Contribution of photosynthetic picoeukaryotes to the picoplanktonic carbon biomass and to total particulate organic carbon in the open ocean.

Carolina Grob

THESE DE DOCTORAT DE L'UNIVERSITE PIERRE ET MARIE CURIE
(PARIS VI)

LABORATOIRE D'OCEANOGRAPHIE DE VILLEFRANCHE

Présentée par

Carolina Grob

Pour obtenir le grade de

DOCTEUR de l'UNIVERSITÉ PIERRE ET MARIE CURIE

Sujet de la thèse :

Contribution des picoeucaryotes photosynthétiques à la biomasse picoplanctonique et au carbone organique particulaire total dans l'océan ouvert

soutenue le : 14 Mai 2007

devant le Jury composé de :

Mme Vivian Lutz	Docteur	Rapporteur
Mr Josep Gasol	Docteur	Rapporteur
Mme Carmen Morales	Professeur	Examinateur
Mr William K. W. Li	Docteur	Examinateur
Mr Alain Saliot	Professeur	Examinateur
Mr Hervé Claustre	Directeur de recherches CNRS	Co-directeur de thèse
Mr Osvaldo Ulloa	Professeur	Co-directeur de thèse

Dedicated to my family.

Dedicado a mi familia.

Dediée à ma famille.

ACKNOWLEDGMENTS

First of all I would like to thank fate for sitting Dr. Ricardo Galleguillos and Dr. Osvaldo Ulloa side by side on a Concepción-Santiago flight back in 2002. I had just finished my undergraduate degree and Osvaldo was looking for someone to work with him on *Prochlorococcus* cell cycle. Dr. Galleguillos told him that I was looking for a job and after a short interview Osvaldo hired me for 6 months. Those 6 months made me realize that I really liked Oceanography and I started my Ph. D. in 2003.

I would like to thank all the organisms that provided me with financial support during my thesis: the Chilean National Commission for Scientific and Technological Research (CONICYT) through the FONDAP Program and a graduate fellowship; the French-Chilean ECOS (Evaluation and Orientation of the Scientific Cooperation)-CONICYT program, the French program PROOF (Processus Biogeochimiques dans l'Océan et Flux), Fundación Andes and the Observatoire Oceanologique of Villefranche (OOV).

I am specially grateful to Dr. Osvaldo Ulloa and Dr. Hervé Claustre for receiving me in their laboratories, for giving me the chance to participate in the BIOSOPE cruise and for guiding me in the best way during my thesis and leaving me at the same time the autonomy necessary to accomplish this wonderful experience. It is Dr. Oscar Pizarro that I have to thank for including me in his ECOS-CONICYT project that allowed me to do my thesis in co-tutoring between Chile and France.

I would like to sincerely thank all the scientists that have inspired and motivated me and whose advices were very enriching. I would also like to thank all the technicians, engineers and crew members, without whom I could not have done this. To all my friends from Villefranche and Concepción thank you very much for all the moments shared and specially for all the good beers drunk regardless of the day of the week.

Finally I would like to thank my family (my father and mother, Géraldine, Vanessa, Cotín and Boris) for all their patience, comprehension and unconditional support.

AGRADECIMIENTOS

Primero que nada quisiera agradecer al destino por haber sentado a los Drs. Ricardo Galleguillos y Osvaldo Ulloa juntos en un vuelo Concepción-Santiago en el 2002. Recién había terminado mi tesis de pregrado y Osvaldo andaba buscando a alguien para trabajar con él en el ciclo celular de *Prochlorococcus*. El Dr. Galleguillos le dijo que yo estaba buscando trabajo, tras lo cual Osvaldo me entrevistó y contrató finalmente por 6 meses. Esos 6 meses me ayudaron a darme cuenta que en realidad me gustaba mucho la Oceanografía y es por eso que empecé mi doctorado en el 2003.

Agradezco a todos los organismos que me financiaron durante la realización de esta tesis: Comisión Nacional de Investigación Científica y Tecnológica (CONICYT), a través del programa FONDAP y una beca de postgrado; el programa franco-chileno ECOS (Evaluación y Orientación de la Cooperación Científica)-CONICYT, el programa Francés PROOF (Processus Biogeochimiques dans l'Océan et Flux), Fundación Andes y el Observatorio Oceanológico de Villefranche (OOV).

Un muy especial agradecimiento para los doctores Osvaldo Ulloa y Hervé Claustre por acogerme en sus respectivos laboratorios, por permitirme participar en el crucero BIOSOPE y por guiarme de la mejor forma posible durante esta tesis, dándome al mismo tiempo la autonomía necesaria para llevar a cabo esta maravillosa experiencia. Fue gracias al Dr. Oscar Pizarro, quién me incluyó en su proyecto ECOS-CONICYT, que pude realizar mi tesis en co-tutela entre Chile y Francia.

Por miedo de olvidar a alguien, quisiera agradecer en forma general a todos los científicos que me inspiraron y motivaron durante mi tesis y cuyos consejos fueron muy enriquecedores. Me gustaría agradecer también a todos los técnicos, ingenieros y tripulantes, sin los cuales no hubiera podido llevar esta tesis a buen término. Quisiera agradecer además a todos mis amigos de Villefranche y Concepción por todos los momentos compartidos y sobre todo por todas esas bien merecidas cervezas bebidas sin importar el día de la semana.

Finalmente quisiera agradecer a mi familia (papá, mamá, Géraldine, Vanessa, Cotín y Boris) por su paciencia, comprensión y apoyo incondicional.

REMERCIEMENTS

Le destin a voulu que MM Ricardo Galleguillos et Osvaldo Ulloa voyagent ensemble dans un vol Concepción-Santiago en 2002. Je finissais alors mes études de Biologie Marine et Osvaldo cherchait quelqu'un pour travailler avec lui sur le cycle cellulaire de *Prochlorococcus*. Sur les conseils du Dr. Galleguillos et après un court entretien, Osvaldo m'a embauché pendant 6 mois. Ce contrat m'a permis de me rendre compte que l'Océanographie me plaisait vraiment et j'ai commencé mon doctorat en 2003.

Je veux remercier les organismes qui m'ont aidés financièrement pendant ma thèse: la Commission Chilienne pour la Recherche Scientifique et Technologique (CONICYT) à travers le programme FONDAP et une bourse de doctorat, le programme franco-chilien ECOS (Evaluation et Orientation pour la Coopération Scientifique)-CONICYT, le programme Français PROOF (Processus Biogeochimiques dans l'Océan et Flux), la Fondation Andes et l'Observatoire d'Océanologie de Villefranche (OOV).

Je voudrais tout particulièrement remercier MM Osvaldo Ulloa et Hervé Claustre pour m'avoir accueilli dans leur laboratoire respectives, permis de participer à la mission BIOSOPE, efficacement encadré pendant le déroulement de ma thèse tout en me laissant l'autonomie nécessaire à la réalisation de cette belle expérience. J'ajoute que c'est grâce à M. Oscar Pizarro qui m'a intégrée le projet Ecos-CONICYT qui j'ai pu réaliser ma thèse en co-tutelle entre le Chili et la France.

Par peur d'oublier quelqu'un, j'aimerais remercier sincèrement tous les scientifiques qui m'ont inspirée, motivée et dont les conseils furent pour moi très formateurs. Je voudrais remercier aussi les techniciens, ingénieurs et membres d'équipage, sans qui je n'aurais pu mener cette thèse à bien. Au-delà, j'adresse un grand merci à tous les amis de Villefranche et de Concepción pour tous les moments partagés et notamment les bonnes bières bien méritées quelque soit le jour de la semaine.

Enfin, je voudrais remercier ma famille (mon père et ma mère, Géraldine, Vanessa, Cotín et Boris) pour toute leur patience, compréhension et soutien inconditionnels.

ABSTRACT

Contribution of photosynthetic picoeukaryotes to the picoplanktonic carbon biomass and to total particulate organic carbon in the open ocean.

María Carolina Grob Varas
University of Concepción - University of Pierre and Marie Curie (Paris VI)
Ph. D. program in Oceanography, 2007

Drs. Osvaldo Ulloa and Hervé Claustre, thesis co-directors

It has been known since the early eighties that picophytoplankton (<2-3 μm) constitutes an important fraction of the total photosynthetic biomass and primary production in the open ocean. Three main groups have been identified within the picophytoplankton: two cyanobacteria, i.e., *Prochlorococcus* and *Synechococcus*, and picophytoeukaryotes belonging to different taxa. Although cyanobacteria, specially *Prochlorococcus*, tend to dominate numerically, the picophytoeukaryotes have been shown to dominate in some cases the picophytoplanktonic biomass and production, due to their bigger size and higher intracellular carbon content.

In the present work it was hypothesized that the spatial variability in picophytoplankton (i.e., *Prochlorococcus*, *Synechococccus* and picophytoeukaryotes) carbon biomass is essentially determined by the picophytoeukaryotes and that this group contributes significantly to the diel variability in the total particulate organic carbon (POC) concentration. In order to test these hypotheses, picophytoplankton as well as bacterioplankton (i.e, Bacteria + Archaea) abundances and carbon biomasses were assessed during two different oceanographic cruises (BEAGLE and BIOSOPE) carried out across the eastern South Pacific (between Tahiti and the coast of Chile) during austral spring time. Whereas abundances were always determined through flow cytometry, biomasses were estimated using carbon conversion factors from the literature (BEAGLE) or from group-specific contributions to the total particle beam attenuation coefficient (c_p), a proxy for POC (BIOSOPE).

The general tendency in picoplankton abundances and biomasses was to increase from oligo- (or hyper-oligo-) to mesotrophic conditions in the eastern South Pacific (*Prochlorococcus*, *Synechococcus*, picophytoeukaryotes and bacterioplankton reaching up to 116, 21, 7 and 860 x 10^{11} cells m^{-2}, respectively), with a slight decrease towards

eutrophic conditions for all except the bacterioplankton, *Prochlorococcus* not being detected near the coast. Picophytoeukaryotes constituted an important fraction of the picophytoplankton (>50% in most of the studied area) and total phytoplankton carbon biomass (>20% in the open ocean), being indeed essential in determining the spatial variability of the former. However, this group's contribution to the diel variability in the c_p-derived POC concentration was not significant (~10%). Daily rates of change (d^{-1}) in picophytoplankton biomass, on the other hand, presented a significant positive correlation to those in c_p ($r = 0.7$; $p < 0.001$). The usefulness of c_p as a proxy for photosynthetic carbon biomass, compared to chlorophyll *a*, is briefly discussed.

Picophytoeukaryotes carbon biomass was much more important than previously thought, equally or more important than that of *Prochlorococcus* in the open ocean. This group could therefore be playing a very important ecological and biogeochemical role in subtropical gyres, which extend over a vast area of the world's ocean.

RESUMEN

Contribución de los picoeucariontes fotosintéticos a la biomasa picoplanctónica y al carbono orgánico particulado total en el océano abierto.

María Carolina Grob Varas
Universidad de Concepción - Universidad de Pierre y Marie Curie (Paris VI)
Programa de Doctorado en Oceanografía, 2007

Drs. Osvaldo Ulloa y Hervé Claustre, co-directores de tesis

El picofitoplancton (<2-3 μm) constituye una fracción importante de la biomasa fotosintética total y de la producción primaria en el océano abierto. Dentro del picofitoplancton se han identificado tres grupos principales: las cianobacterias *Prochlorococcus* y *Synechococcus*, y picofitoeucariontes pertenecientes a distintos taxa. Si bien las cianobacterias, especialmente *Prochlorococcus*, tienden a dominar en número, se ha visto que los picofitoeucariontes pueden llegar a dominar la biomasa y producción picofitoplanctónica, debido a su mayor tamaño y contenido intracelular de carbono.

El presente trabajo se realizó bajo las hipótesis que la variabilidad espacial de la biomasa picofitoplanctónica (i.e., *Prochlorococcus*, *Synechococccus* y picofitoeucariontes) está esencialmente determinada por los picofitoeucariontes y que este grupo contribuye en forma significativa a la variabilidad diurna de la concentración del carbono orgánico particulado total (COP). Para contrastar dichas hipótesis se determinaron las abundancias y biomasas picofitoplanctónicas y bacterioplanctónicas (i.e, Bacteria + Archaea) en términos de carbono durante los cruceros oceanográficos BEAGLE y BIOSOPE realizados a través del sector este del Pacífico Sur (entre Tahiti y la costa de Chile), durante la primavera austral. En ambos casos las abundancias fueron determinadas mediante citometría de flujo, mientras que las biomasas se estimaron usando factores de conversión de la literatura (BEAGLE) o a través de las contribuciones específicas de cada grupo al coeficiente de atenuación particulado (c_p), que es un proxy de la concentración de COP (BIOSOPE).

Las abundancias y biomasas picoplanctónicas tendieron a aumentar desde condiciones oligo- (o hyper-oligo-) hasta condiciones mesotróficas en el Pacífico Sur-este (*Prochlorococcus*, *Synechococcus*, picofitoeucariontes y el bacterioplancton alcanzando

hasta 116, 21, 7 y 860 x 10^{11} cel m^{-2}, respectivamente), con una leve disminución hacia condiciones eutróficas en todos los grupos excepto el bacterioplancton, sin detectarse *Prochlorococcus* cerca de la costa. Los picofitoeucariontes constituyeron una fracción importante de la biomasa picofito- (>50% en gran parte del área de estudio) y fitoplanctónica total (>20% en el océano abierto), determinando efectivamente la variabilidad espacial de la primera. La contribución de este grupo a la variabilidad diurna del COP, sin embargo, no fue significativa (~10%). Las tasas de cambio diurno (d^{-1}) de la biomasa picofitoplanctónica, por otra parte, presentaron una correlación positiva significativa con aquellas de c_p ($r = 0.7$; $p < 0.001$). Se discute brevemente la utilidad de c_p como proxy de la biomasa fotosintética, comparado con la clorofila *a*.

La biomasa de los picofitoeucariontes resultó ser mucho más importante de lo que se creía hasta ahora, siendo equivalente o más importante que aquella de *Prochlorococcus* en el océano abierto. Por lo tanto, este grupo pudiera estar jugando un rol ecológico y biogeoquímico muy importante en los giros subtropicales, que se extienden a lo largo de vastas áreas del océano mundial.

RESUME

Contribution des picoeucaryotes photosynthétiques à la biomasse picoplanctonique et au carbone organique particulaire total dans l'océan ouvert.

María Carolina Grob Varas
Université de Concepción - Université de Pierre et Marie Curie (Paris VI)
Programme de Doctorat en Océanographie, 2007

MM Osvaldo Ulloa et Hervé Claustre, co-directeurs de thèse

Le picophytoplancton (diamètre <2-3 μm) constitue une fraction importante de la biomasse phytoplanctonique totale et de la production primaire dans l'océan ouvert. Parmi le picophytoplancton, trois groupes principaux ont été identifiés: les cyanobactéries *Prochlorococcus* et *Synechococcus*, et des picophytoeucaryotes appartenant à des taxa différents. Bien que les cyanobactéries, spécialement *Prochlorococcus*, dominent généralement en nombre, les picophytoeucaryotes peuvent dans certains cas dominer la biomasse et production picophytoplanctoniques, grâce à leur taille et contenu intracellulaire de carbone plus élevés.

Ce travail s'appuie sur les hypothèses que la variabilité spatiale de la biomasse picophytoplanctonique dans l'océan ouvert (i.e., *Prochlorococcus*, *Synechococccus* et picophytoeucaryotes) est essentiellement déterminée par les picophytoeucaryotes et que ce groupe contribue significativement à la variabilité journalière de la concentration du carbone organique particulaire total (COP). Pour tester ces hypothèses, les abondances du picophytoplancton, ainsi que celles du bacterioplancton (i.e, Bacteria + Archaea) ont été déterminées lors de deux campagnes océanographiques dans le Pacifique Sud Est entre Tahiti et la côte chilienne (BEAGLE et BIOSOPE). Dans les deux cas les abondances ont été déterminées par cytométrie en flux, alors que les biomasses en carbone ont été estimées en utilisant des facteurs de conversion tirés de la littérature (BEAGLE) ou à travers les contributions des différents groupes planctoniques au coefficient d'atténuation particulaire (c_p), un proxy de la concentration de COP (BIOSOPE).

La tendance générale est une augmentation des abondances et biomasses picoplanctoniques entre les conditions oligo- (ou hyper-oligo) et mesotrophiques dans le Pacifique Sud Est (*Prochlorococcus*, *Synechococcus*, picophytoeucaryotes et

bacterioplancton atteignant jusqu'à 116, 21, 7 et 860 x 10^{11} cel m^{-2}, respectivement), avec une légère diminution vers les eaux eutrophiques côtières pour tous sauf le bacterioplancton, les *Prochlorococcus* n'ayant pas été détectés sur la côte. Les picophytoeucaryotes représentaient une fraction importante de la biomasse picophytoplanctonique (>50% dans la plupart de la zone d'étude) et phytoplanctonique totale (>20% dans l'océan ouvert), déterminant la variabilité spatiale de la première. De plus, la contribution de ce groupe à la variabilité journalière de la concentration de COP n'était pas significative (~10%). Les taux de changement journaliers de c_p (d^{-1}), d'une autre parte, étaient significativement corrélés à ceux de la biomasse picophytoplanctonique ($r = 0.7$; $p < 0.001$). L'utilité de c_p comme proxy de la biomasse picophytoplanctonique est brièvement discutée par rapport à celle de la chlorophylle *a*.

La biomasse des picophytoeucaryotes était beaucoup plus importante de ce qui était initialement anticipé, étant souvent plus importants que celle des *Prochlorococcus* dans l'océan ouvert. Les picophytoeucaryotes jouerait donc un rôle écologique et biogéochimique dominant dans les gyres subtropicaux, lesquelles occupent une vaste superficie de l'océan mondial.

TABLE OF CONTENTS

FIGURES

Fig. 1. (a) Global, annual average net primary productivity on land and in the ocean during 2002 (kgC m^{-2} y^{-1}). The yellow and red areas show the highest rates (2-3 kgC m^{-2} y^{-1}), whereas the green, blue, and purple shades show progressively lower productivity. Downloaded from http://earthobservatory.nasa.gov/Newsroom/NPP/npp.html. (b) Global, annual average marine primary production between September 1997 and August 1998 (gC m^{-2}). Downloaded from http://marine.rutgers.edu/opp/swf/Production/results. SPSG stands for South Pacific Subtropical Gyre.

Fig. 2. Distribution of different planktonic groups according to their size fraction. Although in this figure picoplankton is defined to be between 0.2 and 2 μm, the upper limit has also been defined at 3μm. Modified from Sieburth et al. (1978).

Fig. 3. Electronic microscopy images of *Prochlorococcus* (a, scale bar is 5 μm), *Synechococcus* (b, same scale as a) and *Micromonas pusilla* (c), one of the most common picophytoeukaryotic cells found in the coastal ocean (1 to 3 μm). Cyanobacteria images were downloaded from www.sb-roscoff.fr/Phyto/gallery and *M. pusilla* from www.smhi.se/oceanografi/oce_info_data/plankton_checklist.

Fig. 4. Surface chlorophyll *a* concentrations estimated from satellite and *in situ*. Red dots indicate the geographical location of the stations where surface chlorophyll *a* was measured *in situ*. Note that the lowest estimated concentrations are observed in the South Pacific Subtropical Gyre (SPSG). From Maritorena, *pers. comm*.

Fig. 5. The data used in the present work was obtained during two different oceanographic cruises: (1) BEAGLE (Blue Earth Global Expedition, JAMSTEC; Uchida & Fukasawa 2005) and (2) BIOSOPE (BIogeochemistry & Optics SOuth Pacific Experiment). Empty and filled circles along 32.5ºS indicate the locations where surface and water column samples were taken during the BEAGLE cruise, respectively. Squares indicate the locations of stations sampled at high frequency (every 3h; MAR, HNL, GYR, EGY and UPW) during the BIOSOPE cruise. Filled circles between these long stations indicate the location of the stations sampled at local noon time during BIOSOPE.

Fig. 6. Schematic diagram of a flow cell. During picophytoplankton analyses, samples enter the flow cytometer through this compartment, where cells are aligned thanks to the laminar flow assured by the sheath fluid. Once they are aligned, cells pass one by one in front of the laser beam. Downloaded from http://biology.berkeley.edu/crl/flow_cytometry_basic.html.

Fig. 7. Schematic diagram of the internal structure of a flow cytometer, including the flow cell. After being hit by the blue laser beam, the signals that can be recovered from the cells in the sample are forward light scatter (FSC), side scatter (SSC), yellow-green fluorescence (FL1, usually from the dies used to stain bacterioplankton cells), orange fluorescence (FL2, from *Synechococcus* ficoerythrin for instance), red fluorescence (FL3, from chlorophyll *a*, mono- as well as divinyl). Additional signals can be retrieved when using flow cytometers equipped with a second (red) laser (e.g., FL4).

Fig. 8. Example of cytograms. (a) Picophytoplankton populations (*Prochlorococcus*, *Synechococcus* and picophytoeukaryotes) are differentiated based on their forward scatter (FSC) and chlorophyll fluorescence signals. Reference beads of 1 μm are included in the sample. (b). Bacterioplankton is differentiated based on their FSC and the yellow-green fluorescence signal of the DNA dye used (SYBR-Green I). HDNA and LDNA stand for bacterioplankton with high and low DNA content, respectively.

Fig. 9. Example of bacterioplankton DNA distribution. Bacterioplankton DNA being stained with SYBR-Green I, high DNA (HDNA) and low DNA (LDNA)-containing bacterioplankton can be identified in the yellow-green (FL1) signal distribution of this die. Bottom vertical arrow indicates the approximate limit between HDNA and LDNA-containing bacteriopalnkton populations.

Fig. 10. Example of forward light scatter cytometric signal (FSC) distribution for reference beads (a) and picophytoeukaryotes (b). Mean FSC for beads were obtained by fitting a Gaussian curve (dark line in (a)), whereas for picophytoeukaryotes we used the whole signal's distribution, except for the outliers observed at both ends of the distribution that have already been removed from this figure (b). Note that 3 different picophytoeukaryotes peaks, each one of them probably corresponding to a different population, can be clearly identified from this group's FSC distribution (b).

Fig. 11. Schematic diagram of the stream-in-air droplet principle used by the fast cell sorting system of the FACSAria flow cytometer. The identified cells of interest are first charged with the charging electrode and then deflected by the deflection plates according to the charge that has been given to them. These cells are ultimately collected in different collection tubes.

Fig. 12. Example of the Coulter Counter's particle size distribution for a picophytoeukaryotes population isolated *in situ* using fast cell sorting. Both the original size distribution (light line) and the data used to calculate the arithmetic mean of the identified picophytoeukaryotes population (dark line) are shown.

Fig. 13. Simplified scheme of light attenuation by a particle. The incident light is attenuated through absorption and scattering by that particle.

Fig. 14. Relationship between particle attenuation (c_p) and particulate organic carbon (POC). The solid circles, the linear fit (continuous line), and the equation correspond to measurements performed at 5ºS, 150ºW. The open circles correspond to values derived from a power law model linking c_p to POC (Loisel & Morel, 1998) fitted to a linear relationship (POC = 506.71 c_p + 2.32 and r^2 = 0.99) shown as the dashed line. Extracted from Claustre et al. (1999).

Fig. 15. Example of volume distribution of particles in terms of μm^3 ml^{-1} per 1 μm obtained using a HIAC particle counter. A peak assumed to correspond to a large phytoplankton group (>3 μm) is observed around 5 μm. Vertical dashed lines indicate the beginning and end of the identified peak and the diagonal arrow shows the approximate (App.) location of the logarithmic base line for the volume distribution of particles. Only the data within these limits was considered to calculate the average size for this group, as its arithmetic mean. The number of particles within the same limits was taken as cell abundance for the identified phytoplankton group.

Fig. 16. Example of a hypothetical data set from 40 m depth for which the daily rate of change was calculated. Each dot corresponds to a different sample. Samples were taken every 3h during 2 to 4 days. A regression line was fitted to the whole data set. The slope of this regression line (black line) was then normalized to the average value for the whole data set. Finally, the normalized slope was standardized to 24h to obtain a daily rate of change (d^{-1}).

Fig. 17. Schematic representation of the log-log relationships between mean cell size and abundance (a) and between mean cell size and carbon biomass (b) expected from ecological theory.

Fig. 18. Water-columned integrated *Prochlorococcus* (a), *Synechococcus* (b), picophytoeukaryotes (c) and bacterioplankton abundances (x 10^{11} cells m^{-2}) estimated during both cruises. Although during the BEAGLE cruise the data was integrated between the surface and 200 m, the abundances registered below 200 m were negligible enough for these results to be comparable to those integrated between the surface and 1.5 Ze during BIOSOPE.

Fig. 19. Picophytoeukaryotes (a) and *Prochlorococcus* (b) general increasing trends observed at 160-170 m (solid lines) as a response to an increase in light availability during the 4 days of sampling at GYR station. The slightly negative (a) and almost negligible (b) trends observed at 190 m (dashed lines) are presented to highlight the increases observed at 160-170 m.

Fig. 20. Surface irradiance (mmole quanta m^{-2} s^{-1}) the day before arriving to GYR station (Fri, Friday 11th) and during the 4 days of sampling at this station (Monday 12th to Wednesday 16th), November 2003. From Claustre, *pers. comm.*

Fig. 21. Water-column integrated picophytoeukaryotes carbon biomasses estimated across the eastern South Pacific. In order to compare the data from both cruises, original BEAGLE data were divided by 2, according to the mean picophytoeukaryotes intracellular carbon content estimated during BIOSOPE. The latter was 2 times lower than the conversion factors from the literature used during the BEAGLE cruise. O, M and E (top of the figure panel) stand for oligo-, meso- and eutrophic conditions.

Fig. 22. Picophytoeukaryotes contribution to integrated picoplankton (filled circles and solid line) and picophytoplanktonic (empty circles and dotted line) carbon biomass (C) during the BIOSOPE (a) and BEAGLE (b) cruises. For the BIOSOPE cruise (a), picophytoeukaryotes contribution to total phytoplankton carbon biomass (dashed line) is also presented. Note that BEAGLE integrated data starts at 110ºW, whereas that of BIOSOPE begins at 142ºW.

Fig. 23. Total particle beam attenuation coefficient (c_p) ratios to the vegetal compartment attenuation coefficient (c_{veg}) and to the non-vegetal compartment

attenuation coefficient (c_{nveg}). Notice the much higher variability in the c_p to c_{veg} ratio. Data from the BIOSOPE cruise.

Fig. 24. Mean diel cycles of picophytoeukaryotes abundance in cells ml^{-1} (a) and attenuation cross-section (σ_c) in x 10^{12} m^2 $cell^{-1}$ (b) between the surface and 60 m, at MAR station. The average and standard deviation (vertical lines) values for each sampling time (i.e., 3, 6, 9, 12, 15, 18, 21 and 24 h) were obtained using the data collected during the 2 sampling days. σ_c for each time of the day were obtained as indicated in Chapter 2.3.1.

Fig. 25. Mean diel cycle of integrated (0 to 1.5 Ze) particle beam attenuation (c_p) at MAR station. Vertical lines indicate the standard deviations for each sampling time.

Fig. 26. Relationship between daily rates of change (d^{-1}) in *Prochlorococcus* (*Proc*), *Synechococcus* (*Syn*) and picophytoeukaryotes (Euk) carbon biomass and daily rates of change of total particle attenuation (c_p) (a) and cytometric chlorophyll fluorescence (FL3) (b). In (a), the correlation coefficient (r) was calculated for the mean rates of change (considering all *Proc*, *Syn* and Euk biomasses rates of change) and c_p. In (b), n. s. stands for not significant.

Fig. 27. Daily rates of change (d^{-1}) of *Prochlorococcus* (*Proc*) and *Synechococcus* (*Syn*) abundances (abund), total particle beam attenuation coefficient (Total c_p) and picophytoeukaryotes attenuation coefficient (c_{euk}) at MAR (a), HNL (b), GYR (c) and EGY (d). In the case of cyanobacteria, daily rates of change in abundance are representative of daily rates of change in their attenuation coefficients, because the latter were estimated using an average cell size (see Chapter 2.3.1).

Fig. 28. The picoplankton food web: This oceanic food web based on picoplankton shows the paths of organic carbon flux determined by Richardson and Jackson. On the left is the classical "microbial loop" (gray). The two red boxes (large zooplankton and particulate organic detritus) are two carbon pools that, according to Richardson and Jackson, receive substantial export of picoplankton carbon. This new information suggests that the role of picoplankton in carbon export and fish production needs further investigation in both observations and models. Modified from Barber, 2007.

LIST OF ABBREVIATIONS

PP : primary production

FSC: flow cytometric forward light scatter signal normalized to reference beads and expressed in relative units

Picophytoplankton: includes photosynthetic cyanobacteria (*Prochlorococcus* and *Synechococcus*) and picophytoeukaryotes

Picophytoeukaryotes: photosynthetic eukaryotic organisms ≤ 3 µm

Bacterioplankton: includes all Bacteria and Archaea

Picoplankton: includes picophytoplankton and bacterioplankton

Tchl*a*: total chlorophyll *a* (monodivinyl + divinyl chlorophyll *a*)

POC: total particulate organic carbon

DOC: total dissolved organic carbon

c_p**:** total particle beam attenuation coefficient (m^{-1})

c_{veg}**:** part of the total particle beam attenuation coefficient due to vegetal particles (pico- and larger phytoplankton cells)

c_{nveg}**:** part of the total particle beam attenuation coefficient due to non-vegetal particles (bacterioplankton, heterotrophic protists and detritus)

c_{proc}**:** *Prochlorococcus*-specific attenuation coefficient

c_{syn}**:** *Synechococcus*-specific attenuation coefficient

c_{euk}**:** picophytoeukaryotes-specific attenuation coefficient

c_{bact}**:** bacterioplankton-specific attenuation coefficient

c_{het}**:** heterotrophic protists'-specific attenuation coefficient

c_{det}**:** detritus-specific attenuation coefficient

CHAPTER 1

GENERAL INTRODUCTION

1. GENERAL INTRODUCTION

Nearly half of the Earth's primary production (PP) takes place in the ocean (Field et al., 1998; Fig. 1a). Mean global marine PP is estimated in the order of 45 (Longhurst et al., 1995) to 60 Gt C y^{-1} (Carr et al., 2006 and references therein), 86% of which occurs in the open ocean (Chen et al., 2003). This is due primarily to its large area, since PP rates per unit area in the open ocean are much lower than in coastal regions (Fig. 1b).

In the open ocean the photosynthetic biomass is dominated by small phytoplankton cells that fall within the picoplankton size fraction (i.e., < 2-3 μm in diameter; Fig. 2). Picophytoplankton also constitutes the background photosynthetic biomass in more productive waters where most of the biomass is constituted by larger phytoplankton cells belonging to the nano- (2-3 to 20 μm) and microphytoplankton (>20 μm), such as in coastal regions (Fig. 3).

Within the picophytoplankton, three groups have been commonly differentiated: two within the cyanobacteria - the genera *Prochlorococcus* (Chisholm et al., 1988) and *Synechococcus* (Waterbury et al., 1979) - and the other one within the picophytoeukaryotes, which includes different phylogenetic taxa in the Eukarya domain (Fig. 3). Until now, most of the organisms included in the latter group are only known by their genetic sequences (Moon-van der Staay et al., 2001; López-García et al., 2001; Not et al., 2007).

Because cyanobacteria tend to dominate numerically in the open ocean, most picophytoplankton studies have focused on this group. It has been recognized, however, that picophytoeukaryotes can in some cases dominate the picophytoplanktonic PP (e.g., Li, 1994 & 1995; Worden et al., 2004) and also the carbon biomass in this size fraction (e.g., Zubkov et al., 2000), but the studies have been restricted in space and time. Thus, very little is still known about the diversity (e.g., Not et al., 2007), ecology and biogeochemical role of this group, which is the focus of this thesis.

Apart from the three autotrophic groups mentioned above, picoplankton also includes the bacterioplankton, conformed by Bacteria and Archaea commonly assumed to be essentially heterotrophic. The bacterioplankton is known to use between 10 and 60% of the organic matter produced during photosynthesis, mainly in the form of dissolved organic matter (DOC) (Fuhrman, 1992 and references therein). At first, this group was

believed to remineralize all of this organic matter to inorganic nutrients and CO_2. However, bacterioplankton is now known to also use this DOC for their own growth, hence fixing it into new living carbon biomass available for grazers such as flagellates and ciliates, which will in turn be consumed by larger organisms (Fuhrman, 1992 and references therein). Thus, instead of being reconverted into inorganic nutrients and CO_2, this biomass will be available for higher trophic levels and escape immediate remineralization. The role of bacterioplankton in carbon flow is therefore undoubtedly important through this microbial loop.

In coastal regions, where the photosynthetic biomass is dominated by large cells, the organic matter produced is preferentially consumed by higher trophic levels and exported to the sediments and open ocean. In the open ocean, on the other hand, most of the primary production is assumed to be locally remineralized or take part of the microbial loop in the euphotic zone, due to the small size of the autotrophic cells (e.g., Legendre & Le Fèvre, 1995 and references therein). It has been recently suggested, however, that the role of picophytoplankton in the open ocean carbon export to the deep ocean could be much more important than previously thought, and could therefore be significantly contributing to global carbon export and sequestration (Richardson & Jackson, 2007; Barber, 2007). Therefore, the role of picophytoplankton in carbon production and export in the open ocean could be much more important than previously thought and needs to be re-evaluated.

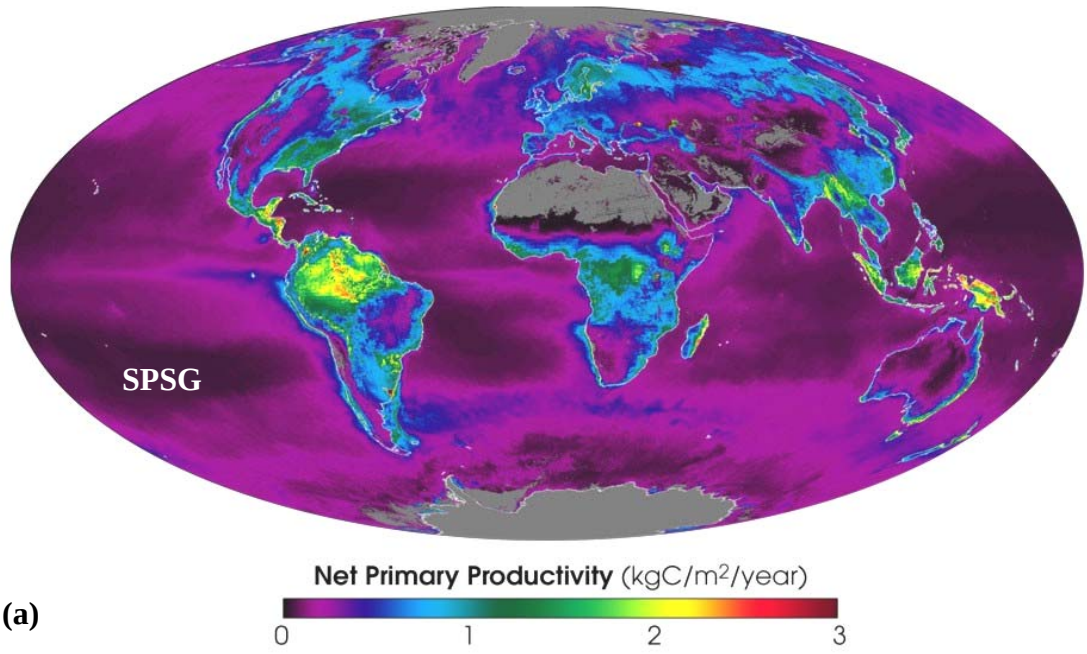

(a)

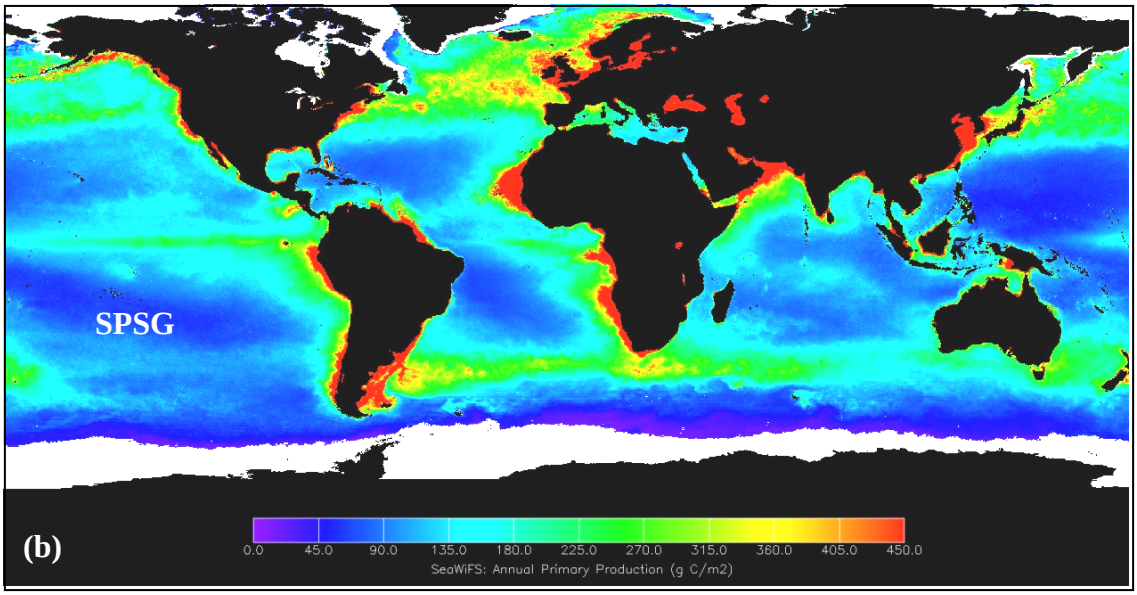

Fig. 1. (a) Global, annual average net primary productivity on land and in the ocean during 2002 (kgC m^{-2} y^{-1}). The yellow and red areas show the highest rates (2-3 kgC m^{-2} y^{-1}), whereas the green, blue, and purple shades show progressively lower productivity. Downloaded from http://earthobservatory.nasa.gov/Newsroom/NPP/npp.html. (b) Global, annual average marine primary production between September 1997 and August 1998 (gC m^{-2}). Downloaded from http://marine.rutgers.edu/opp/swf/Production/results. SPSG stands for South Pacific Subtropical Gyre.

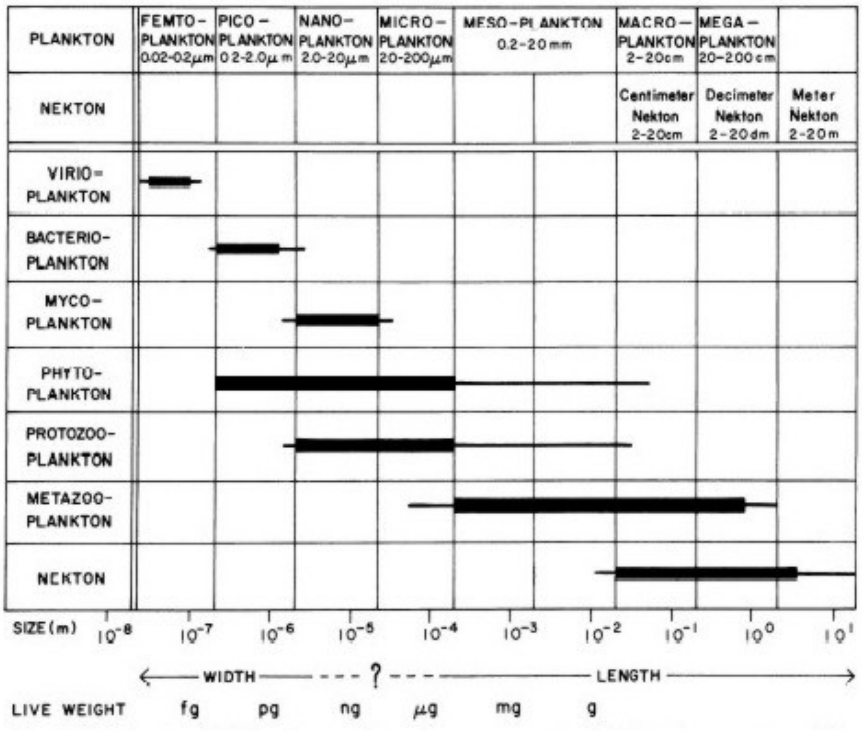

Fig. 2. Distribution of different planktonic groups according to their size fractions. Although in this figure picoplankton is defined to be between 0.2 and 2 µm, the upper limit has also been defined at 3µm.Modified from Sieburth et al. (1978).

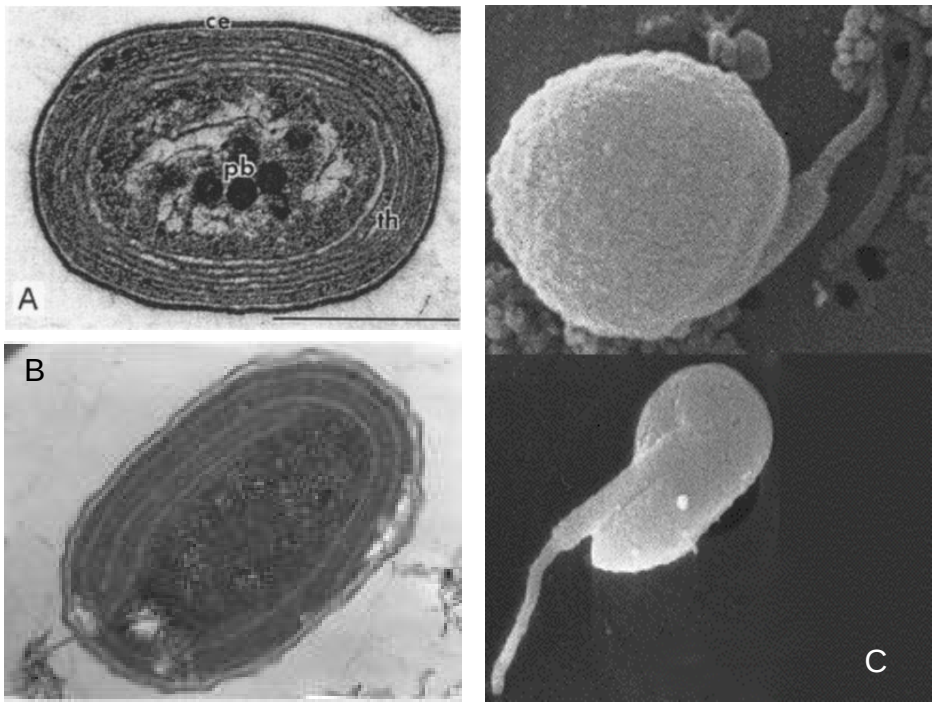

Fig. 3. Electronic microscopy images of *Prochlorococcus* (a, scale bar is 5 μm), *Synechococcus* (b, same scale as a) and *Micromonas pusilla* (c), one of the most common picophytoeukaryotic cells found in the coastal ocean (1 to 3 μm). Cyanobacteria images were downloaded from www.sb-roscoff.fr/Phyto/ gallery and *M. pusilla* from www.smhi.se/ oceanografi/oce_info_data/plankton_checklist/others.

1.1 Picoplankton group-specific abundances, biomasses and contributions to total particle beam attenuation coefficient (c_p)

Due to their very small size, it was only after the development of flow cytometry that picophytoplankton cells could be detected, differentiated (primarily among the three groups mentioned above) and counted on regular bases and at the large scale (e.g., Li & Wood, 1988 and references therein). Macroecological studies indicate that picophytoplankton abundance tends to decrease with increasing chlorophyll *a* concentrations and to increase with increasing stratification (usually accompanied by low nutrients) and temperature (Li, 2002). As a result, 66% of the variance in picophytoplankton abundance can be explained by temperature (the dominant factor), nitrate and chlorophyll *a* concentration (Li, *in press*). At the group-specific level, it has been shown that higher *Prochlorococcus* abundances are observed in more stratified waters and at temperatures above 10ºC (Partensky et al., 1999a), whereas *Synechococcus* and picophytoeukaryotes are more abundant when mixing prevails (e.g. Blanchot and Rodier, 1996; Shalapyonok et al.; 2001). Bacterioplankton abundance, on

the other hand, is known to be directly related to chlorophyll *a* concentrations (e.g., Gasol & Duarte, 2000) and to dominate the total picoplankton abundance (e.g., Zubkov et al., 2000). The relationship with chlorophyll *a* can have a positive or negative slope, indicating bottom-up or top-down control on bacterioplankton abundance, respectively (Li et al., 2004).

Cell abundances are usually used to estimate carbon biomasses by applying volume-based carbon conversion factors (e.g., Li et al., 1992; Campbel & Vaulot, 1993; Zubkov et al. 1998). When cell volumes are not available, cell-specific conversion factors can also be used (e.g., Blanchot et al., 2001; Sherr et al., 2005). Picophytoeukaryotes are bigger in size and present a higher intracellular chlorophyll *a* and carbon content than *Prochlorococcus* or *Synechococcus* (e.g., Raven, 1986 and references therein). The above implies that lower picophytoeukaryotes abundances could reach similar or higher carbon biomasses than cyanobacteria. Furthermore, maximal growth rates per unit cell volume (1 μm^3) seem to be higher for picophytoeukaryotes than for the numerically dominant *Prochlorococcus* (Raven 2005 and references therein). The amount of carbon passing through the picophytoeukaryotic compartment could hence be significant in the open ocean and their role in energy and carbon flow could be much more important than previously thought. In the present thesis work I tried to determine the relevance of this group in terms of carbon biomass, not only within the picoplanktonic size fraction, but also in relation to the total particulate organic carbon.

An alternative approach to determining carbon biomasses is through the deconvolution of the total particle beam attenuation coefficient, c_p, corresponding to the beam attenuation coefficient measured at 660 nm (m^{-1}). This coefficient has proven to be a good proxy for the concentration of total particulate organic carbon (POC, mg m^{-3}) (e.g. Claustre et al., 1999). Vegetal as well as non-vegetal particles contribute to c_p. The contributions by the different vegetal and non-vegetal groups of particles, i.e., the group-specific contributions, can be estimated using optical theory. For this, the size, refractive index and abundance of each group needs to be known or at least assumed. Using this optically-based approach it has been estimated, for example, that in the equatorial Pacific 1-3 µm picophytoeukaryotes cells contributed with 28–46% to c_p, and therefore POC, whereas the numerically dominant *Prochlorococcus* represented 8-12% and *Synechococcus* was negligible (Chung et al., 1996; DuRand & Olson, 1996;

Claustre et al, 1999). Thus, the contribution to picophytoeukaryotes to the total particulate organic carbon in the open ocean can be considerable.

During the 24h diel (i.e., day-night) period, differences of up to 2-fold between a diurnal maximum and nocturnal minimum in c_p have been observed (e.g., Chung et al., 1998; Claustre et al., 1999). Although the non-vegetal particles tend to dominate this coefficient (e.g., Chung et al., 1998; Claustre et al., 1999; Oubelkheir et al., 2005), its diel cycle resembles that of most phytoplantkonic cells that grow and divide within 24h. Little is known, however, about the influence of the different groups that contribute to c_p on the diel variability observed in this coefficient. When assuming a constant refractive index, group-specific attenuation coefficients are determined by size and abundance. Therefore, when assuming no diel changes in the refractive index, diel changes in group-specific attenuation coefficients are expected to be determined by changes in these two variables, resulting from growth and mortality processes. Diel variability in the cytometric forward light scatter signal (FSC), a proxy for cell size (e.g., Olson et al., 1993), and abundance have been observed in both cyanobacteria (DuRand & Olson, 1996; Binder & DuRand, 2002) and picophytoeukaryotes (Vaulot & Marie, 1999). Using the optically-based approach described above, it would therefore be possible to determine the influence of the diel variability in picoplankton-specific attenuation coefficient on that of c_p. Such approach is used in the second part of this thesis (see below).

Determining the spatial and temporal variability in the photosynthetic carbon biomass distribution among the different picophytoplanktonic groups can be useful to improve primary production estimates in the open ocean. Determining the contribution to the photosynthetic biomass by larger phytoplankton groups (nano- and microphytoplankton) towards more productive regions can help defining the limits of the area within which the small size fraction, and especially picophytoeukaryotes, dominate and are important for the ecology of the pelagic ecosystem. This is particularly important if we consider that the spatial variability in c_p, and therefore POC, seems to be determined by the vegetal particles (e.g., Claustre et al., 1999; Ouberkheir et al., 2005) and that the picophytoeukaryotes could be dominating this compartment in the open ocean. Complementing the above with information on the non-vegetal group's contributions to the c_p-derived POC can give an idea on the fate of the carbon being produced. For instance, the ratio of biomass autotrophs : bacterioplankton < 1 will

indicate that the turn over rate of autotrophs must be faster than that of bacterioplankton to be able to keep up with their carbon demand (Fuhrman et al., 1989). Knowing the distribution of carbon biomass among the different contributors can therefore be helpful to identify the underlying biogeochemical pathways and ecosystem functioning.

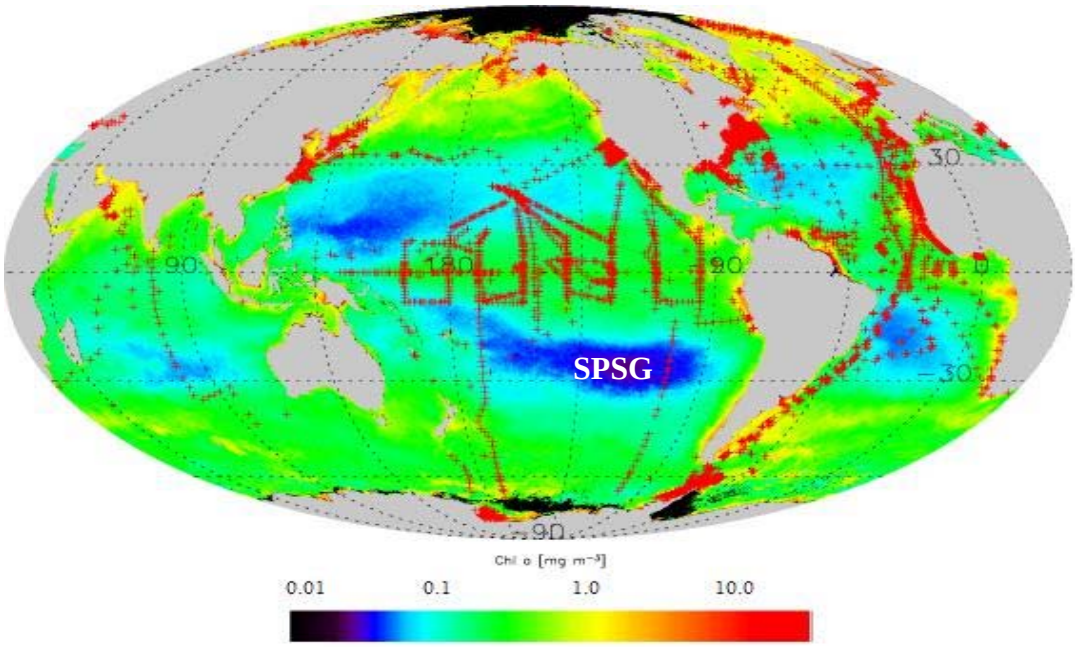

Fig. 4. Surface chlorophyll *a* concentrations estimated from satellite and *in situ*. Red dots indicate the geographical location of the stations where surface chlorophyll *a* was measured *in situ*. Note that the lowest estimated concentrations are observed in the South Pacific Subtropical Gyre (SPSG). From Maritorena, *pers. comm*.

Picoplankton studies have been carried out in different regions of the world's ocean except for most of the South Pacific Subtropical Gyre (SPSG). Based on the consistently low surface chlorophyll *a* concentrations (Fig. 4) and primary production rates (Fig. 1b) estimated from space, Claustre & Maritorena (2003) defined the SPSG as "the Earth's largest oceanic desert". More recently, Morel et al. (2007) have stated that the clearest waters of the world's ocean are located at the centre of this gyre. Furthermore, SeaWiFS satellite images indicates that the poor conditions encountered at the centre of the gyre differ greatly from the typical high nutrients-low chlorophyll waters encountered at the western and equatorial borders of the gyre, and from the highly productive upwelling waters of the Chilean and Peruvian coasts. The eastern South Pacific constitutes a unique scenario for studying group-specific contributions, and particularly picophytoeukaryotes contribution to the total picophytoplanktonic carbon biomass and total particulate organic carbon (POC) across extreme trophic

conditions, including oligo- (≤ 0.1 mg m^{-3} of surface chlorophyll *a*), meso- (> 0.1 & ≤ 1 mg m^{-3}) and eutrophic (> 1 mg m^{-3}) areas (Antoine et al., 1996). The eastern South Pacific was therefore chosen as the study area for this work.

The ***main objective*** of the present work is:

To determine the contribution of oceanic picophytoeukaryotes to the picophytoplanktonic carbon biomass and to total particulate organic carbon (POC), and to their spatial and temporal variability in the euphotic layer of the open ocean.

Based on the background given above, the two following working hypothesis were posed:

Hypothesis 1: *The spatial variability of picophytoplanktonic carbon biomass in the euphotic zone of the eastern South Pacific is essentially determined by the picophytoeukaryotes.*

Hypothesis 2: *The picophytoeukaryotes contribute significantly to the diel variability in the total particulate organic carbon (POC) concentration.*

The two **specific objectives** established to guide the present thesis work:

(1) To determine the contribution of picoeukaryotes to the picophytoplanktonic carbon in the euphotic zone of the eastern South Pacific based on flow cytometry.

(2) To evaluate the contribution of picophytoeukaryotes to the total particle beam attenuation coefficient (a proxy for POC) and its diel variability in the euphotic zone of oligotrophic and mesotrophic regions of the eastern South Pacific.

Organization of the thesis

The methods used during the development of this thesis are described in detail in **Chapter 2**. The first part of the present work resulted in the publication of the scientific article "Picoplankton abundance and biomass across the eastern South Pacific Ocean along latitude 32.5° S", here included in **Chapter 3**. The data collected during the second part of the thesis was used in the elaboration of a new manuscript entitled "Contribution of picoplankton to the particle beam attenuation coefficient (c_p) and organic carbon concentration (POC) in the eastern South Pacific", here included in

Chapter 4, which has already been submitted for publication. In Chapters 3 and 4, the articles' abstracts have also been included in Spanish and French.

Chapter 5 includes a general discussion on the results presented in the two previous chapters. Several ideas regarding the relevance of this work at the larger spatial and temporal scale are also exposed. Finally, based on the questions rising from this thesis, some perspectives to the present work are presented in **Chapter 6**.

CHAPTER 2

METHODS

2. METHODS

Samples and data were collected during two oceanographic cruises across the Eastern South Pacific, during austral spring time:

(1) Leg-2 of the Japanese expedition BEAGLE (Blue Earth Global Expedition, JAMSTEC; Uchida & Fukasawa 2005), between Tahiti (~149.5º W) and the coast of Chile (~71.5º W) along 32.5ºS, from September 12th to October 12th, 2003 (Fig. 5).

(2) The French expedition BIOSOPE (BIogeochemistry & Optics SOuth Pacific Experiment), between the Marquesas Islands (~ 8.39ºS; 141.24ºW) and the coast of Chile (~ 34.55ºS; 72.39ºW), from October 26th to December 11th, 2004 (Fig. 5).

Additionally, phytoplankton cells from culture were used in laboratory work to establish direct relationships between the flow cytometric forward scatter signal (FSC) and both mean intracellular carbon content (see Chapter 2.2.3) and cell size (see Chapter 2.4.2).

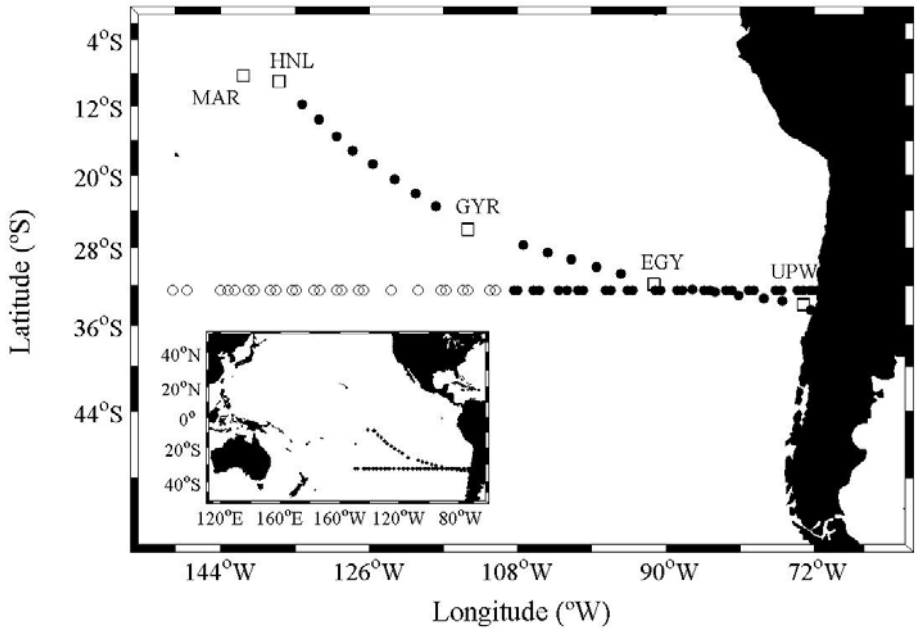

Fig. 5. The data used in the present work was obtained during two different oceanographic cruises: (1) BEAGLE (Blue Earth Global Expedition, JAMSTEC; Uchida & Fukasawa 2005) and (2) BIOSOPE (BIogeochemistry & Optics SOuth Pacific Experiment). Empty and filled circles along 32.5ºS indicate the locations where surface and water column samples were taken during the BEAGLE cruise, respectively. Squares indicate the locations of stations sampled at high frequency (every 3h; MAR, HNL, GYR, EGY and UPW) during the BIOSOPE cruise. Filled circles between these long stations indicate the location of the stations sampled at local noon time during BIOSOPE.

2.1 Flow cytometry

Originally developed for clinical analyses, flow cytometry was first applied to phytoplankton analyses in the early eighties (e.g., Olson et al., 1983 & 1985). This technique allows counting cells on individual bases, i.e. one by one, and differentiate populations according to their optical properties. In brief, during flow cytometric analyses a very small volume of sea water (0.5 ml) is drawn through a thin tube into the flow cell where cells are aligned one after the other thanks to a constant laminar flow generated by the sheath fluid (Fig. 6).

One by one these cells are excited with a laser beam to record their emitted natural (from pigments) or added fluorescence (from fluorochromes; see Chapter 2.1.1) using different collectors, mirrors and filters (Fig. 7; see Marie et al., 2005 for details). Among the different fluorescence signals that can be detected are the red chlorophyll fluorescence (FL3), orange phycobilins fluorescence (FL2) and yellow-green induced bacterioplankton fluorescence (FL1) (Fig. 7). At the same time the forward (FSC) and side light scatter (SSC) signals are detected, the former being a proxy for cell size and the latter for cell complexity.

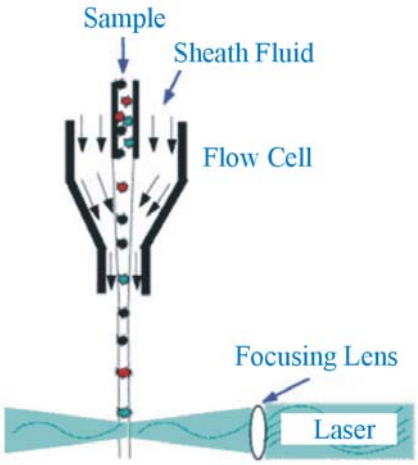

Fig. 6. Schematic diagram of a flow cell. During picophytoplankton analyses, samples enter the flow cytometer through this compartment, where cells are aligned thanks to the laminar flow assured by the sheath fluid. Once they are aligned, cells pass one by one in front of the laser beam. Downloaded from http://biology.berkeley.edu/crl/ flow_cytometry_basic.html.

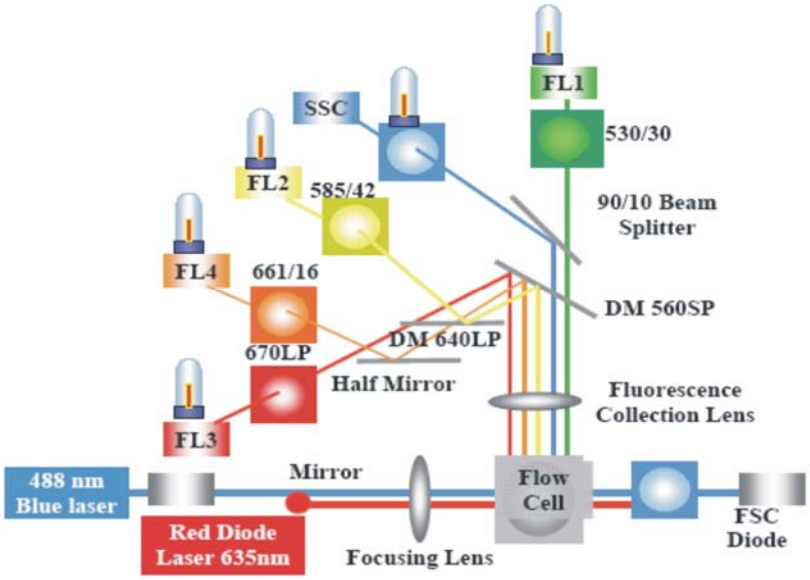

Fig. 7. Schematic diagram of the internal structure of a flow cytometer, including the flow cell. After being hit by the blue laser beam, the signals that can be recovered from the cells in the sample are forward light scatter (FSC), side scatter (SSC), yellow-green fluorescence (FL1, usually from the dies used to stain bacterioplankton cells), orange fluorescence (FL2, from *Synechococcus* phycoerythrin for instance), red fluorescence (FL3, from chlorophyll *a*, mono- as well as divinyl). Additional signals can be retrieved when using flow cytometers equipped with a second (red) laser (e.g., FL4).

2.1.1 Picoplankton abundance

During the BEAGLE cruise samples for flow cytometry were taken at 25 surface stations (< 5 m) between Tahiti and Easter Island (~109º W) and at 6 different depths between the latter and the coast of Chile (surface, 10, 50, 100, 150 and 200 m). All samples were fixed on board with paraformaldehyde at 1% final concentration and quick-frozen in liquid nitrogen (see Chapter 3). During BIOSOPE, samples were taken at 6 to 14 different depths from the surface up to 300 m, the position of the deepest sampling being established according to the depth where the irradiance was reduced to 1% of its surface value. In this case picophytoplankton analyses were performed on board on fresh samples, whereas for bacterioplankton they were fixed with paraformaldehyde at 1% or glutaraldehyde at 0.1% final concentration and quick-frozen in liquid nitrogen (see Chapter 4). In both cases (i.e., BEAGLE and BIOSOPE) fixed samples were analysed on land within two months after the end of the corresponding cruise.

Prochlorococcus, *Synechococcus*, picophytoeukaryotes and bacterioplankton abundances were determined using a FACSCalibur (Becton Dickinson) flow cytometer,

equipped with a 488 nm blue laser. Picophytoplanktonic populations (cyanobacteria and picophytoeukaryotes) were differentiated based on their forward scatter (FSC) and chlorophyll *a* fluorescence (FL3) signals (Fig. 8a) according to Marie et al. (2000). Bacterioplankton samples were stained with the fluorochrome SYBR-Green I (Molecular Probes) to differentiate this population based on FSC and the yellow-green fluorescence (FL1) of this DNA dye (Fig. 8b; Marie et al., 2000). The error associated to abundances determined using flow cytometry is ≤ 5%.

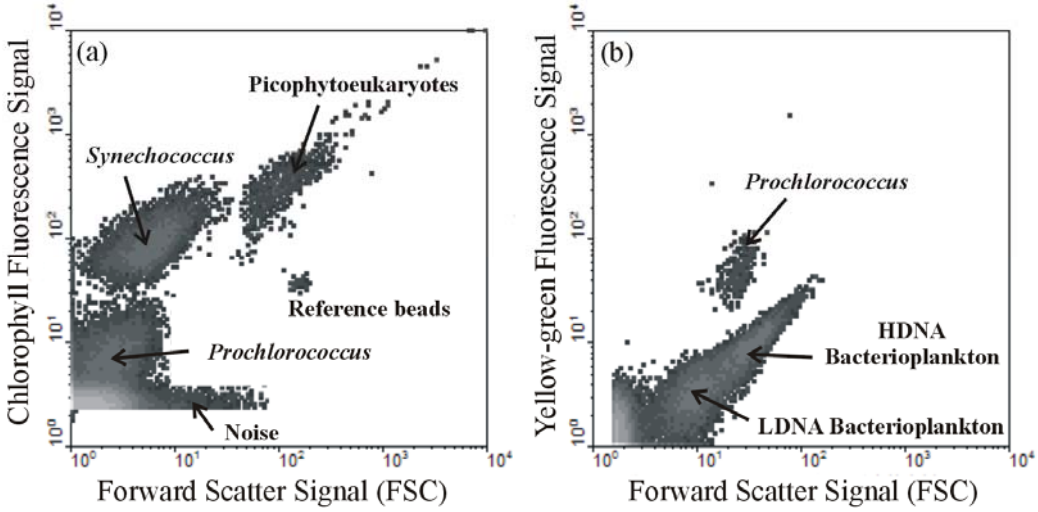

Fig. 8. Example of cytograms. (a) Picophytoplankton populations (*Prochlorococcus*, *Synechococcus* and picophytoeukaryotes) are differentiated based on their forward scatter (FSC) and chlorophyll fluorescence signals. Reference beads of 1 µm are included in the sample. (b). Bacterioplankton is differentiated based on their FSC and the yellow-green fluorescence signal of the DNA dye used (SYBR-Green I). HDNA and LDNA stand for bacterioplankton with high and low DNA content, respectively.

Abundances for the weakly fluorescent surface *Prochlorococcus* populations were determined by fitting a Gaussian curve (see Chapter 3) or from divinyl-chlorophyll *a* concentrations assuming an intracellular content of 0.23 fg (see Chapter 4). Flow cytometry data acquisition was always performed with the Cell Quest Pro software (Becton Dickinson) on log mode using 256 channels (see, for example, Fig. 9) and then analysed with the Cytowin software (Vaulot, 1989).

2.1.2 High-DNA (HDNA) and low-DNA (LDNA) containing bacteria

HDNA- and LDNA-containing bacteria were differentiated based on the yellow-green (FL1) fluorescence signal of the fluorochrome added to their DNA. Higher fluorescence indicates higher DNA content. It was therefore assumed that the first and second peaks observed in the FL1 signal distribution corresponded to LDNA- and HDNA-containing bacteria, respectively (Fig. 9). Assuming a similar distribution for both populations, the

proportion of total bacterioplankton counts corresponding to HDNA- and LDNA-containing bacteria was determined by establishing a limit between these two populations (vertical arrow in Fig. 9) and counting the cells before and after this limit. This analysis was performed only for the BEAGLE cruise data.

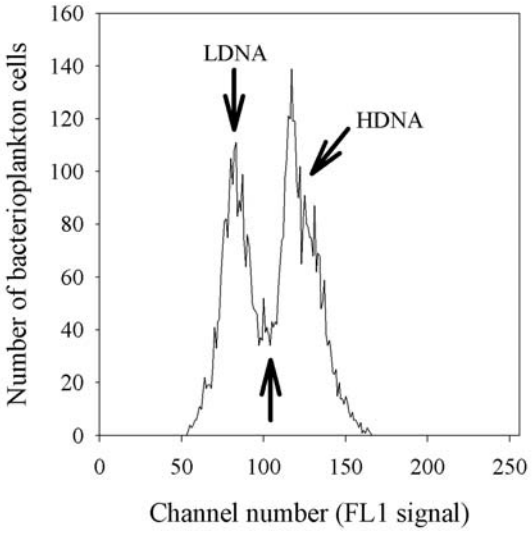

Fig. 9. Example of bacterioplankton DNA distribution. Bacterioplankton DNA being stained with SYBR-Green I, high DNA (HDNA) and low DNA (LDNA)-containing bacterioplankton can be identified in the yellow-green (FL1) signal distribution of this die. Bottom vertical arrow indicates the approximate limit between HDNA and LDNA-containing bacteriopalnkton populations.

2.1.3 Mean normalized forward scatter signal

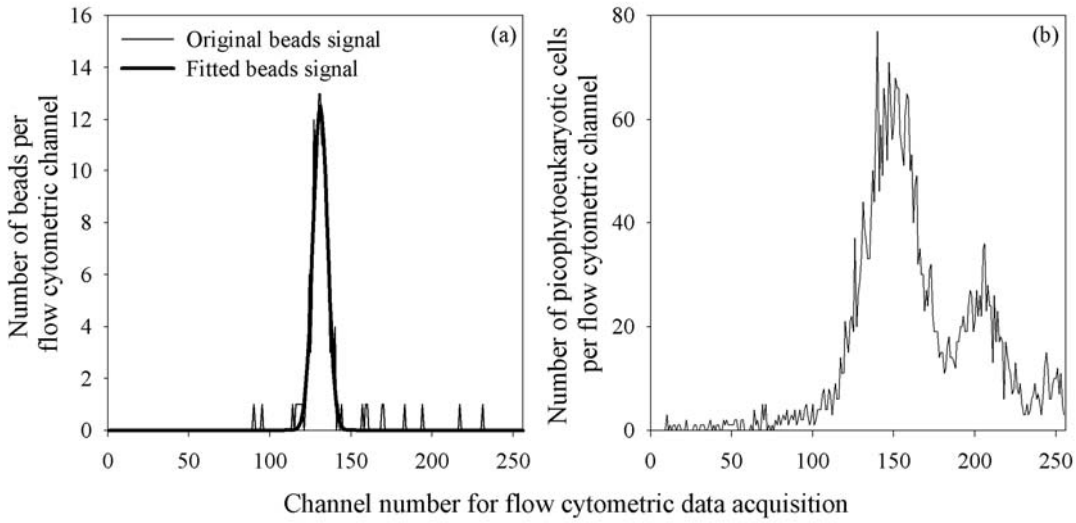

Fig. 10. Example of forward light scatter cytometric signal (FSC) distribution for reference beads (a) and picophytoeukaryotes (b). Mean FSC for beads were obtained by fitting a Gaussian curve (dark line in (a)), whereas for picophytoeukaryotes we used the whole signal's distribution, except for the outliers observed at both ends of the distribution that have already been removed from this figure (b). Note that 3 different picophytoeukaryotes peaks, each one of them probably corresponding to a different population, can be clearly identified from this group's FSC distribution (b).

Mean forward scatter (FSC) and chlorophyll *a* fluorescence (FL3) signals for the reference beads were obtained by fitting a Gaussian curve to the original 256-channels signal distribution (Fig. 10a). For cyanobacteria, population size distributions represented by FSC were assumed to follow a normal distribution and the peak of such distribution was taken as the mean. *Prochlorococcus* and *Synechococcus* FSC distributions were however not always available, because the flow cytometer parameters were set to target the higher FSC signals of the bigger picophytoeukaryotic cells (remember that FSC is a proxy for cell size). In this case of picophytoeukaryotes, FSC signals were obtained by calculating the arithmetic mean of the whole signal's distributions, except for the outliers usually observed in the first and last 5 to 10 channels of such distribution (Fig. 10b). FL3 signals for all three groups were obtained as for the picophytoeukaryotes FSC, except that in this case no outliers were observed (not shown).

2.2 Mean picoplankton cell size

2.2.1 Isolating picoplankton populations: FACSAria cell sorting

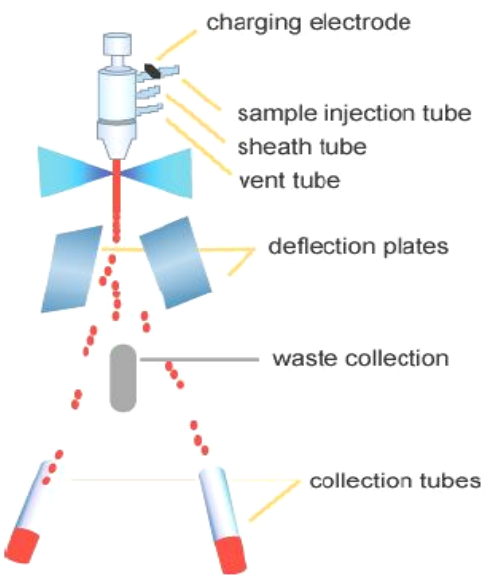

Fig. 11. Schematic diagram of the stream-in-air droplet principle used by the fast cell sorting system of the FACSAria flow cytometer. The identified cells of interest are first charged with the charging electrode and then deflected by the deflection plates according to the charge that has been given to them. These cells are ultimately collected in different collection tubes.

The stream-in-air droplet sorting system of the FACSAria flow cytometer allows rapid sorting of a high number of cells. The mechanism consists on creating spaced droplets containing the cells of interest and charging them electrically (positively or negatively). The charged droplet passes then trough an electrostatic field between the deflection plates, is deflected towards the plate of opposite charge and collected into the corresponding collection tube (Fig. 11). Using this mechanism, during the BIOSOPE cruise picophytoplankton populations were isolated *in situ* from fresh samples. Each population was then analyzed with the FACSCalibur flow cytometer to obtain their mean FSC signals (see Chapter 2.1.3). Mean cell size for the

different isolated populations was determined using the Coulter Counter (see Chapter 2.2.2). This is the first time ever that this kind of measurement has been performed onboard on fresh populations isolated *in situ*.

2.2.2 Determining actual mean cell size: Coulter Counter measurements

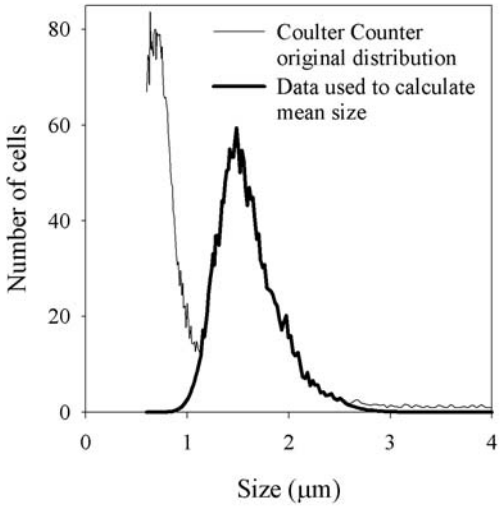

Fig. 12. Example of the Coulter Counter's particle size distribution for a picophytoeukaryotes population isolated *in situ* using fast cell sorting. Both the original size distribution (light line) and the data used to calculate the arithmetic mean of the identified picophytoeukaryotes population (dark line) are shown.

Actual mean cell size for populations isolated *in situ* (see Chapter 2.2.1) and for phytoplankton cells from culture were determined using a Coulter Counter. Average population cell sizes were calculated as the arithmetical mean of the whole group's distribution (Fig. 12). The same populations were simultaneously analysed through flow cytometry to obtain their mean normalized FSC signals (see Chapter 2.1.3). A direct relationship was then established between FSC and size using both, populations isolated *in situ* and culture cells (see Fig. 3a in Chapter 4). Using this relationship it was possible to estimate mean cell size for picophytoeukaryotes populations in almost every sample analyzed during the BIOSOPE cruise. In the case of cyanobacteria, their FSC signals were available in enough samples to obtain mean cell sizes representatives of the whole transect (see Chapter 4).

2.3 Estimating particulate organic carbon concentration (POC, mg m^{-3}) from the particle beam attenuation coefficient (m^{-1})

The inherent optical properties of sea water (IOP's) depend exclusively on the medium and the different substances in it (Preisendorfer, 1961). One of the main IOP's is the light attenuation coefficient (c, m^{-1}), which is determined by light absorption (a, m^{-1}) and scattering (b, m^{-1}) at any given wavelength λ (Eq. 1).

$$c(\lambda) = a(\lambda) + b(\lambda) \quad (1)$$

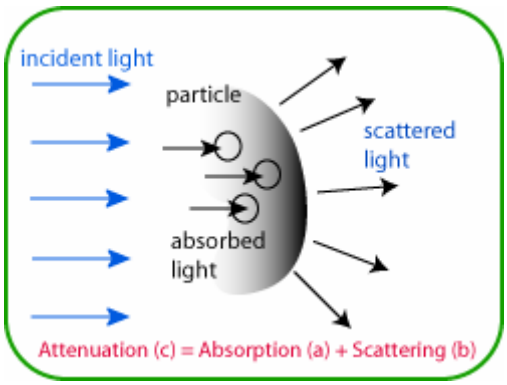

Fig. 13 Simplified scheme of light attenuation by a particle. The incident light is attenuated through absorption and scattering by that particle.

Particles (Fig. 13), water and coloured dissolved organic matter (CDOM) contribute to the beam attenuation coefficient. At 660 nm, however, attenuation due to CDOM is considered to be negligible (Bricaud et al., 1981) and a constant value can be used for water. Beam attenuation at 660 nm can therefore be considered as representative of particle load. The total particle beam attenuation coefficient (c_p) in the ocean is determined by both vegetal and non-vegetal particles between 0.5 and 20µm (Behrenfeld & Boss, 2006 and references therein). During the BIOSOPE cruise c_p profiles were obtained using a C-Star transmissometer (Wet Labs, Inc.) attached to the CTD rosette. The C-Star data was treated and validated as described in Claustre et al. (1999). Total particulate organic carbon concentrations (POC, mg m^{-3}) were estimated from c_p by using a conversion factor of 500, based on an empirical relationship established by Claustre et al. (1999) between the two variables (Fig. 14). This relationship was validated during the BIOSOPE cruise.

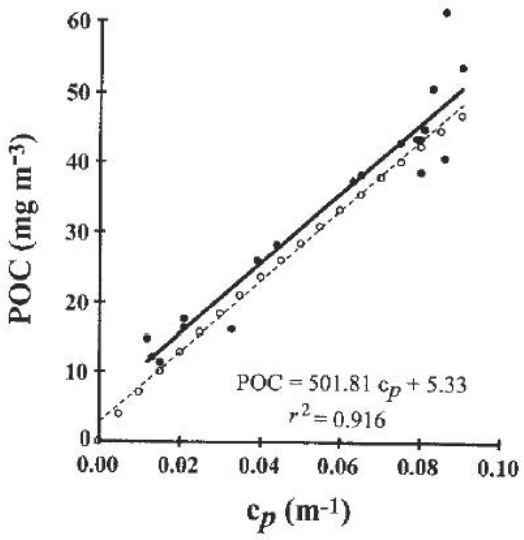

Fig. 14. Relationship between particle attenuation (c_p) and particulate organic carbon (POC). The solid circles, the linear fit (continuous line), and the equation correspond to measurements performed at 5ºS, 150ºW. The open circles correspond to values derived from a power law model linking c_p to POC (Loisel & Morel, 1998) fitted to a linear relationship (POC = 506.71 c_p + 2.32 and r^2 = 0.99) shown as the dashed line. Extracted from Claustre et al. (1999).

2.3.1 Group-specific attenuation coefficients resolving the different particle contributors to c_p

Vegetal (c_{veg}) as well as non-vegetal (c_{nveg}) particles contribute to the total particle beam attenuation coefficient (Eq. 2).

$$c_P = c_{veg} + c_{nveg} \quad (2)$$

Whereas *Prochlorococcus* (c_{proc}), *Synechococcus* (c_{syn}), picophytoeukaryotes (c_{euk}) and larger phytoplankton (>3 µm, c_{large}) contribute to the vegetal part of the signal (Eq. 3),

$$c_{veg} = c_{proc} + c_{syn} + c_{euk} + c_{large} \quad (3)$$

bacterioplankton (c_{bact}), heterotrophic protists (c_{het}) and detritus (c_{det} = non living particles) contribute to the non-vegetal one (Eq. 4),

$$c_{nveg} = c_p - c_{veg} = c_{bact} + c_{het} + c_{det} = c_{bact} + 2c_{bact} + c_{det} = 3c_{bact} + c_{det} \quad (4)$$

where c_{het} is assumed to be approximately $2c_{bact}$ (Morel and Ahn, 1991). Finally, once c_{veg}, c_{bact} and therefore c_{het} are determined, c_{det} is obtained directly by difference (Eq. 5).

$$c_{det} = c_{nveg} - c_{bact} - c_{het} = c_{nveg} - c_{bact} - 2c_{bact} = c_{nveg} - 3c_{bact} \quad (5)$$

At 660 nm, particle absorption is negligible and beam attenuation and scattering are equivalent (Loisel and Morel, 1998). Group-specific contributions to c_p are therefore equivalent to their contributions to b_p. c_{proc}, c_{syn}, c_{euk}, c_{large} and c_{bact} can hence be estimated by determining the group-specific scattering coefficients,

$$b_i\ (m^{-1}) = N_i\ [s_i\ Q_{bi}] = N_i\ \sigma_{bi} \quad (6)$$

- ✓ i = proc, syn, euk, large or bact.
- ✓ N_i (cells m^{-3}), i.e., picoplankton abundances, and mean cell sizes (through the relationship established with FSC, see Chapter 2.2.2) were determined using flow cytometry (see Chapters 2.1.1 & 2.2.2).
- ✓ s (m^2 $cell^{-1}$), i.e., the mean geometrical cross sections, were calculated from size.
- ✓ Q_{bi} (dimensionless), i.e., the optical efficiency factors, were computed through the anomalous diffraction approximation at 660 nm (Van de Hulst, 1957) assuming a refractive index of 1.05 for all groups (Claustre et al., 1999).

✓ [s_i Q_{bi}] or σ_{bi} corresponds to the scattering cross-sections (m^2 $cell^{-1}$).

For *Prochlorococcus* and *Synechococcus* we used mean sizes obtained from a few samples, whereas for the picophytoeukaryotes we used the mean cell size estimated for each sample (see Supp. Mat.). For samples where picophytoeukaryotes abundance was too low to determine their size we used the nearest sample's value. For bacterioplankton we used a value of 0.5 µm, as used by Claustre et al. (1999).

In the case of larger phytoplankton (>3 µm), however, mean cell size and abundance were determined either from the Coulter Counter's particle distribution as indicated in Chapter 2.2.2, or from the HIAC particle counter data (Royco; Pacific Scientific). When detected in the Coulter Counter particle distribution, mean cell size and abundance for large phytoplankton were determined as indicated in Chapter 2.2.2. Data collected with the HIAC were represented in the form of volume distribution of particles standardized to 1 µm (μm^3 ml^{-1} per 1 µm). Small peaks are easier to identify using this representation (Fig. 15). In this example shown in Fig. 15, a large peak, assumed to correspond to a phytoplankton population, can clearly be seen around 4.5 and 5 µm. The average size of this population was calculated as the arithmetic mean of all data included within the identified peak, between its beginning and end, above the approximate location of the logarithmic baseline. Those data points were then added to obtain the approximate cell abundance.

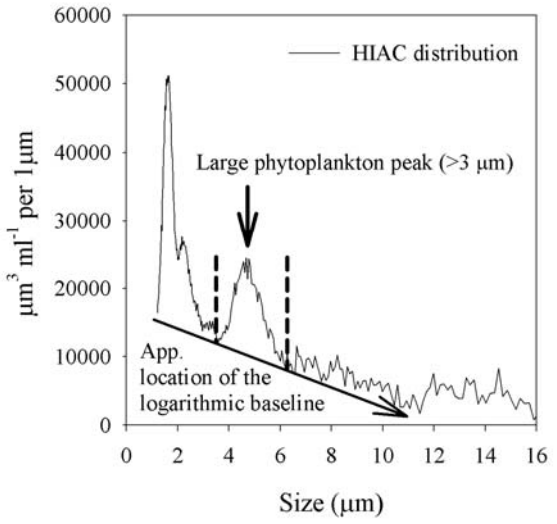

Fig. 15. Example of volume distribution of particles in terms of μm^3 ml^{-1} per 1 µm obtained using a HIAC particle counter. A peak assumed to correspond to a large phytoplankton group (>3 µm) is observed around 5 µm. Vertical dashed lines indicate the beginning and end of the identified peak and the diagonal arrow shows the approximate (App.) location of the logarithmic base line for the volume distribution of particles. Only the data within these limits was considered to calculate the average size for this group, as its arithmetic mean. The number of particles within the same limits was taken as cell abundance for the identified phytoplankton group.

2.4 Picophytoplankton carbon biomass

For the BEAGLE cruise data, carbon conversion factors from the literature were used to estimate *Prochlorococcus* (53 fgC cell^{-1}; e.g., Campbell et al., 1994, Partensky et al., 1996), *Synechococcus* (100 fgC cell^{-1}; e.g., Zubkov et al., 2000, Shalapyonok et al., 2001), picophytoeukaryotes (1500 [e.g., Zubkov et al., 2000] and 530 [Worden et al., 2004] fgC cell^{-1} for oceanic and coastal cells, respectively) and bacterioplankton (12 [e.g., Fukuda et al., 1998] and 27 [e.g., Troncoso et al., 2003] fgC cell^{-1} for oceanic and coastal cells, respectively) biomasses from cell abundance. For the BIOSOPE cruise, however, a direct relationship between the flow cytometric FSC signal and intracellular carbon content was established using phytoplankton cells from culture (see Fig. 2b in Chapter 4). This relationship was then applied to FSC data available for picophytoeukaryotes and *Synechococcus* to obtain their intracellular carbon content and estimate their biomasses. *Prochlorococcus* FSC signals were, however, smaller than the lower limit of the established relationship and their intracellular carbon content was estimated by applying a volume-based conversion factor derived from *Synechococcus* (see Chapter 4).

Picophytoeukaryotes carbon biomasses were estimated through two different approaches based on FSC signals: (1) by establishing a direct relationship with intracellular carbon content (see above) and (2) by establishing a relationship with size, which allowed us to calculate c_{euk} and its contribution to c_p, which we assume to be equivalent to this group's contribution to POC (see Chapter 2.3.1). Both approaches gave very similar results, indicating that the premise that all picophytoeukaryotic organisms have the same refractive index (~ 1.05) was valid for the study area, even if we know that this group is constituted by diverse taxa (e.g. Moon-van der Staay et al., 2001). The above validates the use of optical techniques and theory to determine picophytoeukaryotes contribution to POC, under the sole condition of using real mean cell sizes.

In the case of cyanobacteria, however, carbon biomasses calculated using the intracellular carbon contents estimated directly (*Synechococcus*) or indirectly (*Prochlorococcus*) from FSC (see above) were higher than those estimated from their contributions to c_p. This overestimation of carbon biomasses can be explained by the fact that only one *Synechococcus* and no *Prochlorococcus* populations were included in

the FSC-intracellular carbon content relationship. The conversion factors obtained from such relationship for these two small groups seem, therefore, to be biased. For this reason, it was assumed that group-specific contributions to c_p for cyanobacteria, as well as for large phytoplankton, bacterioplankton and heterotrophic protists were equivalent to their contributions to POC, as proven for picophytoeukaryotes.

2.5 Temporal variability

2.5.1 Diel cycle

During BIOSOPE, picophytoplankton abundance and flow cytometric signals (when possible) were collected every 3 hours during 2 to 4 days at stations MAR, HNL, GYR and EGY. Mean diel cycles were obtained by calculating the average values for each sampling time (i.e., 3, 6, 9, 12, 15, 18, 21 and 24h) considering all the days sampled.

2.5.2 Daily rates of change

Daily rates of change (d^{-1}) were additionally estimated for each one of these long stations. These data were first linearly interpolated to obtain regular matrices with matching depths. Whereas matrices' lines represented the different depths sampled, columns corresponded to the different samplings times. Samples were taken every 3 hours during 2 days at the MAR and HNL sites and during 4 days at the GYR (90 to 270 m) and EGY sites. For each depth and each station we proceeded as follows: first, a regression line was fitted to the entire sampling period data set (Fig. 16). Second, the slope of this regression line was normalized to the data set's mean. Finally, given that the data were taken every 3 hours, daily rates of change (d^{-1}) were obtained by standardizing the normalized slopes to 24 h (d^{-1}). Correlations between daily rates of change of the total picophytoplankton carbon biomass and c_p were then established without considering MAR data.

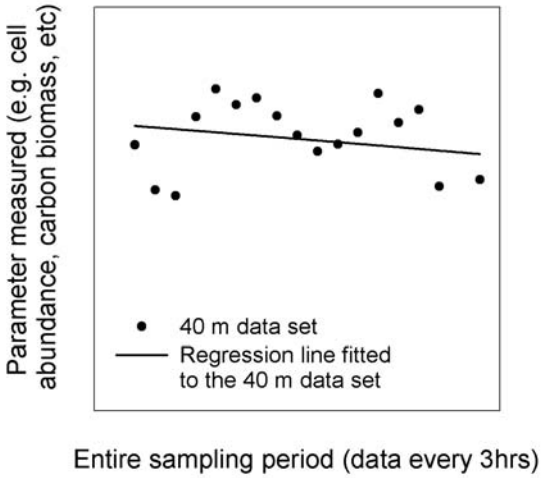

Fig. 16. Example of a hypothetical data set from 40 m depth for which the daily rate of change was calculated. Each dot corresponds to a different sample. Samples were taken every 3h during 2 to 4 days. A regression line was fitted to the whole data set. The slope of this regression line (black line) was then normalized to the average value for the whole data set. Finally, the normalized slope was standardized to 24h to obtain a daily rate of change (d^{-1}).

CHAPTER 3

PICOPLANKTON ABUNDANCE AND BIOMASS ACROSS THE EASTERN SOUTH PACIFIC OCEAN ALONG LATITUDE 32.5ºS

3. PICOPLANKTON ABUNDANCE AND BIOMASS ACROSS THE EASTERN SOUTH PACIFIC OCEAN ALONG LATITUDE 32.5ºS.

Resumen. Se determinó la distribución del picoplancton (< 2-3 μm de diámetro) en una transecta en el este del Pacífico Sur, entre el sur de Tahiti y la costa de Chile a lo largo de los 32.5ºS de latitud, a principios de la primavera austral en el 2003. De acuerdo a la disponibilidad de nutrientes y a las características hidrográficas, las abundancias de *Synechococcus*, picofitoeucariontes y bacterioplancton aumentaron y aquella de *Prochlorococcus* disminuyó desde el sector oligo- hacia el sector eutrófico. El bacterioplancton dominó a lo largo de toda la transecta (> 75% de la abundancia picoplanctónica total). Como era de esperar, *Prochlorococcus* fue el fitoplancter más abundante bajo condiciones oligo- (concentración de clorofila *a* ≤ 0.1 mg m^{-3}) y mesotróficas (> 0.1 y ≤ 1 mg m^{-3}). Contrariamente a otras regiones subtropicales, en este sector del Pacífico Sur los picofitoeucariontes dominaron la biomasa autotrófica < 2 μm en términos de carbono durante el período muestreado. Las biomasas integradas (0 a 200 m) de *Prochlorococcus*, *Synechococcus*, picofitoeucariontes y bacterioplancton se presentaron en razones de 9:1:14:11 y 3:1:8:6 bajo condiciones oligo- y mesotróficas, respectivamente. La biomasa de los picofitoeucariontes resultó ser 1.4 a 2 veces mayor que aquella de las cianobacterias y levemente mayor (1.2 a 1.3 veces) que aquella del bacterioplancton. Los picofitoeucariontes, por lo tanto, pudieran estar jugando un rol ecológico y biogeoquímico dominante en los giros subtropicales que se extienden a lo largo de vastas áreas del océano mundial.

Palabras clave: picofitoeucariontes, bacterioplancton, biomasa en carbono, cianobacteria, citometría de flujo.

Résumé. La distribution du picoplancton (< 2-3 μm de diamètre) a été déterminée dans le secteur est du Pacifique du Sud, entre le sud de Tahiti et la côte du Chili, le long des 32.5ºS de latitude, au début du printemps austral en 2003. Selon la disponibilité en sels nutritifs et les caractéristiques hydrographiques, les abondances de *Synechococcus*, picophytoeucaryotes et bacterioplankton ont augmenté et celles de *Prochlorococcus* diminué entre les régions oligo- et eutrophes. Le bacterioplancton dominait tout le long du transect (> 75% de l'abondance picoplanctonique totale). Comme anticipé, *Prochlorococcus* était le groupe phytoplanctonique le plus abondant sous conditions oligo- (concentration de chlorophylle *a* ≤ 0.1 mg m^{-3}) et mesotrophes (> 0.1 and ≤ 1 mg m^{-3}). Contrairement à d'autres régions subtropicales, dans ce secteur du Pacifique du Sud et pour la période considérée, les picophytoeucaryotes dominaient la biomasse autotrophe < 2 μm en terme de carbone. Les biomasses intégrées (0 à 200 m) de *Prochlorococcus*, *Synechococcus*, picophytoeucaryotes et bacterioplancton étaient respectivement dans les rapports de 9:1:14:11 et 3:1:8:6 pour les régions oligo- et mesotrophes. La biomasse des picophytoeucaryotes était alors 1.4 à 2 fois plus élevée que celle des cyanobactéries et légèrement plus élevée (1.2 à 1.3 fois) que celle du bacterioplancton. Les picophytoeucaryotes pourraient donc être en train de jouer un rôle écologique et biogéochimique majeur dans les gyres subtropicaux, qui constituent une vaste proportion de l'océan mondial.

Mots clés: picophytoeucaryotes, bacterioplancton, biomasse en carbone, cyanobactéries, cytométrie en flux.

Vol. 332: 53–62, 2007 | MARINE ECOLOGY PROGRESS SERIES
Mar Ecol Prog Ser | Published March 5

Picoplankton abundance and biomass across the eastern South Pacific Ocean along latitude 32.5° S

Carolina Grob[1,2,*], Osvaldo Ulloa[2], William K. W. Li[3], Gadiel Alarcón[2], Masao Fukasawa[4], Shuichi Watanabe[4]

[1]Graduate Programme in Oceanography, and [2]Department of Oceanography & Center for Oceanographic Research in the Eastern South Pacific, University of Concepcion, Casilla 160-C, Concepcion, Chile

[3]Biological Oceanography Section, Bedford Institute of Oceanography, Dartmouth, Nova Scotia B2Y4A2, Canada

[4]Mutsu Institute of Oceanography, Japan Agency for Marine-Earth Science and Technology, 2-15 Natsushima, Yokosuka, Kanagawa 237-0061, Japan

ABSTRACT: The distribution of picoplankton (<2 to 3 µm in diameter) was determined on a transect across the eastern South Pacific Ocean from south of Tahiti to the coast of Chile along 32.5°S latitude during the early austral spring. The abundance of *Synechococcus*, picophytoeukaryotes and bacterioplankton increased from oligo- to eutrophic conditions, while that of *Prochlorococcus* decreased according to nutrient availability and hydrographic characteristics. Bacterioplankton dominated across the transect (>75% total picoplanktonic abundance). As expected, *Prochlorococcus* was the most numerically abundant phytoplankter under very oligotrophic (chlorophyll *a* concentration ≤0.1 mg m^{-3}) and mesotrophic (>0.1 and ≤1 mg m^{-3}) conditions. However, in contrast to other subtropical regions, picophytoeukaryotes appear to dominate the <2 µm autotrophic carbon biomass in this region of the South Pacific Ocean at this time of the year. In the upper 200 m of the water column, the integrated carbon biomass of *Prochlorococcus*, *Synechococcus*, picophytoeukaryotes and bacterioplankton were in the ratios of 9:1:14:11 and 3:1:8:6 under oligo- and mesotrophic conditions, respectively. Thus, picophytoeukaryotes were 1.4- to 2-fold higher in biomass than both cyanobacteria combined, and slightly more important (1.2- to 1.3-fold) than bacterioplankton. Picophytoeukaryotes could therefore play a dominant ecological and biogeochemical role in subtropical gyres, which extend over a vast area of the world's oceans.

KEY WORDS: Picophytoeukaryotes · Bacterioplankton · Carbon biomass · Cyanobacteria · Flow cytometry

INTRODUCTION

Marine picophytoplankton (<2 to 3 µm in diameter) play a very important role in the planktonic community, especially in oligo- and mesotrophic regions of the ocean where they make a large contribution to carbon production, biomass and energy transfer (Stockner 1988). Picoplankton includes cyanobacteria of the genera *Synechococcus* (Waterbury et al. 1979) and *Prochlorococcus* (Chisholm et al. 1988), eukaryotes of diverse taxa (e.g. Moon-van der Staay et al. 2001) and bacterioplankton, which include both *Bacteria* and *Archaea* (Giovannoni & Rappé 2000) that do not carry out oxygenic photosynthesis. Bacterioplankton abundance and chlorophyll *a* (chl *a*) concentration are linearly related across different aquatic ecosystems (Gasol & Duarte 2000), through a positive or negative slope, indicating a bottom-up or top-down control on bacteria, respectively (Li et al. 2004). Such interactions between autotrophic and heterotrophic picoplanktonic organisms strongly influence the fate of biogenic carbon in the open ocean. It is therefore important to characterise this small size fraction of the microbial plankton under different oceanographic, biogeochemical and trophic conditions.

*Email: mgrob@profc.udec.cl

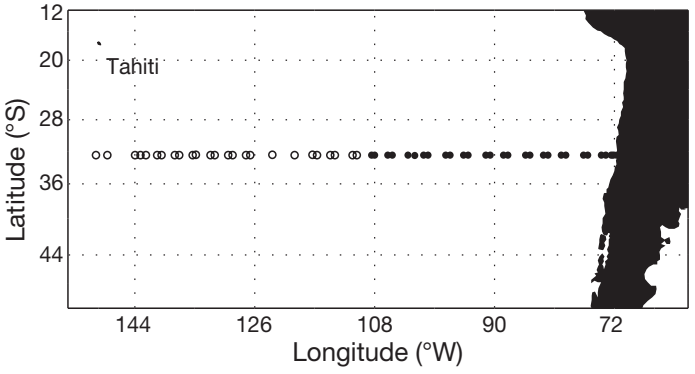

Fig. 1. Stations sampled in the eastern South Pacific at the surface only (○) and at the surface and 10, 50, 100, 150 and 200 m (●)

In the oligotrophic waters studied to date, *Prochlorococcus* and bacterioplankton usually dominate the microbial plankton both in terms of numbers and mass (e.g. Zubkov et al. 2000). Along trophic gradients, *Prochlorococcus* abundance shows opposite patterns to *Synechococcus* and picophytoeukaryotes abundance, becoming a less important component of the carbon standing stock from oligo- to eutrophic conditions (e.g. Partensky et al. 1996, Zubkov et al. 2000). However, because of high cellular carbon and chl *a* content, picophytoeukaryotes can nevertheless contain more biomass than the prokaryotes, even when greatly outnumbered. For instance, in the Arabian Sea the largest eukaryotic phytoplankton cells with higher carbon content were preferentially found in the poorest oceanic waters (Shalapyonok et al. 2001). Satellite images of ocean colour show that the South Pacific subtropical gyre is extremely oligotrophic. This is a large region in which the contribution of picophytoeukaryotes has not been well characterised. Since most (~90%) of the ocean is under oligo- or mesotrophic conditions, the influence of picophytoeukaryotes would have significant impact on the marine primary production, the cycling of bioelements and the ecology of the global ocean.

In this work we present the first detailed picoplankton data set available for the eastern South Pacific Ocean, extending from very oligotrophic to highly productive conditions. We used flow cytometry to: (1) determine the abundance and distribution of *Prochlorococcus*, *Synechococcus*, picophytoeukaryotes and bacterioplankton; (2) analyse the variability in community structure in relation to the trophic conditions and hydrographic characteristics; and (3) determine the contribution of each group to the total picoplanktonic carbon biomass. Our results highlight the importance of picophytoeukaryotes in these oligotrophic waters.

MATERIALS AND METHODS

The study was carried out in the eastern South Pacific Ocean along latitude 32.5° S during the second track (Leg 2) of the Japanese BEAGLE (Blue Earth Global Expedition, Japan Agency for Marine-Earth Science and Technology [JAMSTEC]; Uchida & Fukasawa 2005) cruise, between September 12, and October 12, 2003 (austral spring time). Samples for flow cytometric analyses were taken from surface waters at 25 stations between south of Tahiti (~149.5° W) and Easter Island (~109° W). Between this island and the coast of Chile (~71.5° W), we sampled multiple depths (surface, 10, 50, 100, 150, 200 m) at 29 stations (Fig. 1). Surface samples (Tahiti to Chile) were taken either from CTD casts (i.e. 1 to 3 m), the ship's flow system (i.e. 3 to 5 m), or with a bucket (i.e. 0 m). All samples (surface and water column) were fixed with paraformaldehyde (1% final concentration) and quick-frozen in liquid nitrogen. For bacterioplankton counts, samples were stained with SYBR Green I (Molecular Probes). Cytometric analyses for both picophytoplankton and bacterioplankton were performed with a FACSCalibur (Becton Dickinson) flow cytometer according to Marie et al. (2000a,b). The contribution of high DNA (HDNA)- and low DNA (LDNA)-containing bacteria to total bacterioplankton abundance was estimated according to Li et al. (1995), as a proxy for active and inactive cells, respectively (Gasol et al. 1999). Cell Quest Pro and Cytowin software were used for data acquisition and analysis, respectively. Picoplanktonic populations were differentiated based on their scattering and fluorescence signals (Marie et al. 2000a,b). When surface *Prochlorococcus* populations were not well defined because of their weak fluorescence, their abundance was determined by fitting a Gaussian curve to the data using the Cytowin software. Forward scatter (FSC) and chl *a* fluorescence (FL3) cytometric signals were normalised to reference beads (Fluoresbrite YG Microspheres, calibration grade 1.00 µm, Polysciences) and expressed in relative units (r.u.) to be used as indicators of mean cell size and photoacclimation, respectively (e.g. Campbell & Vaulot 1993).

Prochlorococcus, *Synechococcus* and picophytoeukaryotes abundances were integrated over the water column (0 to 200 m) to determine the contribution of each group to the total number of picophytoplanktonic cells. For calculating water-column-integrated picoplanktonic carbon biomass (IPCB), conversion factors of 53 and 100 fg C cell^{-1} were chosen from the literature as the most representative and conservative values for *Prochlorococcus* and *Synechococcus*, respectively (see Table 1). For open ocean (i.e. oligo- and mesotrophic conditions) and coastal (i.e. eutrophic conditions) picophytoeukaryotes, we used

Table 1. Conversion factors from the literature for *Prochlorococcus* (*Proc*), *Synechococcus* (*Syn*), picophytoeukaryotes (Euk) and bacterioplankton (Bact) carbon biomass (in fg C cell^{-1})

Proc	*Syn*	Euk	Bact	Reference
17–124	–	–	–	Bertilsson et al. (2003) and references therein
32	101	~750–1833	–	Shalapyonok et al. (2001)
29	100	1500	12	Zubkov et al. (2000)
39	82	530	–	Worden et al. (2004)
53	250	2108	–	e.g. Partensky et al. (1996), Campbell et al. (1994)
–	250	–	16 & 20	Fuhrman et al. (1989)
–	–	–	27	Troncoso et al. (2003)
–	–	–	12–30	Fukuda et al. (1998)

1500 and 530 fg C cell^{-1}, respectively, because mean FSC signals (i.e. relative cell size) were significantly lower in the latter than the former populations. The use of the same conversion factor for the whole water column and transect for *Synechococcus* and with depth for the picophytoeukaryotes is justified by the fact that no statistically significant differences were found between mean FSC signals (analyses of variance, $p < 0.001$ for both depth and trophic conditions). Although such differences were indeed significant for *Prochlorococcus* with depth, the use of different conversion factors for the surface and deep populations did not lead to significant differences in the integrated biomass ($p < 0.001$, data not shown). Bacterioplankton biomass was calculated using 12 and 27 fg C cell^{-1} for the open ocean and coastal samples, respectively (see Table 1).

Temperature, salinity and oxygen profiles were obtained with a conductivity–temperature–depth–oxygen profiler (CTDO, Seabird 911 Plus). Nitrate, nitrite, phosphate and silicate concentrations were determined onboard using an autoanalyser and standard techniques. Nutrient concentrations near instrumental detection limit were approximated to 0. Total chl *a* and phaeopigment concentrations were measured fluorometrically (Turner Design, Model 10-AU005CE) for all but 1 of the stations. The missing profile was obtained by triangle-based interpolation. Since no surface hydrographic data were collected, we assumed homogeneous conditions in the top layer and used the 10 m hydrogaphic values as surface values.

To interpret cytometric abundances in relation to the physical and biogeochemical conditions of the water column, we only used data above the depth of 0.1% of surface light intensity, since below this level picophytoplankton growth and therefore distribution should be mostly limited by light. Using Eqs. (3a) and (1b) in Morel & Berthon (1989), we first calculated the euphotic zone depth for each profile (Z_e, corresponding to 1% of surface light intensity) and then the attenuation coefficients (k) using the light attenuation equation (Kirk 1994). For Eq. (3a), we used our surface chl *a* concentrations as their C_{sat}, assuming that it roughly corresponds to what would be measured from satellites. Knowing k for every station, we then determined the 0.1% value of surface light intensity by using the light attenuation equation one more time. To examine vertical changes in normalised cytometric size and fluorescence signals, we computed the optical depth (kz) as k times z for each profile, where z is the actual sampling depth and k is the diffuse attenuation coefficient estimated for each station.

According to surface chl *a* concentrations (mg m^{-3}), we discuss our results in terms of oligo- (≤0.1), meso- (>0.1 and ≤1) and eutrophic (>1) conditions (Antoine et al. 1996). Although this division does not directly take into account the nutrient concentrations, it has been used to characterise the trophic status of the ocean from space and, hence, can be used to place our results in a global bio-optical context.

RESULTS

Picoplankton abundance and community structure

Flow cytometric analyses allowed us to determine the abundance of the cyanobacteria *Prochlorococcus* and *Synechococcus*, and of picophytoeukaryotes and bacterioplankton. A marked increase in FSC and FL3 with the optical depth ($kz > 4.6$) indicates that a more fluorescent *Prochlorococcus* population consisting of larger sized cells replaces a less fluorescent surface population of smaller cells with depth (Fig. 2). A similar pattern was observed for picophytoeukaryotes, although no statistically significant differences were found between the mean FSCs of surface and deep populations ($p < 0.001$). On the other hand, *Synechococcus* mean relative cell size was relatively constant with depth, although their mean fluorescence showed a slight increase towards intermediate depths. It is worth noting that below $kz = 12$ (<0.01% of surface light) the FSC and FL3 signals of all 3 groups are more dispersed because of the very low cell abundance (Fig. 2).

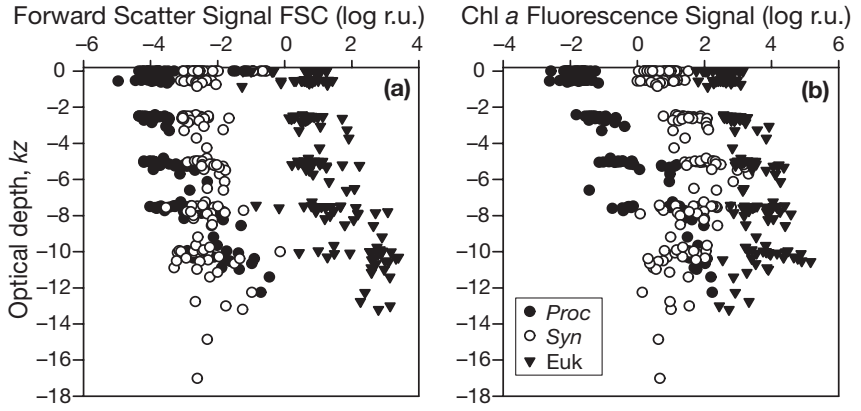

Fig. 2. Forward scatter signal (FSC) (a) and chl *a* fluorescence signal (b) variability with optical depth (*kz*, dimensionless) for*Prochlorococcus* (*Proc*, ●), *Synechococcus* (*Syn*, ○) and picophytoeukaryotes (Euk, ▼); *k*: diffuse attenuation coefficient estimated for each station; *z*: actual sampling depth; r.u. = relative units

With the exception of *Prochlorococcus*, which decreased from the mesotrophic region towards the coast, the abundance of all other cells, as well as the chl *a* concentration, increased from oligo- to eutrophic conditions (Fig. 3, Table 2). Mean (±SD) surface (10 m) nitrogen (nitrate + nitrite), phosphate and silicate concentrations under oligotrophic conditions were 0.51 ± 0.51, 0.22 ± 0.04 and 0.41 ± 0.28 µmol kg^{-1}, respectively. Under meso- and eutrophic conditions nitrogen increased to 1.76 ± 2.30 and 10.06 ± 2.33 µmol kg^{-1}, respectively, while phosphate and silicate reached 0.44 ± 0.26 and 0.35 ± 0.18 µmol kg^{-1} in the former and 1.39 ± 0.37 and 3.34 ± 2.75 µmol kg^{-1} in the latter region, respectively. Maxima *Prochlorococcus*, *Synechococcus*, picophytoeukaryotes and bacterioplankton concentrations were found in the top 50 m of the mesotrophic region (up to ~25, 4, 2 and 140 × 10^4 cells ml^{-1}, respectively) and very close to the Chilean coast for the last 3 groups (up to ~3, 2 and 127 × 10^4 cells ml^{-1}, respectively). Picophytoeukaryotes maxima were associated with a deep chlorophyll maximum (DCM) and the highest chlorophyll concentrations (~2 to 5 mg m^{-3}), respectively (Fig. 3). Water-column-integrated abundance was dominated by bacterioplankton along the whole transect (Table 2). Of the 3 picophytoplanktonic groups, only *Prochlorococcus* integrated abundance was significantly correlated to the mixed-layer depth (Z_m) estimated by Bouman et al. (2006). Mean integrated chl *a* concentration increased from oligo- (17 ± 2 mg m^{-2}) to mesotrophic conditions (26 ± 9 mg m^{-2}) and was highest under eutrophic conditions (212 ± 98 mg m^{-2}). HDNA bacterioplankton represented on average 45 ± 4, 47 ± 5 and 48 ± 10% of total counts under oligo-, meso- and eutrophic conditions, respectively. Their contribution in the open ocean (i.e. oligo- and mesotrophic) was slightly higher above 100 m (3 to 5%) than below this depth.

Integrated bacterioplankton abundance (surface to 0.1% of surface light) was positively and significantly correlated to both *Synechococcus* and picophytoeukaryotes, these 2 picophytoplanktonic groups being strongly correlated to each other (Table 3). *Prochlorococcus* integrated abundance, on the other hand, was not significantly correlated to any of the other groups (Table 3). The relationship between total bacterioplankton abundance and chl *a* concentration observed along the transect (data not shown) lies within the macroecological limits established for the open ocean (Li et al. 2004), and a clear positive slope was observed for chlorophyll concentrations ≤0.2 mg m^{-3} (R^2 = 0.66, $p < 0.0001$). Mean water-column-integrated chl *a* concentrations (0 to 200 m) were ~17, 26 and 212 mg m^{-2} in the oligo-, meso- and eutrophic regions, respectively.

Prochlorococcus abundance was positively related with water temperature (R^2 = 0.54, $p < 0.0001$), and negatively, with inorganic nitrogen (i.e. nitrate + nitrite, R^2 = 0.53, $p < 0.0001$), phosphate (R^2 = 0.51, $p < 0.0001$) and silicate concentrations (R^2 = 0.33, $p < 0.0001$), temperature being negatively correlated to all nutrients and salinity ($p < 0.001$). No statistically significant relationships with these variables were found for *Synechococcus* or the picophytoeukaryotes, except for a very weak negative one between the former and temperature (R^2 = 0.03, $p < 0.05$, data not shown). All 3 groups' abundances exhibited a negative relationship with salinity ($R^2 \geq 0.3$, $p < 0.0001$).

Picoplanktonic carbon biomass

West of Easter Island, mean surface bacterioplankton and *Prochlorococcus* carbon biomasses were equivalent (2.9 mg C m^{-3} in both cases) and higher than those of *Synechococcus* (0.1 mg C m^{-3}) and the pi-

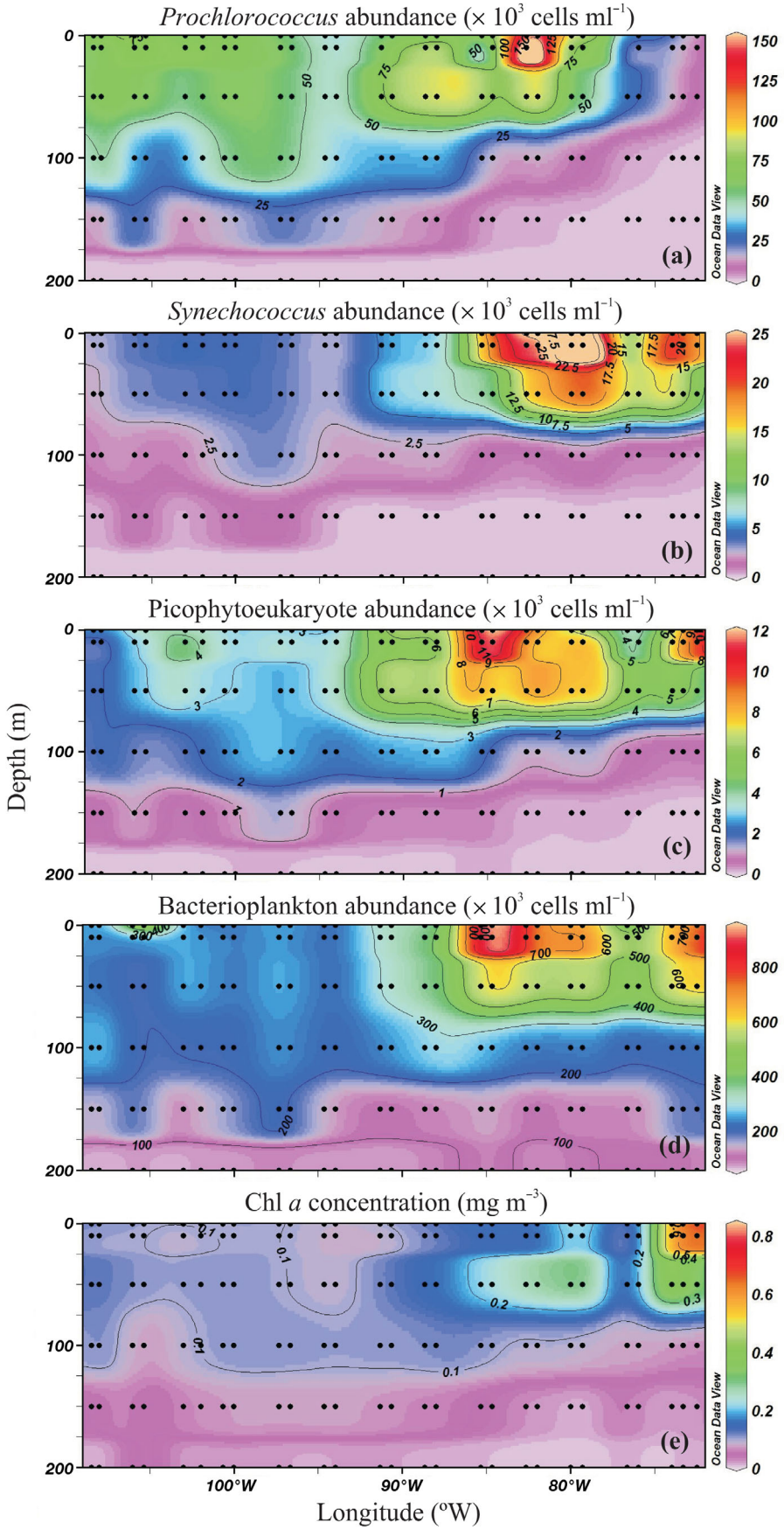

Fig. 3. Water column *Prochlorococcus* (a), *Synechococcus* (b), picophytoeukaryotes (c) and bacterio-plankton abundances (d) in cells ml^{-1}, and chl *a* concentrations (e) in ml m^{-3} (~32.5°S, ~109 to 72.5°W)

Table 2. Mean (±SD) water-column-integrated (0 to 200 m) *Prochlorococcus*, *Synechococcus*, picophytoeukaryotes and bacterioplankton abundance ($\times 10^{11}$ cells m^{-2}) along 32.5° S, between Easter Island and the coast of Chile. The transect range includes the minimum and maximum values found along the transect (when present in the case of *Prochlorococcus*). Campbell & Vaulot (1993) ranges are indicated for comparison. Transect range and Campbell & Vaulot (1993) results for picophytoeukaryotes are presented in bold and italic to highlight the differences observed between them

Group	Oligotrophic	Mesotrophic	Eutrophic	Transect range	Global range published by Campbell & Vaulot (1993)
Prochlorococcus	76 ± 15	62 ± 45	0	5–122	7–200
Synechococcus	4 ± 1	12 ± 6	9 ± 2	2–23	1–20
Picophytoeukaryotes	4 ± 1	6 ± 2	6 ± 2	***2–11***	***0.2–4***
Bacterioplankton	395 ± 44	651 ± 145	919 ± 58	332–1016	–

Table 3. Correlation matrix for picoplankton integrated abundances (surface to 0.1% of surface light) (upper right values: correlation coefficients; ***$p < 0.0001$; ns: not statistically significant)

	Prochlorococcus	*Synechococcus*	Picophytoeukaryotes	Bacterioplankton
Prochlorococcus	1.00	ns	ns	ns
Synechococcus	–	1.00	0.714***	0.854***
Picophytoeukaryotes	–	–	1.00	0.715***
Bacterioplankton	–	–	–	1.00

cophytoeukaryotes (1.5 mg C m^{-3}). East of Easter Island, where we were able to sample through the upper water column (~109 to 72.5° W, 0 to 200 m, IPCB), picophytoeukaryotes had the highest integrated biomass in most of the oligotrophic and part of the mesotrophic region, but bacterioplankton had higher biomass in the rest of the transect (Fig. 4, Table 4). *Prochlorococcus* and bacterioplankton integrated biomass decreased and increased from oligo- to eutrophic conditions, respectively. *Synechococcus* and picophytoeukaryotes integrated biomass, on the other hand, increased from oligo- to meso- and decreased slightly from meso- to eutrophic conditions (Fig. 4). Similar to bacterioplankton abundance, total picoplanktonic carbon biomass (i.e. *Prochlorococcus* + *Synechococcus* + picophytoeukaryotes + bacterioplankton carbon biomass at each sampled point) was positively correlated to chl *a* concentrations ≤0.2 mg m^{-3} ($R^2 = 0.77$, $p < 0.0001$).

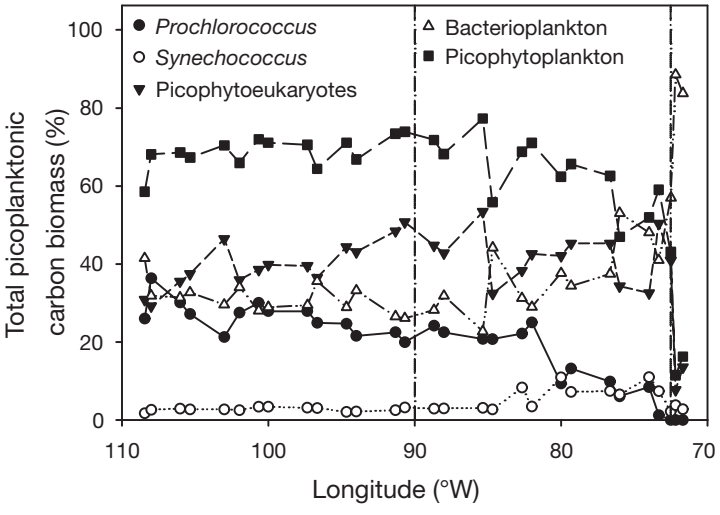

Fig. 4. *Prochlorococcus* (●), *Synechococcus* (○), picophytoeukaryotes (▼), bacterioplankton (△) and picophytoplankton (*Prochlorococcus* + *Synechococcus* + picophytoeukaryotes, ■) contribution to water-column-integrated picoplanktonic carbon biomass. vertical lines indicate limits between oligo- and mesotrophic conditions (90° W) and between meso- and eutrophic conditions (72.5° W)

DISCUSSION

The South Pacific subtropical gyre is by far the most unexplored region of the world's ocean. Until now, virtually the only information concerning phytoplankton at the centre of this gyre was surface chl *a* concentrations estimated through satellite images, whereas bacterioplankton abundance remained completely unknown. The BEAGLE results show some general features typically observed in other oligo-, meso- and eutrophic regions during similar periods of the year, but differ significantly in the more oligotrophic conditions encountered along the transect. Here, the relative biomass composition of the picoplankton community comprising *Prochlorococcus*, *Synechococcus*, picophytoeukaryotes and bacterioplankton was different from other studies of subtropical gyres. Instead of *Prochlorococcus*, it was the picophytoeukaryotes

that dominated the carbon biomass together with the bacterioplankton.

The distribution patterns of picoplanktonic abundance observed across the eastern South Pacific subtropical gyre reflect changes in trophic conditions, nutrient availability and water column stability (Partensky et al. 1996, Zubkov et al. 2000, Shalapyonok et al. 2001, Worden et al. 2004). However, in the oligotrophic region, *Prochlorococcus* abundance was 1 order of magnitude lower than the range established for them elsewhere (1 to 4×10^5 cells ml^{-1}; Partensky et al. 1999) and about half of the values reported for the North and South Atlantic subtropical gyres during spring time (Zubkov et al. 2000). *Synechococccus* abundance was 1 order of magnitude lower and those of picophytoeukaryotes and bacterioplankton similar to the ones reported by Zubkov et al. (2000). However, *Synechococcus* abundance was within the range reported by Partensky et al. (1999) for central gyres. Near the coast *Synechococcus* abundance values were similar to those reported for other upwelling areas, but picophytoeukaryotes abundance was found to be twice the highest reported value (Sherr et al. 2005 and references therein). It is important to highlight that water-column-integrated picophytoplankton abundances observed along the transect were within the global estimates published by Campbell & Vaulot (1993) for both cyanobacteria, but surprisingly higher for picophytoeukayotes (Table 2).

Although the use of linear regressions in microbial ecology has limitations (discussed elsewhere, e.g. Duarte et al. 2000a), our results agree with previous observations on the influence of temperature (e.g. Partensky et al. 1996) and macronutrient availability (e.g. Bertilsson et al. 2003) on the distribution of *Prochlorococcus*. The strong positive correlations between *Synechococcus* and picophytoeukaryotes abundance may be explained by similar nitrogen utilisation abilities (Worden et al. 2004) and growth stimulation towards the coast, provided by the less stable water column and shallower nutricline that allows injection of nutrients to the surface (Partensky et al. 1996, Shalapyonok et al. 2001). The lack of relationships with nutrient concentration does not necessarily contradict the latter, but rather indicates that other factors (e.g. grazing and virus lysis) may be controlling the abundances of these 2 groups as well. The fact that no significant correlations were found between the mixed-layer depth (Z_m) and the integrated abundances of *Synechococcus* and picophytoeukaryotes (0 to 200 m or 0 to Z_m) further indicates this possibility (data not shown). Different time responses of these 2 groups to the addition of nutrients, as observed in mesocosm experiments (Duarte et al. 2000b) and in Norwegian coastal waters (Larsen et al. 2004), could also explain our observations. Limitation by nutrients other than nitrogen, phosphate and silicate cannot be rejected, since, for example, iron has been shown to increase *Prochlorococcus* growth rates (Mann & Chisholm 2000), but appears to have no influence on those of *Synechococcus* or picophytoeukaryotes (Timmermans et al. 2005).

Negative relationships between all 4 picoplanktonic group abundances and salinity, such as the ones found here, have already been observed along a marked salinity gradient for salinities >23.5 (Joshem 2003). *Synechococcus* and picophytoeukaryotes correlations with the bacterioplankton abundance, which is known to covary with phytoplankton biomass, were expected, since all 3 groups tend to increase with nutrient supply (Gasol & Duarte 2000). Higher bacterioplankton abundance in the upwelling area off Chile compared with, for instance, the Mauritarian upwelling region (Zubkov et al. 2000) can be explained by the high productivity levels of the former region (Stuart et al. 2004).

HDNA bacterioplankton is thought to be related to the metabolically active part of the bacterial community (Gasol et al. 1999). However, Sherr et al. (2006) found that when phytoplankton biomass is low, HDNA bacterioplankton represented only a fraction of this active part. Considering the above, our results indicate then a lower limit for active bacterioplankton, averaging 50% (ranging from ~33 to 58%) of the total abundance, which is close to mean HDNA contributions registered elsewhere (Gasol et al. 1999). Although the spatial variability in percent HDNA (increasing from oligo- to eutrophic conditions and with depth) followed the same patterns observed in the North Atlantic, Mediterranean and Northeast Pacific Ocean (Li et al. 1995, Gasol et al. 1999, Sherr et al. 2006), the range of contribution to total bacterioplankton abundance in the eastern South Pacific was usually lower and their dominance was less evident.

Table 4. Mean (±SD) water-column-integrated (0 to 200 m) *Prochlorococcus*, *Synechococcus*, picophytoeukaryotes and bacterioplankton carbon biomass (mg m^{-2}) along latitude 32.5° S, between Easter Island and the coast of Chile. The transect range includes the minimum and maximum values found along the transect (when present in the case of *Prochlorococcus*)

Group	Oligotrophic	Mesotrophic	Eutrophic	Transect range
Prochlorococcus	402 ± 79	327 ± 240	0	28–645
Synechococcus	43 ± 13	121 ± 64	94 ± 23	21–228
Picophytoeukaryotes	617 ± 180	910 ± 311	861 ± 314	368–1657
Bacterioplankton	474 ± 53	781 ± 174	2481 ± 157	400–2592

Different light-adaptation capabilities allow *Prochlorococcus* and picophytoeukaryotes to distribute deeper than *Synechococcus* in the water column (e.g. Partensky et al. 1996, 1999). Increasing fluorescence signals with optical depth (Fig. 2b) may be attributed to: (1) an increase in the synthesis of chl *a* at lower light levels associated with photoacclimation processes or (2) the presence of different picophytoplanktonic ecotypes. The former has been observed in all 3 groups (e.g. Partensky et al. 1996), is usually less pronounced for picophytoeukaryotes than for cyanobacteria (e.g. Campbell & Vaulot 1993) and could be producing the DCM observed in the eastern mesotrophic region (Fig. 3c,e), although the presence of nanophytoplanktonic cells, not considered here, cannot be ruled out. A clear example of the latter is the presence of 2 *Prochlorococcus* populations observed here (Fig. 2a) and also described for other oligotrophic regions (Campbell & Vaulot 1993, Partensky et al. 1996, Zubkov et al. 2000). Using molecular probes, high-light- and low-light-adapted *Prochlorococcus* ecotypes were found to co-dominate in the surface waters of the South Pacific subtropical gyre (Bouman et al. 2006). However, because samples for the detection of ecotypes were collected only at the sea surface, we were unable to determine if the higher fluorescence below the mixed layer and euphotic depths was caused by a shift towards a dominance of low-light ecotypes. Although different *Synechococcus* (e.g. Rocap et al. 2002) and picophytoeukaryotes (e.g. Rodríguez et al. 2005) ecotypes have also been observed in natural samples, flow cytometry data alone do not allow us to identify them or determine their physiological or genetic microdiversity.

Higher chl *a* concentrations near the Chilean coast are mainly due to the presence of larger phytoplankton cells, such as diatoms, that dominate the phytoplanktonic community in upwelling systems (Stuart et al. 2004) and that are usually underestimated by flow cytometry (e.g. Shalapyonok et al. 2001). The positive relationship between chl *a* concentrations ≤ 0.2 mg m^{-3} and bacterial abundance would indicate a bottom-up control on this group in the oligo- and part of the mesotrophic regions, as inferred from macroecological patterns (Li et al. 2004). Towards the coast this relationship would be lost due to the presence of larger cells, or due to a stronger response from autotrophs than from heterotrophs to greater nutrient availability (Duarte et al. 2000a). This would also explain the relationship found with the total picoplanktonic carbon biomass.

In terms of carbon biomass, the picture is quite different from what has been observed in other oligo- and mesotrophic regions of the world's ocean during the same period of the year. The picophytoeukaryotes, instead of *Prochlorococcus* or *Synechococcus* (e.g. Partensky et al. 1996, Zubkov et al. 2000, see Table 1 for conversion factors), dominated the autotrophic biomass along the whole transect, their dominance in the upwelling region being expected (Worden et al. 2004, Sherr et al. 2005 and references therein). Picophytoeukaryotes also co-dominated the IPCB with bacterioplankton along most of the transect (Fig. 4). The latter differs from the results of Fuhrman et al. (1989) for the oligotrophic Sargasso Sea, where the microbial carbon biomass (i.e. bacterioplankton + auto- and heterotrophic nanoflagellates + cyanobacteria) was dominated by the bacterioplankton. Using lower *Prochlorococcus* or *Synechococcus* conversion factors would not modify our conclusions regarding the relative importance of bacterioplankton and picophytoeukaryotes carbon biomass. If, for example, the conversion factor for picophytoeukaryotes was changed to 750 fg C cell^{-1} (i.e. half of what we used), this group's mean contribution to IPCB in the oligo- and mesotrophic regions (~25 and 27%, respectively) would be lower than that of bacterioplankton (~39 and 48%, respectively), but only slightly below that of *Prochlorococcus* in the former (~33%) and higher in the later (~18%) region. Total picophytoplanktonic carbon biomass would still be higher than that of bacterioplankton under both oligotrophic (~61%) and (~52%) mesotrophic conditions. In the eutrophic zone picophytoeukaryotes would represent about one-sixth of the bacterioplankton carbon biomass, but would still be 5 times more important than that of *Synechococcus*. It is worth noting that if this lower conversion factor for picophytoeukaryotes was obtained through the relationship pg C = $0.433 \times$ (biovolume)$^{0.866}$ (Campbell et al. 1994 and references therein), their mean cell size would have to be of 1.54 µm, which is rather conservative. These considerations support a view of the importance of the picophytoeukaryotic carbon stock under the different trophic conditions encountered along the transect during spring time.

Under oligotrophic conditions, mean integrated carbon biomass proportions between *Prochlorococcus*, *Synechococcus*, picophytoeukaryotes and bacterioplankton were ~9:1:14:11, respectively. These proportions changed to ~3:1:8:6 and ~0:1:9:26 in the meso- and eutrophic regions, respectively. This gives bacterioplankton to picophytoplankton carbon biomass ratios of 0.46, 0.5 and 2.6 for the oligo-, meso- and eutrophic regions, respectively. Ratios <1 for bacterioplankton to phytoplankton integrated carbon biomass have been reported as a general feature for different ecological provinces in the North Atlantic Ocean (Li & Harrison 2001), with values ≥1 at low chl *a* concentrations, where picophytoplankton dominates. Considering the above, the higher ratios observed in the meso- and eutrophic regions of the South Pacific subtropical

gyre can then be attributed to the presence of phytoplanktonic cells >3 µm that we did not consider in our analyses. Low ratios, on the other hand, do not necessarily imply that autotrophs are dominant, since heterotrophic organisms other than bacterioplankton need to be taken into account. Indeed, Gasol et al. (1997) have shown that in open-ocean systems of low primary productivity, the ratio of total heterotrophic biomass (i.e. bacteria, protists and mesozooplankton) to total autotrophic biomass is very high. Because of the very oligotrophic conditions encountered in the eastern South Pacific, it is likely that eukaryotic heterotrophic organisms would significantly contribute to the total integrated heterotrophic biomass.

Carbon flow towards higher trophic levels would be more efficient and would tend to escape remineralisation when the picophytoeukaryotes dominate the picophytoplanktonic biomass. Until now, the scenario was that of an open ocean dominated by cyanobacteria, in which an extremely efficient microbial loop would remineralise most of the organic matter produced (Azam 1998). Although very little is known about picophytoeukaryotes, this group would be far more diverse than cyanobacteria (e.g. Moon-van der Staay et al. 2001), which could possibly explain their success in the open ocean. A shift in dominance from cyanobacteria to picophytoeukaryotes such as the one observed during early spring in the eastern South Pacific could imply a shift in the dominant biogeochemical pathways that directly affect carbon fate in the ocean. Despite the fact that our results represent only a snap shot of the situation in the eastern South Pacific, they highlight the importance of the picophytoeukaryotes carbon biomass under trophic conditions where cyanobacteria were expected to dominate all year (e.g. Partensky et al. 1996, Zubkov et al. 2000). Because of their potential influence on the carbon flow, the importance of this group at the annual scale could be significant, even if the observed situation was to be true only for the relatively short sampling period.

In the oligo- and mesotrophic regions of the eastern South Pacific, we have found the carbon biomass of picophytoplankton to be higher than that of bacterioplankton during spring time. However, it will require studies of metabolic processes to place this finding in the perspective of global biogeochemical cycles, especially regarding carbon cycling, and in the global climate system. Production (i.e. primary and secondary) and loss rate (e.g. grazing and virus lysis) measurements, as well as genetic assays and temporal surveys need to be incorporated into a more comprehensive study. The eastern South Pacific Ocean deserves further attention, and the extremely oligotrophic centre of this subtropical gyre (~0.01 mg m^{-3}; Claustre & Maritorena 2003) needs to be included in future studies of global processes.

Acknowledgements. We thank the captain and crew of the RV 'Mirai' and 'Michio Oayama' (GRD/MRI) for the nutrient data. Data collection was facilitated by scholarships provided by POGO and IOCCG and IOC to participants from Chile, Peru and Turkey on Leg 2 of the BEAGLE Expedition. We are also grateful to V. Molina, H. Bouman, G. Yuras, R. Wiff, L. A. Cuevas, V. Stuart, S. Sathyendranath and T. Platt for help and support. This work was funded by the Chilean National Commission for Scientific and Technological Research (CONICYT) through the Funds for Advanced Research in Priority Areas (FONDAP) Programme. Additional support was provided by Fundación Andes and the Japan Agency for Marine–Earth Science and Technology. C.G. was supported by a CONICYT graduate fellowship.

LITERATURE CITED

Antoine D, André JM, Morel A (1996) Oceanic primary production. II. Estimation at global scale from satellite (Coastal Zone Color Scanner) chlorophyll. Global Biogeochem Cycles 10:57–69

Azam F (1998) Microbial control of oceanic carbon flux: the plot thickens. Science 280:694–696

Bertilsson S, Berglund O, Karl DM, Chisholm SW (2003) Elemental composition of marine *Prochlorococcus* and *Synechococcus*: implications for the ecological stoichiometry of the sea. Limnol Oceanogr 48:1721–1731

Bouman HA, Ulloa O, Scanlan D, Zwirglmaier K and 10 others (2006) Oceanographic basis of the global surface distribution of *Prochlorococcus* ecotypes. Science 312: 918–921

Campbell L, Vaulot D (1993) Photosynthetic picoplankton community structure in the subtropical North Pacific Ocean near Hawaii (Station ALOHA). Deep-Sea Res I 40: 2043–2060

Campbell L, Nolla HA, Vaulot D (1994) The importance of *Prochlorococcus* to community structure in the central North Pacific Ocean. Limnol Oceanogr 39:954–961

Chisholm SW, Olson RJ, Zettler ER, Goericke R, Waterbury JB, Welschmeyer NA (1988) A novel free-living prochlorophyte occurs at high cell concentrations in the oceanic euphotic zone. Nature 334:340–343

Claustre H, Maritorena S (2003) The many shades of ocean blue. Science 302:1514–1515

Duarte CM, Agustí S, Gasol JM, Vaqué D, Vazquez-Dominguez E (2000a) Effect of nutrient supply on the biomass structure of planktonic communities: an experimental test on a Mediterranean coastal community. Mar Ecol Prog Ser 206:87–95

Duarte CM, Agustí S, Agawin NSR (2000b) Response of a Mediterranean phytoplankton community to increased nutrient inputs: a mesocosm experiment. Mar Ecol Prog Ser 195:61–70

Fuhrman JA, Sleeter TD, Carlson CA, Proctor LM (1989) Dominance of bacterial biomass in the Sargasso Sea and its ecological implications. Mar Ecol Prog Ser 57:207–217

Fukuda R, Ogawa H, Nagata T, Koike I (1998) Direct determination of carbon and nitrogen contents of natural bacterial assemblages in marine environments. Appl Environ Microb 64:3352–3358

Gasol JM, Duarte CM (2000) Comparative analyses in aquatic microbial ecology: How far do they go? FEMS Microbiol Ecol 31:99–106

Gasol JM, del Giorgio PA, Duarte CM (1997) Biomass distribution in marine planktonic communities. Limnol Oceanogr 42:1353–1363

Gasol JM, Zweifel UL, Peters F, Fuhrman JA, Hagström A (1999) Significance of size and nucleic acid content heterogeneity as measured by flow cytometry in natural planktonic bacteria. Appl Environ Microb 65:4475–4483

Giovannoni S, Rappé M (2000) Evolution, diversity, and molecular ecology of marine prokaryotes. In: Kirchman DL (ed) Microbial ecology of the oceans. Wiley-Liss, New York, p 47–84

Joshem FJ (2003) Photo- and heterotrophic pico- and nanoplankton in the Mississippi River plume: distribution and grazing activity. J Plankton Res 25:1201–1214

Kirk J (1994) Light and photosynthesis in aquatic ecosystems, 2nd edn. Cambridge University Press, New York

Larsen A, Flaten GAF, Sandaa RA, Castberg T, Thyrhaug R, Erga SR, Jacquet S, Bratbak G (2004) Spring phytoplankton bloom dynamics in Norwegian coastal waters: microbial community succession and diversity. Limnol Oceanogr 49:180–190

Li WKW, Harrison WG (2001) Chlorophyll, bacteria and picophytoplankton in ecological provinces of the North Atlantic. Deep-Sea Res II 48:2271–2293

Li WKW, Jellett JF, Dickie PM (1995) DNA distributions in planktonic bacteria stained with TOTO or TO-PRO. Limnol Oceanogr 40:1485–1495

Li WKW, Head EJH, Harrison WG (2004) Macroecological limits of heterotrophic bacterial abundance in the ocean. Deep-Sea Res I 51:1529–1540

Mann EL, Chisholm SW (2000) Iron limits the cell division rate of *Prochlorococcus* in the eastern equatorial Pacific. Limnol Oceanogr 45:1067–1076

Marie D, Partensky F, Simon N, Guillou L, Vaulot D (2000a) Flow cytometry analysis of marine picoplankton. In: Diamond RA, DeMaggio S (eds) In living colors: protocols in flow cytometry and cell sorting. Springer-Verlag, New York, p 421–454

Marie D, Simon N, Guillou L, Partensky F, Vaulot D (2000b) DNA, RNA analysis of phytoplankton by flow cytometry. In: Robinson JP, Darzynkiewicz Z, Dean PN, Orfao A, Rabinovitch PS, Stewart CC, Tanke HJ, Wheeless LL (eds) Current protocols in cytometry, Suppl 11, Unit 11.12. John Wiley & Sons, New York, p 1–16

Moon-van der Staay SY, Wachter RD, Vaulot D (2001) Oceanic 18S rDNA sequences from picoplankton reveal unsuspected eukaryotic diversity. Nature 409:607–610

Morel A, Berthon JF (1989) Surface pigments, algal biomass profiles, and potential production of the euphotic layer: relationships reinvestigated in view of remote-sensing applications. Limnol Oceanogr 34:1545–1562

Partensky F, Blanchot J, Lantoine F, Neveux J, Marie D (1996) Vertical structure of picophytoplankton at different trophic sites of tropical northeastern Atlantic Ocean. Deep-Sea Res I 43:1191–1213

Partensky F, Blanchot J, Vaulot D (1999) Differential distribution and ecology of *Prochlorococcus* and *Synechococcus* in oceanic waters: a review. Bull Inst Oceanogr Monaco 19:457–475

Rocap G, Distel DL, Waterbury JB, Chisholm SW (2002) Resolution of *Prochlorococcus* and *Synechococcus* ecotypes by using 16S–23S ribosomal DNA internal transcribed spacer sequences. Appl Environ Microb 68:1180–1191

Rodríguez F, Derelle E, Guillou L, Gall FL, Vaulot D, Moreau H (2005) Ecotype diversity in the marine picoeukaryote *Ostreococcus* (Chlorophyta, Prasinophyceae). Environ Microbiol 7:853–859

Shalapyonok A, Olson RJ, Shalapyonok LS (2001) Arabian Sea phytoplankton during southwest and northeast monsoons 1995: composition, size structure and biomass from individual cell properties measured by flow cytometry. Deep-Sea Res II 48:1231–1261

Sherr EB, Sherr BF, Wheeler PA (2005) Distribution of coccoid cyanobacteria and small eukaryotic phytoplankton in the upwelling ecosystem off the Oregon coast during 2001 and 2002. Deep-Sea Res II 52:317–330

Sherr EB, Sherr BF, Longnecker K (2006) Distribution of bacterial abundance and cell-specific nucleic acid content in the Northeast Pacific Ocean. Deep-Sea Res I 53:713–725

Stockner JG (1988) Phototrophic picoplankton: an overview from marine and freshwater ecosystems. Limnol Oceanogr 33:765–775

Stuart V, Ulloa O, Alarcón G, Sathyendranath S, Major H, Head EJH, Platt T (2004) Bio-optical characteristics of phytoplankton populations in the upwelling system off the coast of Chile. Rev Chil Hist Nat 77:87–105

Timmermans KR, van der Wagt B, Veldhuis MJW, Maatman A, de Baar HJW (2005) Physiological responses of three species of marine pico-phytoplankton to ammonium, phosphate, iron and light limitation. J Sea Res 53:109–120

Troncoso VA, Daneri G, Cuevas LA, Jacob B, Montero P (2003) Bacterial carbon flow in the Humboldt Current System off Chile. Mar Ecol Prog Ser 250:1–12

Uchida H, Fukasawa M (2005) WHP P6, A10, I3/I4 Revisited data book, Blue Earth Global Expedition 2003 (BEAGLE 2003) Vols 1 and 2. JAMSTEC, Yokosuka, Kanagawa

Waterbury JB, Watson SW, Guillard RRL, Brand LE (1979) Widespread occurrence of a unicellular, marine planktonic, cyanobacterium. Nature 277:293–294

Worden AZ, Nolan JK, Palenik B (2004) Assessing the dynamics and ecology of marine picophytoplankton: the importance of the eukaryotic component. Limnol Oceanogr 49: 168–179

Zubkov MV, Sleigh MA, Burkill PH, Leakey RJG (2000) Picoplankton community structure on the Atlantic Meridional Transect: a comparison between seasons. Prog Oceanogr 45:369–386

Editorial responsibility: Otto Kinne (Editor-in-Chief), Oldendorf/Luhe, Germany

Submitted: November 3, 2005; Accepted: July 24, 2006
Proofs received from author(s): February 20, 2007

CHAPTER 4

CONTRIBUTION OF PICOPLANKTON TO THE TOTAL PARTICULATE ORGANIC CARBON (POC) CONCENTRATION IN THE EASTERN SOUTH PACIFIC

4. CONTRIBUTION OF PICOPLANKTON TO THE TOTAL PARTICULATE ORGANIC CARBON (POC) CONCENTRATION IN THE EASTERN SOUTH PACIFIC

Resumen. Las abundancias y contribuciones de *Prochlorococcus*, *Synechococcus*, picofitoeucariontes y bacterioplancton al coeficiente de atenuación debido a partículas (c_p) y a la concentración de carbono orgánico particulado (COP) fueron determinadas en el Pacífico Sur-este entre las Islas Marquesas y la costa de Chile. Todas las abundancias determinadas mediante citometría de flujo disminuyeron hacia el centro hyper-oligotrófico del giro y fueron máximas cerca de la costa, salvo *Prochlorococcus* que no fue detectado bajo condiciones eutróficas. Tanto la temperatura como la disponibilidad de nutrientes parecieran ser moduladores importantes de la abundancia del picofitoplancton, de acuerdo con las condiciones tróficas predominantes. Si bien las partículas no-algales tienden a dominar la señal de c_p a lo largo de toda la transecta (50 a 83%), esta dominancia parece debilitarse entre condiciones oligo- y eutróficas, siendo las contribuciones por parte de partículas vegetales y no-vegetales similares en condiciones de surgencia madura. La variabilidad espacial del compartimiento vegetal fue más importante que aquella del no-vegetal en determinar el coeficiente de atenuación debido a partículas en la columna de agua. Se observó una correlación significativa entre la variabilidad espacial de la biomasa picofitoplanctónica y aquella de la concentración total de clorofila *a*, por un lado, y la de c_p, por otro. Finalmente, a lo largo de la transecta los picofitoeucariontes constituyeron ~38% de la biomasa fotosintética y coeficiente de atenuación vegetal integrados en la columna de agua, como pudo ser determinado utilizando medidas directas del tamaño de células aisladas por citometría de flujo y teoría óptica. Por lo tanto, el rol de los picofitoeucariontes en el flujo de energía y carbono sería muy importante, incluso bajo condiciones hyper-oligotróficas.

Résumé. Les abondances de *Prochlorococcus*, *Synechococcus*, picophytoeucaryotes et bacterioplancton et la contribution de ces organismes au coefficient d'atténuation particulaire (c_p) et à la concentration de carbone organique particulaire (POC) ont été déterminés à travers le secteur este du Pacifique du Sud, entre les Iles Marquises et la côte du Chili. Toutes les abondances déterminées par cytométrie en flux diminuent vers le centre hyper-oligotrophique du gyre et sont maximales sur la côte, sauf pour *Prochlorococcus* qui n'est pas détecté en conditions eutrophes. La température et la disponibilité en sels nutritifs semblent être d'importants modulateurs de l'abondance picophytoplanctonique, en relation avec les conditions trophiques prédominantes. Bien que les particules non-algales dominent le signal de c_p tout le long du transect (50 à 83%), cette dominance décroît depuis les conditions oligotrophes vers les conditions eutrophes, les contributions algale et non-algale sont semblables en conditions d'upwelling mature. La variabilité spatiale du compartiment végétale est plus importante que celle du non-végétale et détermine ainsi la valeur de c_p dans la colonne d'eau. Le long du transect, la biomasse picophytoplanctonique était significativement corrélée à la concentration totale de chlorophylle *a*, d'un côté, et à c_p, de l'autre. Finalement, le long du transect les picophytoeucaryotes contribuent pour ~38% en moyenne à la biomasse phytoplanctonique en carbone et au signal d'atténuation intégrées. Le rôle des picophytoeucaryotes dans le flux d'énergie et de carbone pourrait donc être important, y compris en conditions hyper-oligotrophes.

“Contribution of picoplankton to the total particulate organic carbon (POC) concentration in the eastern South Pacific”

Carolina Grob[1,2,3*], Osvaldo Ulloa[2], Hervé Claustre[3], Yannick Huot[3], Gadiel Alarcón[2], Dominique Marie[4]

[1]Graduate Programme in Oceanography
[2]Department of Oceanography and Center for Oceanographic Research in the eastern South Pacific,
University of Concepción, Casilla 160-C, Concepción, Chile
[3]CNRS, Laboratoire d'océanographie de Villefranche, 06230 Villefranche-sur-Mer, France ; Université Pierre et Marie Curie-Paris 6, Laboratoire d'océanographie de Villefranche, 06230 Villefranche-sur-Mer, France
[4]Station Biologique, CNRS, INSU et Université Pierre et Marie Curie,
F-29482 Roscoff Ceder, France

*corresponding author: mgrob@profc.udec.cl

Abstract

Prochlorococcus, *Synechococcus*, picophytoeukaryotes and bacterioplankton abundances and contributions to the total particulate organic carbon concentration (POC), derived from the total particle beam attenuation coefficient (c_p), were determined across the eastern South Pacific between the Marquesas Islands and the coast of Chile. All flow cytometrically derived abundances decreased towards the hyper-oligotrophic centre of the gyre and were highest at the coast, except for *Prochlorococcus*, which is not detected under eutrophic conditions. Temperature and nutrient availability appeared important in modulating picophytoplankton abundance, according to the prevailing trophic conditions. Although the non-vegetal particles tended to dominate the c_p signal everywhere along the transect (50 to 83%), this dominance seemed to weaken from oligo- to eutrophic conditions, the contributions by vegetal and non-vegetal particles being about equal under mature upwelling conditions. Spatial variability in the vegetal compartment was more important than the non-vegetal one in shaping the water column particulate attenuation coefficient. Spatial variability in picophytoplankton biomass could be traced by changes in both total chlorophyll *a* (Tchl*a*, i.e., mono + divinyl chlorophyll *a*) concentration and c_p. Finally, picophytoeukaryotes contributed ~38% on average to the total integrated phytoplankton carbon biomass or vegetal attenuation signal along the transect, as determined by direct size measurements on cells sorted by flow cytometry and optical theory. Although there are some uncertainties associated with these estimates, the new approach used in this paper lend further support to picophytoeukaryotes playing a dominant role in carbon cycling in the surface ocean, even under hyper-oligotrophic conditions.

1 Introduction

Global estimates indicate that about half of the earth's primary production (PP) takes place in the ocean (Field et al., 1998). Of a mean global marine PP of 50.7 Gt C y^{-1} estimated through ocean-colour-based models (Carr et al., 2006), 86% would occur in the open ocean (Chen et al., 2003), where the photosynthetic biomass is dominated by three main picophytoplanktonic (<2-3 μm) groups (e.g., Li, 1995): cyanobacteria of the genera *Prochlorococcus* (Chisholm et al., 1988) and *Synechococcus* (Waterbury et al., 1979), and eukaryotes belonging to diverse taxa (Moon-van der Staay et al., 2001).

Although cyanobacteria, especially *Prochlorococcus* (Li & Wood, 1988; Chisholm et al., 1988), tend to dominate in terms of numerical abundance, it has been shown that eukaryotic phytoplankton (usually <3.4 μm) dominates the ultraplankton (<5 μm) photosynthetic biomass in the northern Sargasso Sea (Li et al., 1992) and in the eastern Mediterranean Sea (Li et al., 1993). Across the North and South Atlantic Subtropical Gyres (Zubkov et al., 1998 & 2000) and eastern South Pacific (Grob et al., 2007) picophytoeukaryotes also constituted a considerable fraction of the picophytoplanktonic carbon biomass.

Using flow cytometry cell sorting combined with ^{14}C measurements, Li (1994) made the only simultaneous group-specific primary production rates measurements available in the literature for *Prochlorococcus*, *Synechococcus* and picophytoeukaryotes. Even though he could only apply this methodology at 3 different stations in the North Atlantic Ocean and at a single depth per station, this author's results showed that picophytoeukaryotes contribution to picophytoplankton primary production increased as the *Prochlorococcus* to picophytoeukrayotes abundances ratio decreased. At a coastal Pacific site in the Southern California Bight, on the other hand, Worden et al. (2004) reported that picophytoeukaryotes had the highest picophytoplankton growth rates and contributions to the net community production and carbon biomass on annual bases.

Picophytoeukaryotes can therefore make a significant contribution to the picophytoplanktonic PP and carbon biomass (see above). Carbon being the universal currency in marine ecological modelling, looking inside the pico-autotrophic "black box" to determine the distribution of carbon biomass among the different groups becomes fundamental to better understand the respective role of these groups in the

global carbon cycle. Recent biogeochemical models have made a significant step forward on this subject by incorporating not only different plankton functional types, but also different groups within these functional types (e.g., cyanobacteria, picophytoeukaryotes, nitrogen fixers) in order to reproduce some of the ecosystem's variability (e.g., Bisset et al., 1999; Le Quéré et al., 2005). Different picophytoplanktonic groups have different physiological characteristics such as optimal specific rates of photosynthesis, adaptation to light, photosynthetic efficiencies and maximum specific growth rates (Veldhuis et al., 2005 and references therein). Knowing where one group dominates over the others could therefore help choosing the appropriate physiological parameters to estimate PP from surface chlorophyll *a* concentrations retrieved from space and improve such estimates at the large scale.

The measurement of the particulate attenuation coefficient (c_p) has proven to be a very powerful tool in determining particle load and particulate organic carbon (POC) concentrations at the global (e.g., Gardner, 2006) as well as the regional scale (e.g., Claustre et al., 1999; Oubelkheir et al., 2005). High frequency measurements of c_p signal can also be used to derive rates of change in particulate organic stocks like gross and net community production (Claustre et al., submitted). In situ c_p profiles associated with the simultaneous cytometric determination of the different phytoplanktonic groups and bacterioplankton (Bacteria + Archaea) abundances have the potential to allow the estimation of the contribution of these groups to the bulk c_p, and hence to POC. Group-specific contributions to POC can therefore be estimated from their contributions to c_p. In the equatorial Pacific, for instance, picophytoeukaryotic cells would dominate the vegetal contribution to c_p (Chung et al., 1996; DuRand and Olson, 1996; Claustre et al, 1999). These estimations require however that the mean cell size and refractive index of each group are known or at least assumed (Claustre et al., 1999 and references therein). Total and group-specific beam attenuation coefficients can be obtained at relatively short time scales, but also have the advantage of being amenable to large scale in situ surveys on carbon stocks and cycling, and even to global estimation, since bulk oceanic bio-optical properties can be retrieved from space (e.g., Gardner, 2006).

In the present work we tried to answer the following questions: (1) what is the contribution of the different picoplanktonic groups to POC in the upper ocean? and (2) how does the spatial variability in these group's contributions influence the spatial changes in POC in the upper ocean? For this, we studied the waters of the eastern South Pacific, which present an extreme gradient in trophic conditions: from the hyper-

oligotrophic waters of the central gyre to the eutrophic coastal upwelling waters off South America. Using flow cytometry cell sorting we were able to isolate different picophytoplankton populations in situ to obtain their mean cell sizes, which allowed us to improve estimations on the group-specific attenuation coefficients, and therefore on group-specific contributions to POC.

2 Methods

A total of 24 stations were sampled between the Marquesas Islands (~ 8.4ºS; 141.2ºW) and the coast of Chile (~ 34.6ºS; 72.4ºW) during the French expedition BIOSOPE (BIogeochemistry and Optics SOuth Pacific Experiment) in austral spring time (October 26th to December 11th, 2004) (). Temperature, salinity and oxygen profiles were obtained with a conductivity-temperature-depth-oxygen profiler (CTDO, Seabird 911 Plus). Nutrient concentrations (nitrate, nitrite, ammonium, phosphate and silicate) were determined onboard (see Raimbault et al., this issue). Pigment concentrations from noon profiles (local time) were determined using High Performance Liquid Chromatography (HPLC). For HPLC analyses, water samples were vacuum filtered through 25 mm diameter and 0.7 μm porosity Whatman GF/F glass fibre filters (see Ras et al., this issue), where on average 97% of *Prochlorococcus* cells are retained (Chavez et al., 1995). The above implies a maximum error of 3% on the total divinyl-chlorophyll *a* concentrations (dv-chl*a*, pigment that is specific only to this group) determined using this technique. Daily integrated surface total irradiance was determined from on-board calibrated measurements.

All stations reported here were sampled at local noon time at 6 to 14 different depths from the surface down to 300 m (). The position of the deepest sampling depth was established relative to the position of the bottom of the photic layer, Ze (m) defined as the depth where the irradiance is reduced to 1% of its surface value. Five stations of very different trophic conditions, here referred to as long stations, were also sampled at high frequency (i.e., every 3 hours) during 2 to 4 days: (1) mesotrophic (MAR, Marquesas Islands), (2) high nutrient-low chlorophyll (HNL, ~ 9.0ºS and 136.9ºW), (3) hyper-oligotrophic (GYR, ~ 26.0ºS and 114.0ºW), (4) oligotrophic (EGY, ~ 31.8ºS and 91.5ºW) and (5) eutrophic (UPW, highly productive upwelling region, ~ 34.0ºS and 73.3ºW) (). The coastal-most station (UPX) was additionally sampled to compare it with UPW's upwelling condition ().

Our results are presented in terms of oligo-, meso- and eutrophic conditions according to surface total chlorophyll *a* concentrations (Tchl*a*, chlorophyll *a* + divinyl chlorophyll *a*) of ≤ 0.1, > 0.1 and ≤1, and >1 mg m^{-3}, respectively (Antoine et al., 1996). This division has been used to characterize the trophic status of the ocean from space and we consider it as appropriate to describe the large spatial patterns investigated during the BIOSOPE cruise.

2.1 Picoplankton analyses

Prochlorococcus, *Synechococcus* and picophytoeukaryotes abundances were determined on fresh samples on-board with a FACSCalibur (Becton Dickinson) flow cytometer. For bacterioplankton counts (Bacteria + Archaea), samples fixed either with paraformaldehyde at 1% or glutaraldehyde at 0.1% final concentration and quick-frozen in liquid nitrogen were stained with SYBR-Green I (Molecular Probes) and run in the same cytometer within two months after the end of the cruise. Reference beads (Fluoresbrite YG Microspheres, calibration grade 1.00 µm, Polysciences, Inc) were added to each sample before acquiring the data with the Cell Quest Pro software (Becton Dickinson) in logarithmic mode (256 channels). During data acquisition, between 5 x 10^3 and 300 x 10^3 events were registered in order to count at least 500 cells for each picoplanktonic group. The error associated with abundances determined using flow cytometry is ≤ 5% (D. Marie, *pers. comm.*). The data were then analysed with the Cytowin software (Vaulot 1989) to separate the picoplanktonic populations based on their scattering and fluorescence signals, according to Marie et al. (2000) (see Supp. Mat.).

Surface *Prochlorococcus* abundance for weakly fluorescent populations (i.e, ~7% of total samples) was estimated by fitting a Gaussian curve to the data using Cytowin. When their fluorescence was too dim to fit the curve (e.g. surface and sub-surface samples at the center of the gyre) their abundance was estimated from dv-chl*a* concentrations by assuming an intracellular pigment content of 0.23 fg $cell^{-1}$ (see Supp. Mat.). This intracellular dv-chl*a* content corresponds to the mean value obtained for cells in the surface layer (above ~5% of surface light) by dividing the HPLC-determined dv-chl*a* by the cell number estimated from flow cytometry, considering all but the MAR data (). At the GYR station, *Synechococcus* and picophytoeukaryotes abundances above 100 m were only available for the first morning profile (samples taken above 90 m for the other GYR profiles are unfortunately not available). This profile showed that both

groups' abundances were homogeneous over the first 100 m, so we assumed the abundances measured at 90 - 100 m to be representative of the abundances within the 0-100 m layer. All picoplankton abundances were then integrated from the surface to 1.5 Ze rather than to Ze, because deep chlorophyll maxima (DCM) were observed between these two depths at the center of the gyre.

In order to establish a relationship between actual sizes (i.e., mean cell sizes actually measured) and the mean forward scatter cytometric signal normalized to the reference beads (FSC in relative units, r.u.; see Supp. Mat.), in situ *Prochlorococcus*, *Synechococcus* and picophytoeukaryotes populations were sorted separately on board with a FACS Aria flow cytometer (Becton Dickinson). Each sorted population was then analysed with a Multisizer 3 Coulter Counter (Beckman Coulter) for size (µm) and with the FACS Calibur flow cytometer for FSC. Several *Synechococcus* and picophytoeukaryotes populations isolated in situ could be measured with the Coulter Counter. *Prochlorococcus* size, on the other hand, could only be determined for one population because they were at the detection limit of the instrument. A similar analysis was performed on monospecific cultures of various picophytoplankton species (without pre-sorting) to combine both in situ and laboratory measurements to establish a log-log polynomial relationship between FSC and size (a). We believe that even though the left-most end of the fitted curve is driven by a sole data point, it is still very useful to the relationship because it represents the actual mean cell size of a natural *Prochlorococcus* population (i.e., 0.59 µm), corresponding to a mean FSC of 0.02 r.u.. Based on this relationship established within the picophytoplankton size range we calculated the upper size limit for the FSC settings we used during the whole cruise at 3 µm (i.e., FSC = 0.88 r.u.).

Also using culture cells, we established a direct relationship between the mean cytometric FSC signal and intracellular carbon content to estimate *Synechococcus* and picophytoeukaryotes carbon biomass (b). To obtain intracellular carbon contents, a known volume of each culture population was filtered onto GF/F filters previously precombusted at 400ºC, in triplicate. One blank filter per culture was put aside to be used as controls. The number of phytoplankton and contaminating bacterioplankton cells retained in and passing through the filters were determined using flow cytometry (see Supp. Mat.). The filters were then dried at 60ºC for 24hrs, fumigated with concentrated chlorhydric acid for 6 to 8hrs to remove inorganic carbon and dried again for 6 to 8hrs. Each filter was finally put in a tin capsule and analysed with a Carbon-

Hydrogen-Nitrogen (CHN) autoanalyzer (Thermo Finnigan, Flash EA 1112) (see Supp. Mat). Carbon contents were estimated based on a calibration curve performed using Acetanilide.

Considering both size and carbon content derived from FSC, a conversion factor (in fgC μm^{-3}) was established for *Synechococcus* and then applied to the mean cell size estimated for *Prochlorococcus* to obtain the intracellular carbon content of that group. Picophytoplankton carbon biomass was then calculated by multiplying cell abundance and intracellular carbon content for each group.

2.2 Beam attenuation coefficients specific for each picoplankton group

Profiles of the total particle beam attenuation coefficient at 660 (c_p, m^{-1}), a proxy for POC (e.g. Claustre et al., 1999), were obtained with a C-Star transmissometer (Wet Labs, Inc.) attached to the CTD rosette. Procedures for data treatment and validation have been described elsewhere (Loisel and Morel, 1998; Claustre et al., 1999). Inherent optical properties of sea water (IOP's), such as c_p, depend exclusively on the medium and the different substances in it (Preisendorfer, 1961). The vegetal (c_{veg}) and non-vegetal (c_{nveg}) contribution (Eq. 1) to the particulate attenuation coefficient can therefore be expressed as

$$c_P = c_{veg} + c_{nveg} \quad (1)$$

whereas the *Prochlorococcus* (c_{proc}), *Synechococcus* (c_{syn}), picophytoeukaryotes (c_{euk}) and larger phytoplankton (>3 µm, c_{large}) contribution to the vegetal signal (Eq. 2) can be described by,

$$c_{veg} = c_{proc} + c_{syn} + c_{euk} + c_{large} \quad (2)$$

Bacterioplankton (c_{bact}), heterotrophs (c_{het}) and detritus (c_{det} = non living particles) contribute to the non-vegetal component (Eq. 3) as follows,

$$c_{nveg} = c_p - c_{veg} = c_{bact} + c_{het} + c_{det} = c_{bact} + 2c_{bact} + c_{det} = 3c_{bact} + c_{det} \quad (3)$$

where c_{het} is assumed to be approximately $2c_{bact}$ (Morel and Ahn, 1991). This assumption was adopted in order to be able to roughly estimate the fraction of total particulate organic carbon corresponding to detritus, which is the group of particles contributing to c_p that is not directly measured, i.e., the unaccounted c_p (see below; Eq. 4).

Since particulate absorption is negligible at 660 nm (Loisel and Morel, 1998), beam attenuation and scattering are equivalent, so we can estimate c_{proc}, c_{syn}, c_{euk}, c_{large} and c_{bact} by determining the group-specific scattering coefficients b_i (m^{-1}) = N_i [s_i Q_{bi}], where i = proc, syn, euk, large or bact. We used flow cytometry to retrieve both picophytoplankton cell abundance (N_i, cells m^{-3}) and mean cell sizes (through FSC, see Section 2.1). Mean geometrical cross sections (s, m^2 $cell^{-1}$) were calculated from size, while Q_{bi} (660), the optical efficiency factors (dimensionless), were computed through the anomalous diffraction approximation (Van de Hulst, 1957) assuming a refractive index of 1.05 for all groups (Claustre et al., 1999). For *Prochlorococcus* and *Synechococcus* we used mean sizes obtained from a few samples, whereas for the picophytoeukaryotes we used the mean cell size estimated for each sample (see Supp. Mat.). For samples where picophytoeukaryotes abundance was too low to determine their size we used the nearest sample value, i.e, the mean cell size estimated for the sample taken immediately above or below the missing one. This approximation was applied to ~26% of the samples and although it may seem a large fraction, it corresponds mostly to deep samples where cell abundance was very low. Low cell abundances will result in low biomasses and it is therefore unlikely that the error associated with this approximation will introduce important errors in the carbon biomass estimates. For bacterioplankton we used a value of 0.5 µm, as used by Claustre et al. (1999). Finally, once c_{veg}, c_{bact} and therefore c_{het} are determined, c_{det} is obtained directly by difference (Eq. 4).

$$c_{det} = c_{nveg} - c_{bact} - c_{het} = c_{nveg} - c_{bact} - 2c_{bact} = c_{nveg} - 3c_{bact} \quad (4)$$

Contributions to c_p by larger phytoplanktonic cells in the western and eastern part of the transect were estimated by assuming that peaks larger than 3 µm in the particle size distribution data obtained either with the Coulter Counter or with a HIAC optical counter (Royco; Pacific Scientific) corresponded to autotrophic organisms (see Supp. Mat.). Coulter Counter data were only available for 1 (surface samples, ≤5 m) to 3 different depths. Thus, in order to obtain water column profiles for MAR, HNL, EGY and UPW, the estimated c_{large} were extrapolated by assuming c_{large} = 0 at the depth where no peak >3µm was detected (usually below 50 m). When only surface data were available, c_{large} was assumed to be negligible at the depth where chlorophyll fluorescence became lower than the surface one. Group-specific attenuation signals were integrated from the surface down to 1.5 Ze (water column, $c_{0\ to\ 1.5\ Ze}$) and from the surface to 50 m (surface layer, $c_{0\ to\ 50\ m}$) to estimate their contribution to integrated c_p.

Finally, $c_p(660)$ was converted to particulate organic carbon (POC) by using the empirical relationship established by Claustre et al. (1999) for the tropical Pacific (Eq. 5), which has proven to be valid as part of BIOSOPE (see Stramski et al., this issue).

$$\text{POC (mg m}^{-3}) = c_p(\text{m}^{-1}) \times 500 \text{ (mg m}^{-2}) \quad (5)$$

Through the above relationship c_p explains ~92% of the variance in POC concentration (Claustre et al., 1999). To evaluate the ability of Tchl*a* and c_p to trace spatial changes in picophytoplankton biomass along the transect we used local noon time data within the integration depth (0 to 1.5 Ze) from the stations where no large phytoplankton cells were detected with the particle counters (Coulter or HIAC), i.e., stations 3 to 15 + GYR. We chose these stations because we do not have intracellular carbon content data for larger cells to include in the photosynthetic carbon biomass estimates.

3 Results

The sampled transect included South Pacific Tropical Waters (SPTW), with a clear salinity maximum extending from the surface down to 150 m between HNL and GYR, Eastern South Pacific Central Waters (ESPCW) characterized by salinities of 34.5 to 36 (a) and temperatures of 15 to 20ºC at the centre of the gyre (GYR to EGY) and colder and fresher waters at the Chilean coast (Claustre et al., this issue). Limits between oligo-, meso- and eutrophic conditions were set at 133, 89 and 74.5 ºW according to the measured surface chlorophyll *a* concentrations, as explained above. Under oligotrophic conditions nitrate concentrations were close to 0 µM or undetectable between the surface and 150-200 m, and still very low (~2.5 µM) between the latter depth and 1.5 Ze (b). Expectedly, nutrient concentrations were higher under mesotrophic conditions and highest near the coast (see Raimbault et al., this issue), whereas phosphate was never a limiting factor (Moutin et al., this issue).

The hyper-oligotrophic centre of the South Pacific Subtropical Gyre (SPSG), i.e., the clearest waters of the world's ocean (Morel et al., 2007), was characterized by extremely low surface Tchl*a* concentrations (<0.03 mg m^{-3}; see Ras et al., this issue) and undetectable nutrient levels (see Raimbault et al., this issue), greatly differing from the Marquesas Islands' mesotrophic conditions and the typical High Nutrient – Low Chlorophyll situation (i.e., HNL) encountered at the borders of the gyre, and the upwelling conditions observed at the coast.

3.1 Picoplankton numerical abundance

All groups' abundances tended to decrease towards the centre of the gyre. *Prochlorococcus* was highest at the western (up to 300 x 10^3 cells ml^{-1} around 50 m, associated with SPTW) and eastern (up to 200 x 10^3 cells ml^{-1} in the 50 to 100 m layer) borders of the oligotrophic region (e). Peaks in *Synechococcus* (up to 190 x 10^3 cells ml^{-1}; f), picophytoeukaryotes (10-70 x 10^3 cells ml^{-1}; g) and bacterioplankton abundances (up to 2 x 10^6 cells ml^{-1}; h) were registered near the coast. Deep *Prochlorococcus* (100-150 x 10^3 cells ml^{-1} between 50 and 200 m; e) and picophytoeukaryotes (~2 x 10^3 cells ml^{-1} between 150 and 200 m; g) maxima were recorded at the centre of the gyre following the pattern of Tchl*a* concentrations (~0.15 mg m^{-3}; d), above the deep chlorophyll maximum (DCM) for the former and within the DCM depth range for the latter (e and g). *Synechococcus* reached lower depth ranges than the rest of the groups everywhere along the transect (f). In terms of chlorophyll biomass, the importance of the DCM at the centre of the gyre is highlighted when comparing the surface-to-DCM average ratios for the different long stations: 0.67 ± 0.13 at MAR, 0.44 ± 0.04 at HNL, 0.12 ± 0.02 at GYR and 0.27 ± 0.02 at EGY.

Water column integrated picoplankton abundance (0 to 1.5 Ze) was strongly dominated by bacterioplankton along the whole transect (83 ± 7% of total picoplanktonic cells), followed by *Prochlorococcus* when present (up to 27% under oligotrophic conditions), the contributions by *Synechococcus* (0.1 to 3.7%) and picophytoeukaryotes (0.2 to 3.1%) being almost negligible. When not considering MAR, *Prochlorococcus* showed an evident positive relationship with surface temperature (a), which was representative of the general eastward decrease in water temperature within the integration depth (0 to 1.5 Ze) along the transect (see Claustre et al., this issue). Picophytoeukaryotes and *Synechococcus* abundances did not follow the surface temperature trend. Bacterioplankton, on the other hand, followed the *Prochlorococcus* pattern under oligotrophic conditions (b).

When considering the entire data set, *Prochlorococcus* integrated abundance was negatively correlated to Tchl*a*, whereas bacterioplankton and *Synechococcus* (strongest correlation) were both positively correlated to this variable (Table 1). Bacterioplankton abundance covaried with phytoplankton biomass (Table 1). Except for *Synechococcus* and picophytoeukaryotes, no statistically significant correlations were observed between picoplanktonic groups (Table 1).

3.2 Picoplankton contributions to c_p, a proxy for POC

Mean pico- and large phytoplankton cell sizes used to estimate the group-specific attenuation cross sections are summarized in Table 2 and compared with values from the literature. These values and the standard errors associated with them (Table 2) were obtained using the relationship established between mean FSC and cell size (a). The largest size difference between previous studies and the present one was observed for the picophytoeukaryotes (Table 2). For this group, the attenuation coefficients were determined by changes in both size (decreasing towards the coast; see Supp. Mat.) and abundance, when considering a constant refractive index. As a result, for instance, an average decrease in mean cells size of 0.22 μm (0.0056 μm^3) from MAR to HNL (see Supp. Mat.) counteracts the higher cell abundance in the latter (g; Table 2) to modulate c_{euk} along the transect (and 7). In the case of *Prochlorococcus* the mean value presented in Table 2 was obtained from samples taken at different depths along the entire transect, except at the centre of the gyre where the FSC signal could only be retrieved at depth. Larger cell sizes for this group were always found in deeper samples (not shown).

Along the transect, the shape and magnitude of the vertical c_p profiles were mainly determined by the non-vegetal compartment, with c_p and c_{nveg} presenting the same vertical pattern at all long stations (). At MAR and HNL, c_p was rather homogeneous in the top 50 m and declined below this depth, whereas c_{nveg} decreased systematically with depth (a and b). At GYR c_p and c_{nveg} subsurface maxima were both observed around 100 m, these two variables being highest around 40 m at EGY (c and d). Both c_p and c_{veg} tended to be lower under hyper- and oligotrophic conditions at the centre of the gyre and were highest at UPW (). Both *Prochlorococcus* (when present) and picophytoeukaryotes usually presented subsurface maxima in their attenuation coefficients (e.g., at GYR around 125 m for the former and between 150 and 250 m for the latter; c) except at UPW, where c_{euk} tended to decrease below 30 m (e). UPX profiles were included to highlight the differences observed with UPW, the other upwelling station (e and f). No large phytoplankton peaks (>3 μm) were detected between Station 3 and 15, including GYR.

Total and group-specific integrated attenuation coefficients (0 to 1.5 Ze) tended all to decrease from the western side towards the center of the gyre and increased again towards the coast (a). The integrated non-vegetal attenuation coefficient (detritus + bacterioplankton + heterotrophic organisms) was quite variable, constituting ≥70% of

$c_{0\text{-}1.5\ Ze}$ in most of the transect, reaching the highest (83%) and lowest (50%) contributions at GYR and UPW, respectively (b). Detritus being estimated by difference (Eq. 4), c_{det} and c_{veg}'s contributions to $c_{0\text{-}1.5\ Ze}$ followed a general opposite trend, presenting similar values near the meso-oligotrophic limits (~128 and 87ºW) (b). Detritus contribution to $c_{0\text{-}1.5\ Ze}$ was always ≤50%, the lowest values being associated with highest vegetal contributions (b). Interestingly, between the two extreme trophic conditions encountered at GYR (hyper-oligotrophic; see Claustre et al., submitted) and UPW (eutrophic), $c_{0\text{-}1.5\ Ze}$ and integrated c_{veg} increased ~2- and 6-fold, respectively, whereas integrated c_{nveg} and c_{det} were only ~1.2- and 1.1-fold higher at the upwelling station (a). Furthermore, in terms of contribution to $c_{0\text{-}1.5\ Ze}$, c_{veg} was ~3 times higher at UPW, c_{nveg} and c_{det} representing only about half of the percentage estimated at GYR (b).

Mean integrated *Prochlorococcus* (when present) and picophytoeukaryotes contributions to $c_{0\text{-}1.5\ Ze}$ for the whole transect were equivalent (9.7 ± 4.1 and 9.4 ± 3.8%, respectively), although the latter were clearly more important under mesotrophic conditions in both absolute values (a) and relative terms (b). *Synechococcus* attenuation coefficients were too low (a) to contribute significantly to c_p (only 1.0 ± 1.0% on average), so we did not include them in b. Bacterioplankton attenuation coefficients varied little along the transect and were always lower than all phytoplankton combined (b). Large phytoplankton attenuation coefficients were lower than that of the picophytoplankton (cyanobacteria and picophytoeukaryotes combined) in the western part of the transect and higher or similar near the coast (a), their contributions to c_p following the same trend (included in c_{veg}'s contribution, b).

When comparing $c_{0\text{-}1.5\ Ze}$ to $c_{0\text{-}50\ m}$ and their integrated group-specific attenuation coefficients, it becomes clear that not considering data below 50 m leads to very different results in most of the transect and especially at the centre of the gyre (a and c). For instance, whereas at UPW $c_{0\text{-}1.5\ Ze}$ and $c_{0\text{-}50\ m}$ were equivalent, the former is 2- and the latter 13-fold higher than the corresponding GYR integrated values (a and c). Similarly, there was a 2-fold difference in c_{veg}'s contributions to $c_{0\text{-}1.5\ Ze}$ and $c_{0\text{-}50\ m}$ at the centre of the gyre (b and d).

3.3 Phytoplanktonic carbon biomass stocks and spatial variability

To avoid the use of carbon conversion factors from the literature, in the present work we used two different approaches to estimate the picophyoteukaryotes carbon biomass: (1)

from intracellular carbon content (b; see Section 2.1) and (2) calculating c_{euk} contribution to c_p, the latter assumed to be equivalent to POC (see Section 2.2). Both approaches gave very similar results (Fig. 8), indicating that the premise that all picophytoeukaryotic organisms have the same refractive index (~ 1.05) is valid for the sampled transect, even if we know that this group is usually constituted by diverse taxa (Moon-van der Staay et al., 2001). The above provides strong support for the use of optical techniques and theory to determine picophytoeukaryotes carbon biomass, under the sole condition of using actual mean cell sizes.

The deconvolution of c_p indicates that at the centre of the gyre (~120.36 to 98.39ºW or Station 7 to 14 + GYR) the photosynthetic biomass, which was dominated by picophytoplankton, constituted ~18% of the total integrated c_p or POC (b). Even more interestingly, when looking at the vegetal compartment alone, ~43% of this photosynthetic biomass would correspond to the picophytoeukaryotes (a; filled circles). Let us now assume that the contribution to integrated c_p by all phytoplanktonic groups is representative of their contribution to POC, as proven for the picophytoeukaryotes (see above). Under this assumption, picophytoeukaryotes would constitute 51% of the total phytoplankton carbon biomass (large phytoplankton included) at MAR, about 39% at HNL and GYR and 43% at EGY (a; filled circles). At UPW, however, where mean integrated POC estimated from c_p (see Section 2.2) was ~6 g m^{-2} (right axis on a), picophytoeukaryotes would only constitute 5% of the photosynthetic biomass (Fig. 9a; filled circles). When considering the whole transect, picophytoeukaryotes mean contribution to the total photosynthetic carbon biomass (i.e., c_{euk}'s mean contribution to c_p) was ~38%.

Intracellular carbon contents used to estimate picophytoplankton biomass through the relationship established with FSC (b) are given in Table 2. Contributions to POC by *Prochlorococcus* and *Synechococcus* were ~1.7 and 1.5 times higher when estimated using this approach rather than attenuation coefficients (not shown). Using these higher values for cyanobacteria and assuming that the contribution by large phytoplankton is equivalent to c_{large}'s contribution to c_p, picophytoeukaryotes mean contribution to the total photosynthetic carbon biomass along the transect would be ~ 30%, representing ~28 instead of 43% at the centre of the gyre (Fig. 9a; empty circles). These contributions are slightly lower than the ones estimated through the optically-based approach, with almost all data points being below the 1-to-1 line relating both estimates (Fig. 9b).

Regarding spatial variability, both Tchl*a* ($r = 0.67$, $p < 0.001$) and c_p ($r = 0.53$, $p < 0.001$) were correlated to the dominant picophytoplankton carbon biomass, i.e., *Prochlorococcus* + picophytoeukaryotes, between Stations 3 and 15, GYR included (). The results of a t-test on the z-transformed correlation coefficients (Zokal & Rohlf, 1994) indicates that both correlations are not significantly different ($p > 0.05$). Therefore, Tchl*a* and c_p were equally well correlated to the picophytoplanktonic biomass. *Synechococcus* biomass, on the other hand, was negatively correlated to Tchl*a* (a) and positively to c_p (b). However, despite the differences observed between this cyanobacterium and the other two groups, correlation coefficients calculated for total picophytoplankton biomass (i.e., dominant + *Synechococcus*; not shown) were not significantly different ($p > 0.05$) from those calculated for the dominant groups (). *Synechococcus* had no influence on the general relationships because of its negligible biomass. Tchl*a* and c_p were therefore useful in tracing total picophytoplanktonic carbon biomass in the part of the transect where no large phytoplankton was detected (i.e., Stations 3 to 15 + GYR).

4 Discussion and conclusion

4.1 Picoplankton abundance

Macroecological studies indicate that 66% of the variance in picophytoplankton abundance can be explained by temperature (the dominant factor), nitrate and chlorophyll *a* concentration (Li, in press). It has also been established that higher *Prochlorococcus* abundances are observed in more stratified waters, whereas *Synechococcus* and picophytoeukaryotes are more abundant when mixing prevails (e.g. Blanchot and Rodier, 1996; Shalapyonok et al.; 2001). Across the eastern South Pacific Ocean temperature, especially for *Prochlorococcus* and bacterioplankton (), and nitrate concentration along the transect (see b) appear important in modulating picophytoplankton abundance, their influence varying according to the prevailing trophic conditions.

As expected (e.g., Gasol and Duarte, 2000), integrated bacterioplankton abundances covaried with phytoplankton biomass (Table 1). Integrated picophytoeukaryotes abundance was the only one to vary independently from Tchl*a* when considering the whole transect (Table 1), suggesting that the factors controlling picophytoplankton population, such as sinking, sensitivity to radiation, grazing, viral infection, etc (Raven,

2005) acted differently on this group. Thus, the ecology of picophytoeukaryotes needs to be studied in further detail. Across the eastern South Pacific, surface bacterioplankton concentrations were similar to those found by Grob et al. (2007) at 32.5ºS. However, in the deep layer of the hyper-oligotrophic part of the gyre (200 m) this group was 2.5 times more abundant than published by Grob et al. (2007). Given the correlation between integrated bacterioplankton abundance and Tchl*a* concentration (Table 1), the latter could be attributed to the presence of deep *Prochlorococcus* and picophytoeukaryotes maxima that were not observed by Grob et al. (2007). Such deep maxima are a recurrent feature in the oligotrophic open ocean (e and g; Table 3). Along the transect, picophytoplankton abundances were usually within the ranges established in the literature for oligo-, meso- and eutrophic regions of the world's ocean (see Table 3). It is worth noticing that our estimates for surface *Prochlorococcus* abundance were, to our knowledge, the lowest ever estimated for the open ocean (see Table 3), although a possible underestimation cannot be ruled out.

The presence of the mentioned groups under extreme poor conditions suggests a high level of adaptation to an environment where inorganic nutrients are below detection limit. Although little is known on picophytoeukaryotes metabolism, several cyanobacteria ecotypes have been shown to grow on urea and ammonium (Moore et al., 2002). Ammonium uptake at the centre of the gyre was low but still detectable (Raimbault et al., this issue). Considering that heterotrophic bacteria would be responsible for ~40% of this uptake in marine environments (Kirchman, 2000), the possibility of surface picophytoplankton growing on this form of nitrogen at the centre of the gyre cannot be discarded.

4.2 Picoplankton contribution to cp

The larger increase of integrated c_{veg} as compared to c_{nveg} observed between extreme trophic conditions (see Section 3.2) indicates that across the eastern South Pacific spatial variability in the vegetal compartment was more important than the non-vegetal one in shaping the water column optical properties, at least the particulate attenuation coefficient. As expected (e.g., Chung et al., 1996; Loisel and Morel, 1998; Claustre et al., 1999), c_p and c_{veg} tended to be lower under hyper- and oligotrophic conditions at the centre of the gyre and were highest at UPW. Here, the highest c_p and c_{veg} were associated with mature upwelling conditions characterized by the highest primary

production (Moutin et al., this issue) and Tchl*a* (d), and low nutrient concentration (b; Raimbault et al., this issue).

Although the non-vegetal particles tended to dominate the c_p signal, and therefore POC, regardless of trophic condition (b; e.g., Chung et al., 1998; Claustre et al., 1999; Oubelkheir et al., 2005), this dominance seems to weaken from oligo- to eutrophic conditions (Claustre et al., 1999; this study). Here we showed that under mature upwelling conditions (UPW) the contribution by vegetal and non-vegetal particles may even be equivalent (b), in contrast with the invariant ~ 80% c_{nveg} contribution estimated by Oubelkheir et al. (2005) for different trophic conditions. We therefore emphasize the importance of using complementary data to interpret bio-optical measurements since, for instance, the ~2.3-fold difference in c_{veg}'s contribution to c_p observed between our UPW results and those published by Ouberkheir et al. (2005) seems to be related to the state of development of the upwelling event (mature versus early).

At the hyper-oligotrophic centre of the gyre, c_{euk} contribution to $c_{0\text{-}1.5\ Ze}$ was equivalent to the one possibly overestimated (because of the larger cell size assumed) by Claustre et al. (1999). The above highlights the importance of making good size estimates when decomposing the total attenuation signal since, for example, a difference of 1.02 µm in size leads to a 10-fold difference in the scattering cross-section calculated for picophytoeukaryotes (Claustre et al., 1999; Oubelkheir et al., 2005). In the present work, picophytoplankton populations were isolated on board by flow-cytometry cell sorting in order to measure their actual sizes using a particle counter (see Section 2.1). It is the first time to our knowledge that such direct measurements have been done in the field. For future studies we recommend to measure the different picophytoplankton mean cell sizes in situ for at least a few samples, including surface and deep populations in order to consider possible vertical variability. If these samples are taken under different oceanographic conditions, we also recommend including samples from each one of these conditions.

By establishing a relationship with FSC to estimate actual picophytoplankton cell size (a), we confirmed that picophytoeukaryotes were more important contributors to c_p than cyanobacteria under both meso- and eutrophic conditions (Claustre et al., 1999). The uncertainties in this relationship are larger for cyanobacteria (lower part of the curve; a) than for picophytoeukaryotes. However, *Prochlorococcus* and *Synechococcus*' mean cell sizes measured in situ were ≤0.59 (only one isolated population could be measured

with the Coulter Counter, the rest being too small) and ≤0.87 μm, respectively (see Table A, Supp. Mat.). We therefore believe that these group's mean cell sizes, and therefore their contributions to c_p along the transect, may have been at most over- rather than underestimated by this relationship. Differences in cell size (Table 2) would also explain the much lower *Synechococcus* contribution to c_p observed in the hyper-oligotrophic centre of the gyre compared to that published by Claustre et al. (1999) for the tropical Pacific (16°S, 150°W).

Only data collected at local noon time were used to estimate group-specific attenuation coefficients, to avoid errors associated with the natural diel variability that has been observed in the refractive index of picophytoplankton cells from culture (e.g., Stramski et al., 1995; DuRand & Olson, 1998; DuRand et al., 2002). Here we showed that the premise that all picophytoeukaryotes have the same refractive index (1.05) is valid for the sampled transect when actual mean cell sizes are used. In the case of *Synechococcus*, a high refractive index of 1.083 (Aas, 1996) would only increase this group's mean attenuation cross-section by a negligible 6%. Given their low abundance compared to the other groups, the resulting increase in their contribution to c_p would be even lower.

If *Prochlorococcus* were to have a refractive index of 1.06 for instance, their mean attenuation cross-section would be 43% higher than the one calculated here. Nevertheless, the resulting *Prochlorococcus*' contribution to c_p for the entire transect would only be 4 ± 2% higher. However, this group's contribution to c_{veg} would increase by 18 ± 2% on average, constituting up to 99% of the vegetal compartment under hyper-oligotrophic conditions, which is not possible considering the contribution by picophytoeukaryotes. We therefore believe that the assumption of a refractive index of 1.05 for cyanobacteria is appropriate for the purposes of the present work. It is worth noticing that lower refractive indexes for these two groups would only reduce their contribution to c_p (and therefore POC) and c_{veg}, the contribution by picophytoeukaryotes resulting even more important than stated in this work.

Regarding mean cell size, deep *Prochlorococcus* cells are larger than surface ones (e.g. Li et al., 1993; this study). The former are better represented than the latter in the data set used to estimate mean *Prochlorococcus* cell size for the transect, since surface FSC signals could not be retrieved for a large area at the centre of the gyre. We therefore consider that the mean cell size used here for this group could be at most overestimated,

i.e., biased towards a larger value due to the fewer surface data available. Hence, picophytoeukaryotes' contributions to c_{veg} could only be underestimated. The above highlights the importance of this group in terms of photosynthetic biomass in the open ocean.

Definitively the largest uncertainties in the deconvolution of c_p are related to the determination c_{bact} and c_{het}, which have a direct influence on c_{det}'s estimates (see Section 2.2, Eq. 4). First, bacterioplankton cells were assumed to have a mean cell size of 0.5 μm. Taking the minimum and maximum sizes presented in Table 2 (i.e., 0.46 and 0.73 μm), the scattering cross section for bacterioplankton would be ~28% lower and 4.5 times higher than the one used here, respectively. The lower scattering cross sections for these two groups would imply an underestimation of detritus' contribution to c_p of only 11 ± 3% on average for the entire transect. A scattering cross section 4.5 times higher (i.e., 0.73 μm of mean cell size) would imply a contribution ≥100% to c_p, and therefore POC, by bacteria and heterotrophic protests alone, which seems unrealistic. Based on the above, we consider the assumption of a 0.5 μm mean cell size for bacterioplankton to be appropriate for our estimates, since at most it would slightly underestimate detritus.

Following Claustre et al. (1999), here we assumed that $c_{het} = 2\ c_{bact}$ (see Section 2.2, Eq. 3). The range reported by Morel & Ahn (1993) for this conversion factor is 1.8 to 2.4. Using these values instead of 2 would result in an average increase and decrease in c_{det}'s contribution to c_p across the eastern South Pacific of 2 ± 1% and 4 ± 2%, respectively, which in both cases is negligible. It is worth noticing that even if larger errors were associated with the assumptions made in this work regarding bacterioplankton and heterotrophic protists, our results and conclusions regarding picophytoeukaryotes contributions to c_p, and therefore POC, and to the photosynthetic carbon biomass across the eastern South Pacific would not change.

4.3 Phytoplankton carbon biomass stocks and spatial variability

One of the most important observations of the present study is that spatial variability in the open-ocean, where no large phytoplankton was detected, picophytoplankton carbon biomass can be traced by changes in both Tchl*a* and c_p (). While chlorophyll concentration has widely been used as a proxy for photosynthetic carbon biomass, the use of c_p is more controversial. For instance, although c_p seems to be a better estimate of

phytoplankton biomass than Tchl*a* in Case I waters (Behrenfeld and Boss, 2003) and within the mixed layer of the eastern Equatorial Pacific (Behrenfeld and Boss, 2006), chlorophyll concentration would work better in subtropical stratified waters (Huot et al., this issue). Our results indicate that Tchl*a* and c_p would be equally useful estimates of photosynthetic carbon biomass in the open ocean, where it is mainly constituted by picophytoplankton ($\leq$ 3 μm). However, it is important to highlight that in order to estimate the photosynthetic carbon biomass from c_p it is necessary to have information or make some assumptions on the contributions by vegetal and non-vegetal particles to this coefficient. In this case, picophytoplankton biomass and c_p were positively correlated such as that the former could be retrieved from the latter. Despite of the stated limitations, the bio-optical approach used in the present work could be a good alternative for large scale open ocean surveys, especially considering that c_p measurements are much less time-consuming than determining chlorophyll concentration and can also be obtained at a much higher vertical resolution. Further research should be done to test the ability of c_p in tracing phytoplankton biomass in the ocean.

Although when present *Prochlorococcus* largely dominates in terms of abundance, the picophytoeukaryotes would constitute between 39 and 51% (~ 38% on average) of the total integrated phytoplankton carbon biomass (*Prochlorococcus* + *Synechococcus* + picophytoeukaryotes + large phytoplankton) estimated from c_{euk}'s contribution to c_{veg} (a, filled circles; see Section 3.3). Furthermore, under oligotrophic conditions this group constituted ~43% of the photosynthetic carbon biomass. Previous studies indicate that picophytoeukaryotes largely dominate the vegetal compartment in the equatorial Pacific (DuRand et al., 1996; Claustre et al., 1999) and the picophytoplanktonic carbon biomass across the eastern South Pacific along 32.5ºS (Grob et al., 2007). Here we showed that this group constitutes a very important and in some cases a dominant fraction of c_{veg} across the eastern South Pacific, confirming the findings by Grob et al. (2007). The above also agrees with what has been observed in the North and South Atlantic Subtropical Gyres (Zubkov et al., 2000). Picophytoeukaryotes also dominated the picophytoplanktonic carbon biomass in the coastal region, as previously indicated by Worden et al. (2004) and Grob et al. (2007).

Picophytoeukaryotes contributions obtained by estimating cyanobacteria biomass from intracellular carbon content were probably underestimated compared to those obtained using the bio-optical approach (b) because of the conversion factor used for

Prochlorococcus (Table 2). We believe that establishing a relationship between intracellular carbon content and FSC for this cyanobacterium, as we did for *Synechococcus* and picophytoeukaryotes, would lead to contributions similar to those estimated using attenuation coefficients. It is worth noticing that higher or lower cyanobacteria carbon biomasses would only modify the y-intercept of the biomass relationships with Tchl*a* and c_p (), but not their slope or their strength.

When normalized to 1 μm^3, maximal growth rates estimated for picophytoeukaryotes are higher than for *Prochlorococcus* (Raven 2005 and references therein). Considering that the former are ~16 times larger than the latter in terms of mean cell volume, the amount of carbon passing through the picophytoeukaryotes could be very important. For the same reason, this group could also be the most important contributor to export fluxes in the open ocean, since picophytoplankton share of this carbon pathway seems to be much more important than previously thought (Richardson and Jackson, 2007; Barber 2007). The role of this group in carbon and energy flow would therefore be crucial.

Picophytoeukaryotes carbon biomass in the open ocean seems to be much more important than previously thought. Across the eastern South Pacific, this group's biomass is almost equivalent to that of *Prochlorococcus* under hyper-oligotrophic conditions and even more important under mesotrophic ones. The role of picophytoeukaryotes in biogeochemical cycles needs to be evaluated in the near future. Further attention needs to be focused on this group.

Literature cited

Aas, E.: Refractive index of phytoplankton derived from its metabolite composition. J Plankton Res, 18, 2223-2249, 1996.

Antoine, D., André, J. M. , and Morel, A.: Oceanic primary production II. Estimation at global scale from satellite (Coastal Zone Color Scanner) chlorophyll. Global Biogeochem Cycles, 10, 57-69, 1996.

Barber, R. T.: Picoplankton Do Some Heavy Lifting. Science, 315, 777-778, 2007.

Behrenfeld, M. J. and Boss, E.: The beam attenuation to chlorophyll ratio: an optical index of phytoplankton physiology in the surface ocean? Deep Sea Res Part I, 50, 1537–1549, 2003.

Behrenfeld, M. J. and Boss, E.: Beam attenuation and chlorophyll concentration as alternative optical indices of phytoplankton biomass. J Mar Res, 64, 431–451, 2006.

Bissett, W. P., Walsh, J. J., Dieterle, D. A. , and Carder, K. L.: Carbon cycling in the upper waters of the Sargasso Sea: I. Numerical simulation of differential carbon and nitrogen fluxes. Deep Sea Research I, 46, 205-269, 1999.

Blanchot, J. and Rodier, M.: Picophytoplankton abundance and biomass in the western Tropical Pacific Ocean during the 1992 El Nino year: Results from flow cytometry. Deep-Sea Res, 43, 877-896, 1996.

Campbell, L. and Vaulot, D.: Photosynthetic picoplankton community structure in the subtropical North Pacific Ocean near Hawaii (station ALOHA). Deep Sea Research I, 40, 2043-2060, 1993.

Carr, M.-E., Friedrichs, M. A. M., Schmeltz, M., Aita, M. N., Antoine, D., Arrigo, K. R., Asanuma, I., Aumont, O., Barber, R., Behrenfeld, M., Bidigare, R., Buitenhuis, E. T., Campbell, J., Ciotti, A., Dierssen, H., Dowell, M., Dunne, J., Esaias, W., Gentili, B., Gregg, W., Groom, S., Hoepffner, N., Ishizaka, J., Kameda, T., Quéré, C. L., Lohrenz, S., Marra, J., Mélin, F., Moore, K., Morel, A., Reddy, T. E., Ryan, J., Scardi, M.,

Smyth, T., Turpie, K., Tilstone, G., Waters, K. , and Yamanaka, Y.: A comparison of global estimates of marine primary production from ocean color. Deep Sea Research II, 53, 741–770, 2006.

Chavez, F. P., Buck, K. R., Bidigare, R. R., Karl, D. M., Hebel, D., Latasa, M. , and Campbell, L.: On the chlorophyll a retention properties of glass-fiber GF/F filters. Limnol Oceanogr, 40, 428-433, 1995.

Chen, C.-T. A., Liu, K.-K. , and MacDonald, R. W.: Continental margin exchanges. Ocean Biogeochemistry, in: The Role of the Ocean Carbon Cycle in Global Change, edited by Fasham, M. J. R., IGBP Book Series, Springer, 53-97, 2003.

Chisholm, S. W., Olson, R. J., Zettler, E. R., Goericke, R., Waterbury, J. B. , and Welschmeyer, N. A.: A novel free-living prochlorophyte occurs at high cell concentrations in the oceanic euphotic zone. Nature, 334, 340-343, 1988.

Chung, S. P., Gardner, W. D., Richardson, M. J., Walsh, I. D. , and Landry, M. R.: Beam attenuation and microorganisms: spatial and temporal variations in small particles along 14O”W during the 1992 JGOFS EqPac transects. Deep Sea Research II, 43, 1205-1226, 1996.

Chung, S. P., Gardner, W. D., Landry, M. R., Richardson, M. J. , and Walsh, I. D.: Beam attenuation by microorganisms and detrital particles in the Equatorial Pacific. J Geophys Res, 103 (C6), 12,669-12,681, 1998.

Claustre, H., Morel, A., Babin, M., Cailliau, C., Marie, D., Marty, J. C., Tailliez, D. , and Vaulot, D.: Variability in particle attenuation and chlorophyll fluorescence in the Tropical Pacific: Scales, patterns, and biogeochemical implications. J Geophys Res, 104 (C2), 3401-3422, 1999.

DuRand, M. D. and Olson, R. J.: Contributions of phytoplankton light scattering and cell concentration changes to diel variations in beam attenuation in the equatorial Pacific from flow cytometric measurements of pico-, ultra- and nanoplankton. Deep Sea Res Part II, 43, 891-906, 1996.

DuRand, M. D. and Olson, R. J.: Diel patterns in optical properties of the chlorophyte Nannochloris sp.: Relating individual-cell to bulk measurements. Limnol Oceanogr, 43, 1107-1118, 1998.

DuRand, M. D., Green, R. E., Sosik, H. M. , and Olson, R. J.: Diel variations in optical properties of Micromonas pusilla (Prasinophyceae). J Phycol, 38, 1132-1142, 2002.

Falkowski, P. G., Barber, R. T. , and Smetacek, V.: Biogeochemical Controls and Feedbacks on Ocean Primary Production. Science, 200-206, 1998.

Field, C. B., Behrenfeld, M. J., Randerson, J. T. , and Falkowski, P.: Primary Production of the Biosphere: Integrating Terrestrial and Oceanic Components. Science, 281, 237-240, 1998.

Gardner, W. D., Mishonov, A. V. , and Richardson, M. J.: Global POC concentrations from in-situ and satellite data. Deep Sea Research II, 53, 718–740, 2006.

Gasol, J. M. and Duarte, C. M.: Comparative analyses in aquatic microbial ecology: how far do they go? FEMS Microbiol Ecol, 31, 99-106, 2000.

Grob, C., Ulloa, O., Li, W. K. W., Alarcón, G., Fukasawa, M. , and Watanabe, S.: Picoplankton abundance and biomass across the eastern South Pacific Ocean along latitude 32.5° S. Mar Ecol Prog Ser, 332, 53–62, 2007.

Gundersen, K., Heldal, M., Norland, S., Purdie, D. A. , and Knap, A. H.: Elemental C, N, and P cell content of individual bacteria collected at the Bermuda Atlantic Time-series Study (BATS) site. Limnol Oceanogr, 47, 1525–1530, 2002.

Kirchman, D. L.: Uptake and regeneration of inorganic nutrients by marine heterotrophic bacteria, in: Microbial ecology of the oceans, edited by Kirchman, D.L., Wiley-Liss, NewYork, 261–288, 2000.

Landry, M. R., Brown, S. L., Neveux, J., Dupouy, C., Blanchot, J., Christensen, S. , and Bidigare, R. R.: Phytoplankton growth and microzooplankton grazing in high-nutrient, low-chlorophyll waters of the equatorial Pacific: Community and taxon-specific rate assessments from pigment and flow cytometric analyses. Journal of Geophysical Research, 108, 8142-8156, 2003.

Le Quéré, C, Harrison, S. P., Prentice, I. C., Buitenhuis, E. T., Aumont, O., Bopp, L., Claustre, H., Cunha, L. C. D., Geider, R., Giraud, X., Klaas, C., Kohfeld, K. E., Legendre, L., Manizza, M., Platt, T., Rivkin, R. B., Sathyendranath, S., Uitz, J., Watson, A. J. , and Wolf-Gladrow, D.: Ecosystem dynamics based on plankton functional types for global ocean biogeochemistry models. Glob Change Biol, 11, 2016–2040, 2005.

Li, W. K. W., Zohary, T., Yacobi, Y. Z. , and Wood, A. M.: Ultraphytoplankton in the eastern Mediterranean Sea: Towards deriving phytoplankton biomass from flow cytometric measurements of abundance fluorescence and light scatter. Mar Ecol Prog Ser, 102, 79-87, 1993.

Li, W. K. W.: Primary production of prochlorophytes, cyanobacteria, and eucaryotic ultraphytoplankton: Measurements from flow cytometric sorting. Limnol Oceanogr, 39, 169-175, 1994.

Li, W. K. W.: Composition of ultraphytoplankton in the Central North Atlantic. Mar Ecol Prog Ser, 122, 1-8, 1995.

Li, W. K. W.: Plankton Populations and Communities, in: Marine Macroecology, edited by Witman, J. and Kaustuv, R., University of Chicago Press, in press.

Loisel, H. and Morel, A.: Light scattering and chlorophyll concentration in case 1 waters: A reexamination. Limnol Oceanogr, 43, 847-858, 1998.

Mackey, D. J., Blanchot, J., Higgins, H. W. , and Neveux, J.: Phytoplankton abundances and community structure in the equatorial Pacific. Deep Sea Research II, 49, 2561–2582, 2002.

Marie, D., Partensky, F., Simon, N., Guillou, L. , and Vaulot, D.: Flow cytometry analysis of marine picoplankton. In: Diamond R.A., DeMaggio S. (ed.). In Living Colors: Protocols in Flow Cytometry and Cell sorting. Vol., 421-454 pp., 2000.

Moon van der Staay, S. Y., Wachter, R. D. , and Vaulot, D.: Oceanic 18S rDNA sequences from picoplankton reveal unsuspected eukaryotic diversity. Nature, 409, 607-610, 2001.

Moore, L. R., Post, A. F., Rocap, G. , and Chisholm, S. W.: Utilization of different nitrogen sources by the marine cyanobacteria *Prochlorococcus* and *Synechococcus*. Limnol Oceanogr, 47, 989-996, 2002.

Morel, A. and Ahn, Y.-H.: Optics of heterotrophic nanoflagellates and ciliates: A tentative assessment of their scattering role in oceanic waters compared to those of bacterial and algal cells. J Mar Res, 49, 177-202, 1991.

Morel, A., Ahn, Y.-W., Partensky, F., Vaulot, D. , and Claustre, H.: *Prochlorococcus* and *Synechococcus* : a compartive study of their size, pigmentation and related optical properties. J Mar Res, 51, 617-649, 1993.

Morel, A., Gentili, B., Claustre, H., Babin, M., Bricaud, A., Ras, J. , and Tièche, F.: Optical properties of the "clearest" natural waters. Limnol Oceanogr, 52, 217-229, 2007.

Not, F., Valentin, K., Romari, K., Lovejoy, C., Massana, R., Töbe, K., Vaulot, D. , and Medlin, L. K.: Picobiliphytes: A Marine Picoplanktonic Algal Group with Unknown Affinities to Other Eukaryotes. Science, 315, 253-255, 2007.

Oubelkheir, K., Claustre, H. , and Babin, A. S.: Bio-optical and biogeochemical properties of different trophic regimes in oceanic waters. Limnol Oceanogr, 50, 1795–1809, 2005.

Preisendorfer, R. W.: Application of radiative transfer theory to light measurements in the sea. Monogr., 10, 11-30, Int Union Geod Geophys, Paris, 1961.

Raven, J. A., Finkel, Z. V. , and Irwin, A. J.: Picophytoplankton: bottom-up and top-down controls on ecology and evolution. Vie Milieu, 55, 209-215, 2005.

Richardson, T. L. and Jackson, G. A.: Small Phytoplankton and Carbon Export from the Surface Ocean. Science, 315, 838-840, 2007.

Shalapyonok, A., Olson, R. J. , and Shalapyonok, L. S.: Arabian Sea phytoplankton during Southwest and Northeast Monsoons 1995: composition, size structure and biomass from individual cell properties measured by flow cytometry. Deep-Sea Res Part II, 48, 1231-1261, 2001.

Sherr, E. B., Sherr, B. F. , and Wheeler, P. A.: Distribution of coccoid cyanobacteria and small eukaryotic phytoplankton in the upwelling ecosystem off the Oregon coast during 2001 and 2002. Deep Sea Research II, 52, 317–330, 2005.

Sokal, R. R., and F. J. Rohlf. Biometry the principles and practice of statistics in biological research, W.H. Freeman and Company, New York, 1994.

Stramski, D., Shalapyonok, A. , and Reynolds, R.: Optical characterization of the oceanic unicellular cyanobacterium *Synechococcus* grown under a day-night cycle in natural irradiance. J Geophys Res, 100, 13295-13307, 1995.

Ulloa, O., Sathyendranath, S., Platt, T. , and Quiñones, R. A.: Light scattering by marine heterotrophic bacteria. J Geophys Res, 97, 9619-9629, 1992.

Van de Hulst, H. C.: Light scattering by small particles, Wiley, New York, 1957.

Vaulot, D.: CYTOPC: Processing software for flow cytometric data. Signal and Noise, 2:8. 1989.

Vaulot, D. and Marie, D.: Diel variability of photosynthetic picoplankton in the equatorial Pacific. J Geophys Res, 104 (C2), 3297-3310, 1999.

Veldhuis, M. J. W. and Kraay, G. W.: Phytoplankton in the subtropical Atlantic Ocean: towards a better assessment of biomass and composition. Deep Sea Research I, 51, 507–530, 2004.

Veldhuis, M. J. W., Timmermans, K. R., Croot, P. , and Wagt, B. V. D.: Picophytoplankton; a comparative study of their biochemical composition and photosynthetic properties. J Sea Res, 53, 7 – 24, 2005.

Waterbury, J. B., Watson, S. W., Guillard, R. R. L. , and Brand, L. E.: Widespread occurrence of a unicellular, marine planktonic, cyanobacterium. Nature, 277, 293-294, 1979.

Worden, A. Z., Nolan, J. K. , and Palenik, B.: Assessing the dynamics and ecology of marine picophytoplankton: The importance of the eukaryotic component. Limnol Oceanogr, 49, 168–179, 2004.

Zubkov, M. V., Sleigh, M. A., Burkill, P. H. , and Leakey, R. J. G.: Picoplankton community structure on the Atlantic Meridional Transect: a comparison between seasons. Prog Oceanogr, 45, 369–386, 2000.

Acknowledgments

This work was supported by the Chilean National Commission for Scientific and Technological Research (CONICYT) through the FONDAP Program and a graduate fellowship to CG; the ECOS (Evaluation and Orientation of the Scientific Cooperation, France)-CONICYT Program, the French program PROOF (Processus Biogeochimiques dans l'Océan et Flux), Centre National de la Recherche Scientifique (CNRS), the Institut des Sciences de l'Univers (INSU), the Centre National d'Etudes Spatiales (CNES), the European Space Agency (ESA), the National Aeronautics and Space Administration (NASA) and the Natural Sciences and Engineering Research Council of Canada (NSERC). This is a contribution of the BIOSOPE project of the LEFE-CYBER program. Dominique Tailliez and Claudie Bournot are warmly thanked for their efficient help in CTD rosette management and data processing. We also thank the scientific party and the Captain and crew of the RV L'Atalante during the BIOSOPE Expedition; Fanny Thièche for her help with laboratory work; Laura Farías and Mauricio Gallegos for organic carbon analyses, Bernard Gentili for PAR data processing and Rodrigo Wiff for help with statistical analyses.

Table 1. Correlation matrix for log integrated (0 to 1.5 Ze) picoplankton abundances (*Proc* = *Prochlorococcus*, *Syn* = *Synechococcus*, Euk = picophytoeukaryotes and Bact = bacterioplankton; x 10^{11} cells m^{-2}) and log total chlorophyll *a* (Tchl*a*; mg m^{-2}), considering the entire transect. Picophytoplankton = *Proc* + *Syn* + Euk; picoplankton = *Proc* + *Syn* + Euk + Bact.

	Proc	*Syn*	Euk	Bact	Tchl*a*
Proc	1.00	n.s	n.s	n.s	-0.42*
Syn	-	1.00	0.68**	n.s	0.82**
Euk	-	-	1.00	n.s	n.s
Bact	-	-	-	1.00	0.46*
Picophytoplankton	-	-	-	-	0.58*
Picoplankton	-	-	-	-	0.61**

Upper right values show correlation coefficients with their corresponding level of significance:
** significance level <0.0001; * significance level <0.05; n.s., not statistically significant

Table 2. Picoplankton mean cell size (μm), volume (μm^3) and intracellular carbon content (fgC $cell^{-1}$)

Group	Mean cell size (μm)	Mean cell volume (μm^3)	Intracellular carbon content (fgC $cell^{-1}$)	Reference
Prochlorococcus	0.68 ± 0.08	0.17	29 ± 11***	1
	0.74	0.21	-	2
	0.7	0.18	-	3
	0.63±0.2	0.13	29	4
Synechococcus	0.86 ± 0.1* and 1.16 ± 0.02**	0.33 and 0.82	60 ± 19* and 140 ± 9**	1
	0.90	0.38		2
	1.2	0.90		3
	0.95 ± 0.31	0.45	100	4
Picophytoeukaryotes	1.74 ± 0.13 (range = 1.37 to 1.99)	2.76	730 ± 226 (range = 257 to 1266)	1
	1.26	1.05	-	2
	2.28	6.21	-	3
	2.35	6.8	1500	4
Large phytoplankton	3.3 (MAR) to ~20 (UPW)	18.8 to 4189	-	1
	10 to 22	523.6 to 5575.28	-	2
	6 to 13	113.1 to 1150.35	-	5
Bacterioplankton	0.5	0.07	-	1, 3
	0.56	0.09	-	2
	0.46 ± 0.14	0.05	-	4
	0.52 to 0.63	0.07 to 0.13	-	6
	0.15 to 0.73	0.002 to 2	-	7

[1] This study
[2] Chung et al., 1998; Equatorial Pacific
[3] Claustre et al., 1999; tropical Pacific Ocean
[4] Zubkov et al., 2000; North and South Atlantic Subtropical Gyres
[5] Oubelkheir et al., 2005; Mediterranean Sea
[6] Ulloa et al., 1992; Sargasso Sea
[7] Gundersen et al., 2002; Bermuda Atlantic Time Series (BATS)
* For most of the transect and ** for UPX, the most coastal station
*** Obtained using the conversion factor 171 ± 15 fgC μm^3 derived from *Synechococcus* (see Section 2.1)

Table 3. *Prochlorococcus*, *Synechococcus* and picophytoeukaryotes abundances (x 10^3 cells ml^{-1}) registered during spring time in different regions of the world's ocean under varying trophic conditons.

Trophic condition	*Prochlorococcus*	*Synechococcus*	Picophytoeukaryotes	Reference
Hyper-oligotrophic	16-18*	1.2-1.6*	0.76-1.3*	1 (GYR)
	150-160 (125 m)	0.8-1.4 (125 m)	1.8-2.3 (175 m)	
Oligotrophic	35-40*	6.9-8.6*	4.5-4.9*	1 (EGY)
	200-250 (50-75 m)	20 (50 m)	14 (60 m)	
	240 (0 to 100 m)	1.5 (0 to 100 m)	0.8-1 (0 to 100 m)	2
	30*	0.7*	0.5*	3
	200 (120 m)	1-1.5 (50-125 m)	2 (140-150 m)	
	100-150*	3-30*	0.6-2*	4
	100 (120 m)	1 (120-160 m)	1-2 (80-120 m)	
	115*	0.2-1 (0 to 100 m)	0.25-0.5*	5
	150-200 (50-100 m)		Up to 3 (100 m)	
	60 (0 to 100 m)	2.5 (0 to 50-100 m)	2-4*	6
			2 (100 m)	
HNL	200 (surf)	10-28 (surf)	5-9 (0 to 80 m)	1
	270 (30-60 m)	25 (50 m)		
	150-300 (0 to 80 m)	3-5 (0 to 80 m)	0.6-1 (0 to 100 m)	3
	200 (0 to 50 m)	8 (0 to 100 m)	3 (0 to 100 m)	7
	100 (80 m)			
	200 (30 and 60 m)	15 and 13 (30 and 60 m)	6 and 5 (30 and 60 m)	8
Mesotrophic	50-60 (0 to 80 m)	17-20 (0 to 60 m)	3-5 (0 to 80 m)	1 (MAR)
	30-200*	5-44*	3-18*	6
	1-40 (100 m)	0.2-3 (100 m)	0.4-4 (100 m)	
Eutrophic	-	60-200	5-10	1 (UPW)
	-	50-250	10-60	9
	-	Up to 150	Up to 80-90	10

*Surface data

[1] This study
[2] Campbell and Vaulot, 1993; Subtropical North Pacific (ALOHA)
[3] Vaulot et al., 1999; Subtropical Pacific (16ºS ; 150ºW). These authors considered their surface *Prochlorococcus* abundances as "severely underestimated".
[4] Zubkov et al., 2000; North and South Atlantic Subtropical Gyres
[5] Veldhuis and Kraay; 2004; Eastern North Atlantic Subtropical Gyre
[6] Grob et al., 2007; Eastern South Pacific
[7] Mackey et al., 2002;
[8] Landry et al., 2003;
[9] Worden et al., 2004; Southern California Bight, North Pacific
[10] Sherr et al., 2005; Oregon upwelling ecosystem, North Pacific

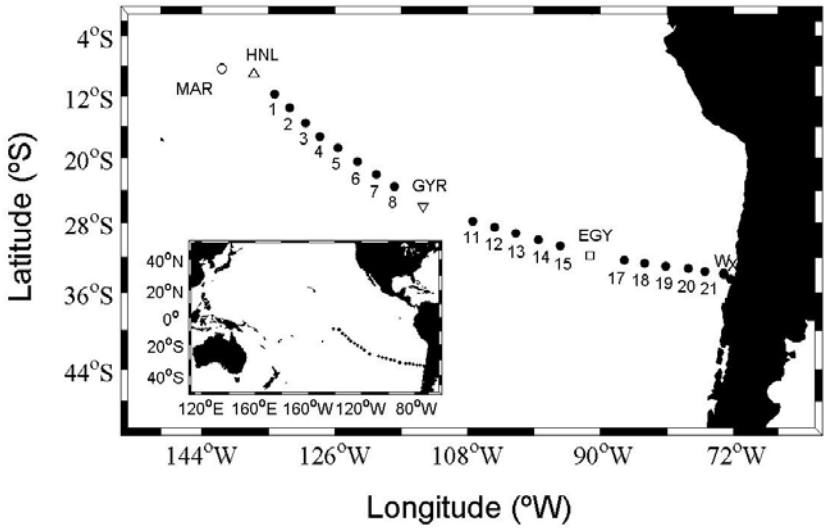

Fig. 1. BIOSOPE transect. In this study we include data from stations 1-8, 11-15 and 17-21, MAR, HNL, GYR, EGY, UPW (W) and UPX (X).

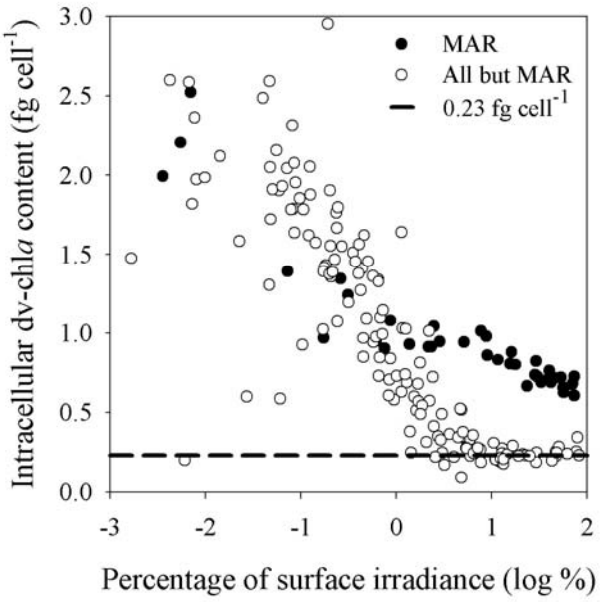

Fig. 2. *Prochlorococcus* intracellular dv-chl*a* content (fg cell^{-1}) as a function of the percentage of surface irradiance at MAR (●) and the rest of the transect (○). Dashed line indicates the average surface intracellular dv-chl*a* content established at 0.23 fg cell^{-1}.

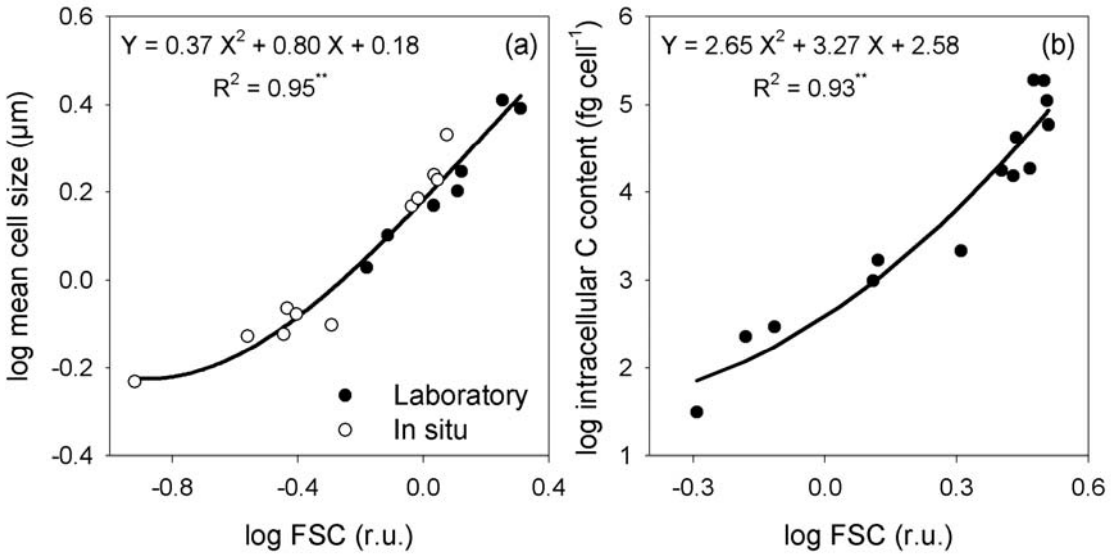

Fig. 3. Log-log relationships established between the flow cytometric forward scatter signal (FSC), expressed in units relative to reference beads (relative units, r.u.), and mean cell size in µm (a) and intracellular carbon (C) content in fig cell^{-1} (b). In (a), mean cell sizes measured on natural populations isolated in situ (empty circles) as well as on populations from culture (filled circles) are included. Mean intracellular carbon contents in (b) were obtained from culture cells. Carbon measurements were performed on triplicate with ≤ 5% of standard deviation ** indicates $p < 0.0001$.

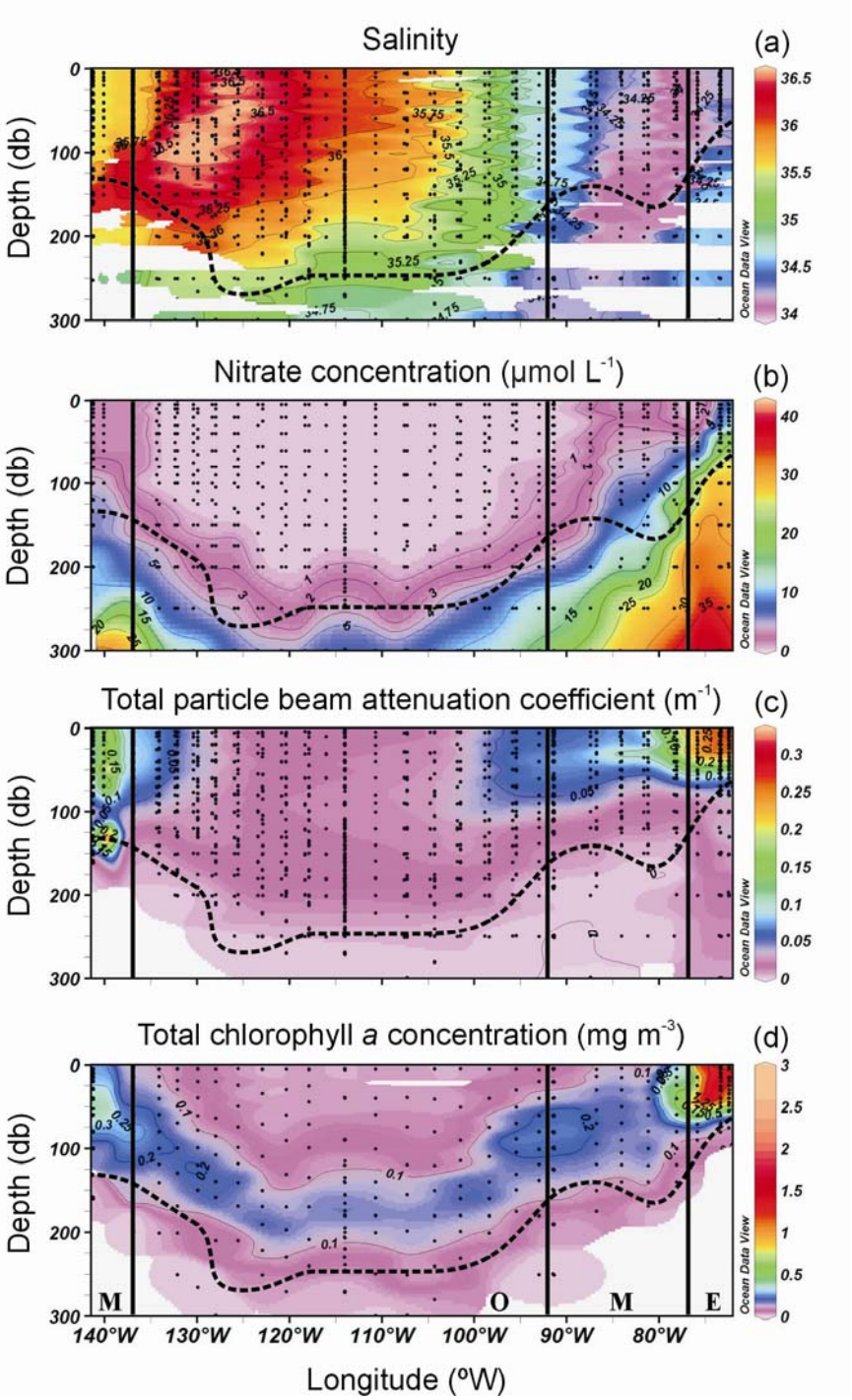

Fig. 4. Salinity (a), nitrate concentrations in µmol L^{-1} (b), total particulate attenuation coefficient in m^{-1} (c), total chlorophyll *a* concentration in mg m^{-3} (d), *Prochlorococcus* (e), *Synechococcus* (f), picophytoeukaryotes (g) and bacterioplankton (h) abundances (x 10^3 cells ml^{-1}). Vertical black lines indicate from left to right the limits between meso- (M), oligo- (O), meso- (M) and eutrophic (E) conditions. Horizontal black dashed line corresponds to the depth of the 1.5 Ze. Black dashed square in (e) indicates where *Prochlorococcus* abundances were estimated from dv-chl*a* concentration.

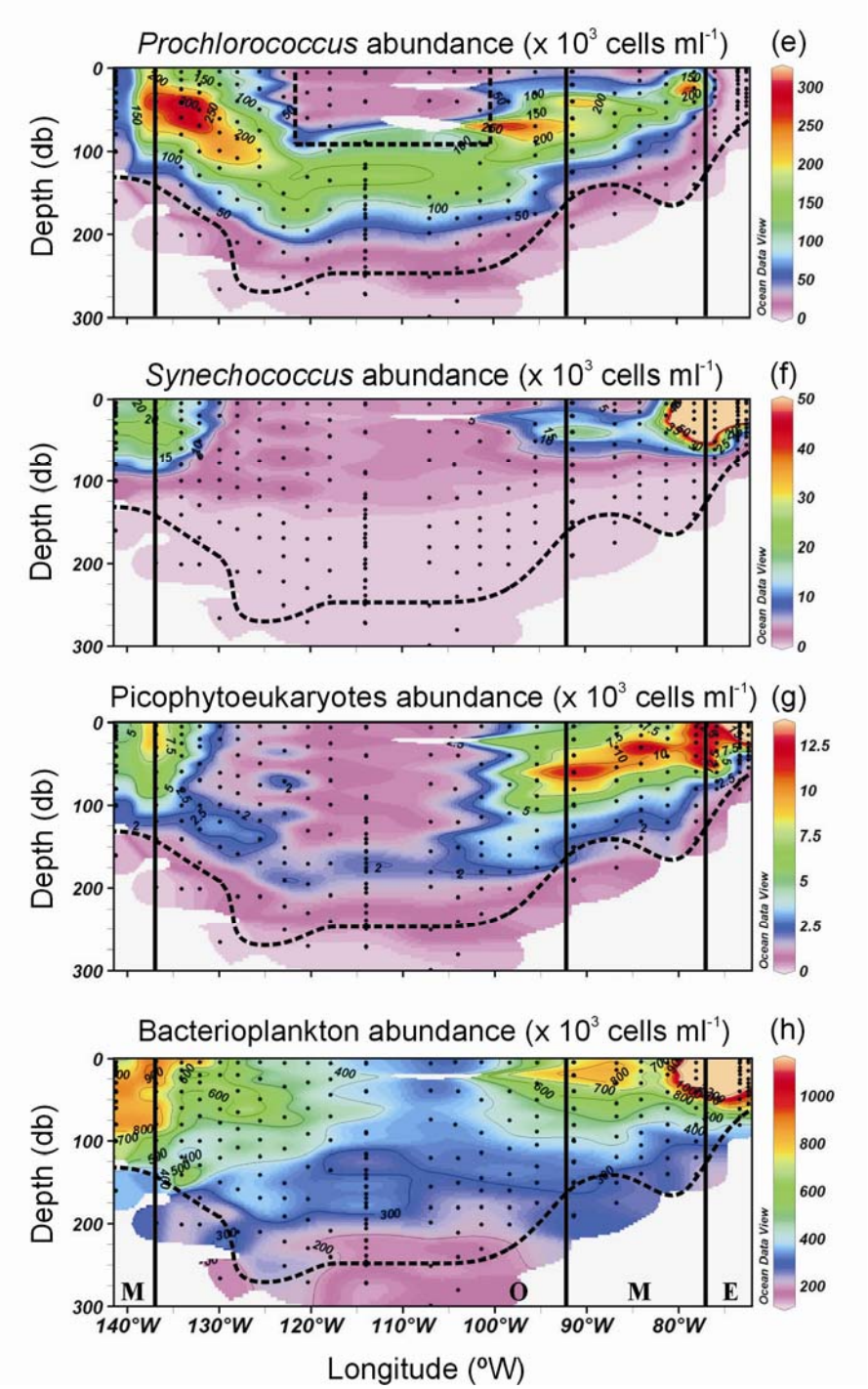

Fig. 4. Continued…

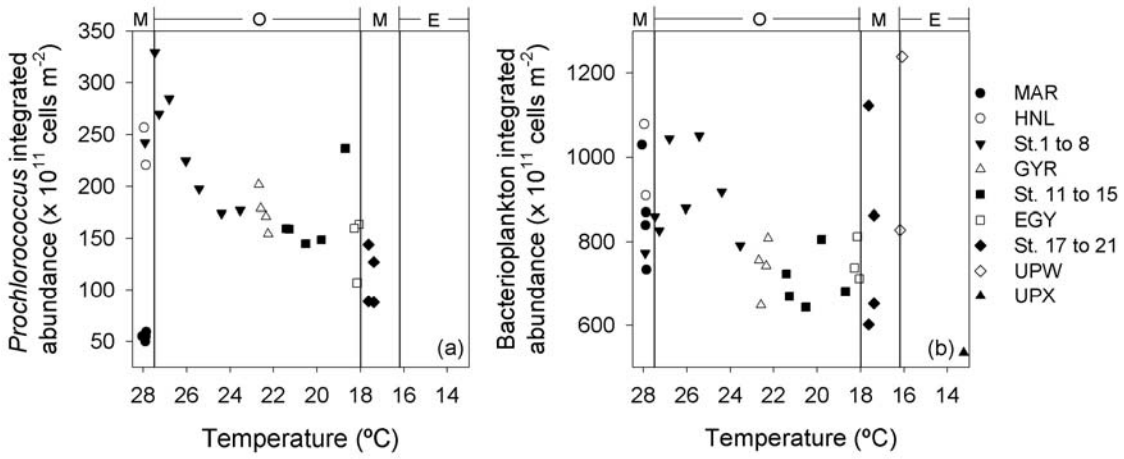

Fig. 5. *Prochlorococcus* (a), and bacterioplankton (b) integrated abundances (0 to 1.5 Ze, x 10^{11} cells ml^{-1}) as a function of surface temperature, which was representative of the general eastward decrease in water temperature within the integration depth (0 to 1.5 Ze) along the transect. Vertical lines indicate the limits established between meso- (M), oligo- (O) and eutrophic (E) conditions.

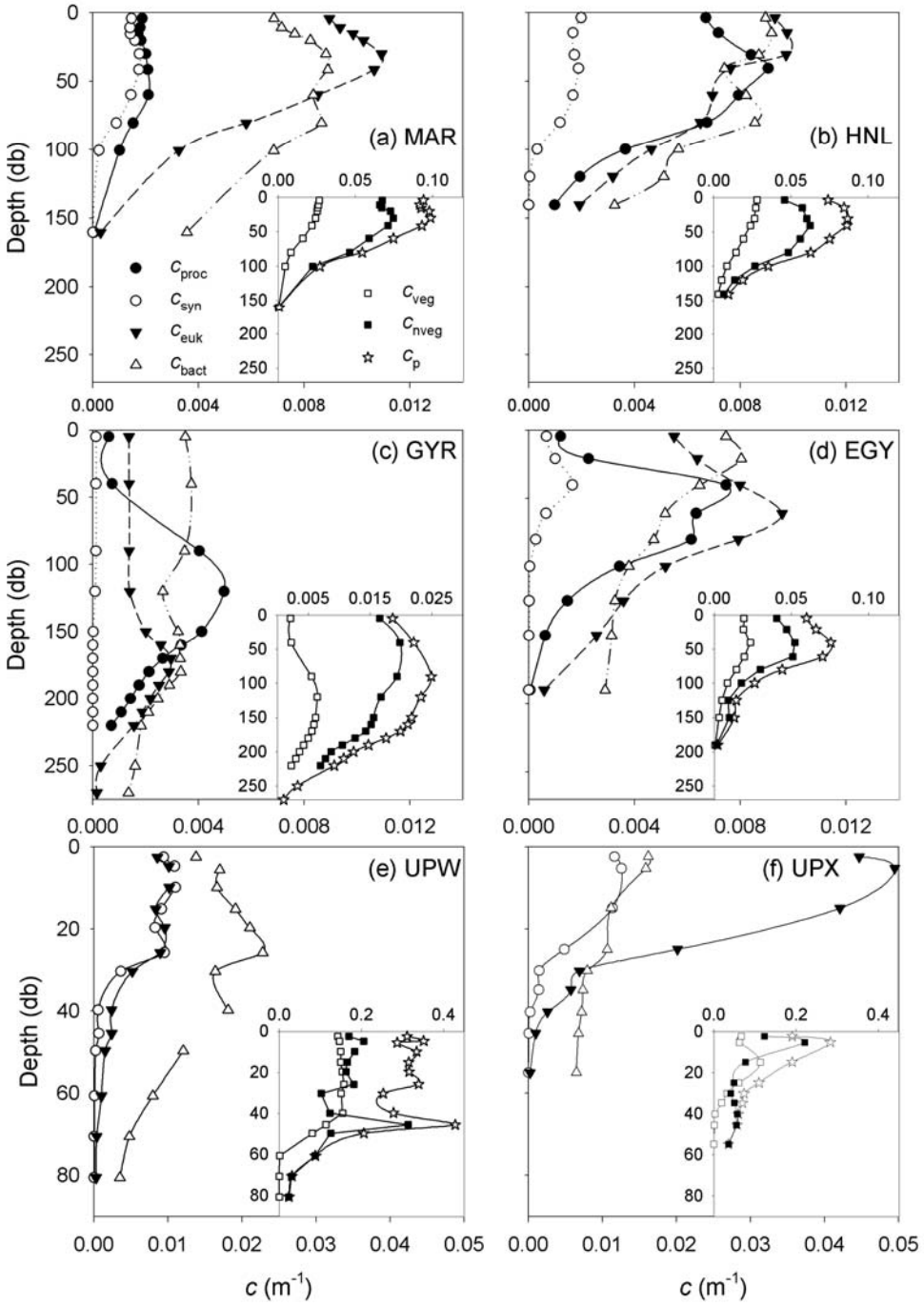

Fig. 6. Mean group-specific particle beam attenuation coefficients for *Prochlorococcus* (c_{proc}), *Synechococcus* (c_{syn}), picophytoeukaryotes (c_{euk}), bacterioplankton (c_{bact}). Insets contain the vegetal (c_{veg}), non-vegetal (c_{nveg}), and total particulate attenuation coefficients (c_p) in m^{-1}. For MAR (a), HNL (b), GYR (c), EGY (d), UPW (e) and UPX (f). Note that UPW and UPX scales are equal to each other and different from the rest. For MAR, HNL, GYR and EGY all scale are the same except for GYR's c_p, c_{veg} and c_{nveg}.

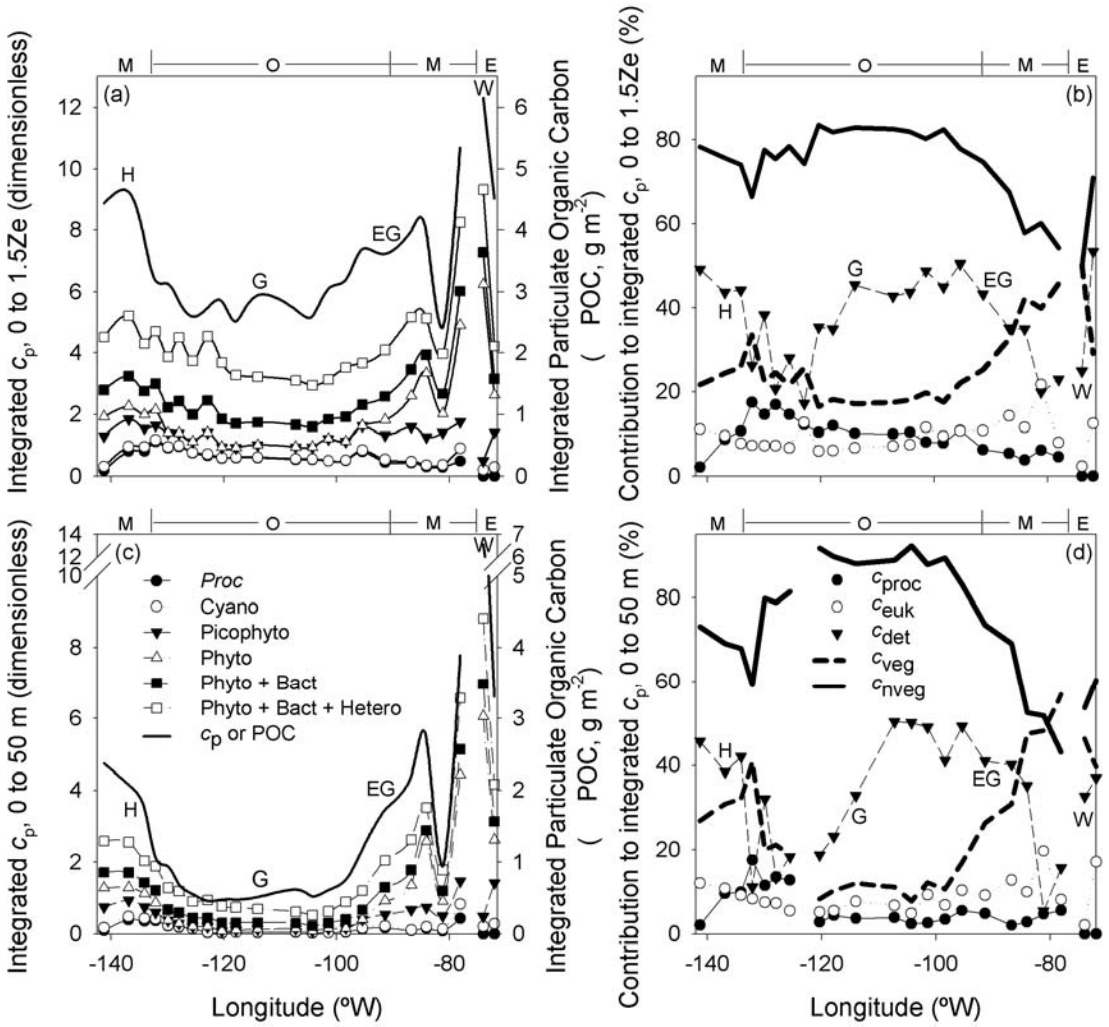

Fig. 7. Integrated attenuation coefficients for *Prochlorococcus* (*Proc*), *Proc* + *Synechococcus* (Cyano), Cyano + picophytoeukaryotes (Picophyto), Picophyto + nanophytoplankton (Phyto), Phyto + bacterioplankton (Phyto + Bact), Phyto + Bact + heterotrophic protists (Phyto + Bact + Hetero) and Phyto + Bact + Hetero + detritus (c_p) in the 0 to 1.5 Ze layer (a) and the 0 to 50 m layer (c). The contributions by *Prochlorococcus* (c_{proc}), picophytoeukaryotes (c_{euk}), detritus (c_{det}), vegetal (c_{veg}) and non-vegetal (c_{nveg}) to the corresponding total integrated attenuation coefficients are shown in (b) and (d). The top black lines in (a) and (c) correspond to the total integrated particle beam attenuation coefficient (c_p, left hand axis) and particulate organic carbon concentration (POC, right hand axis) estimated from c_p using Claustre et al. (1999) relationship (see Section 2.2; Eq. 5). M, O and E stand for meso-, oligo- and eutrophic conditions (top of each panel). H, G, EG and W indicate HNL, GYR, EGY and UPW stations.

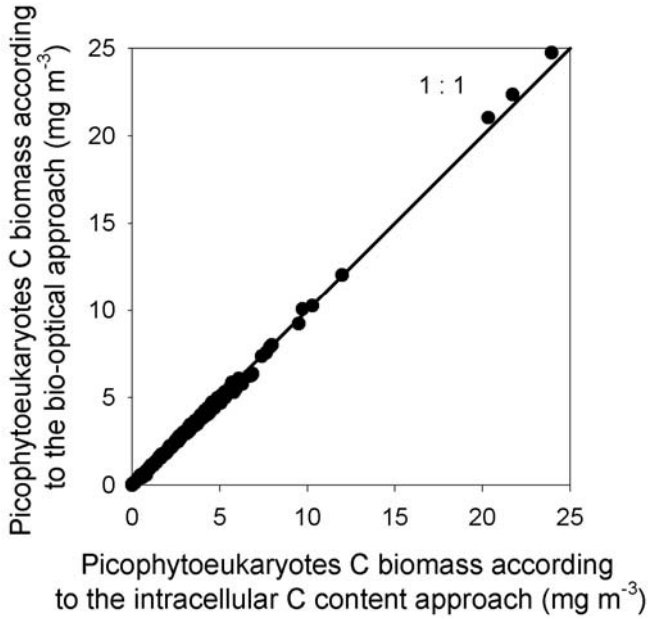

Fig. 8. Picophytoeukaryotes carbon biomass estimated from intracellular carbon content (see Section 2.1) compared to that estimated by calculating c_{euk} contribution to c_p, the latter assumed to be equivalent to POC (see Section 2.2). Note that both approaches gave very similar results. 1 : 1 indicates the 1-to-1 line relating both estimates.

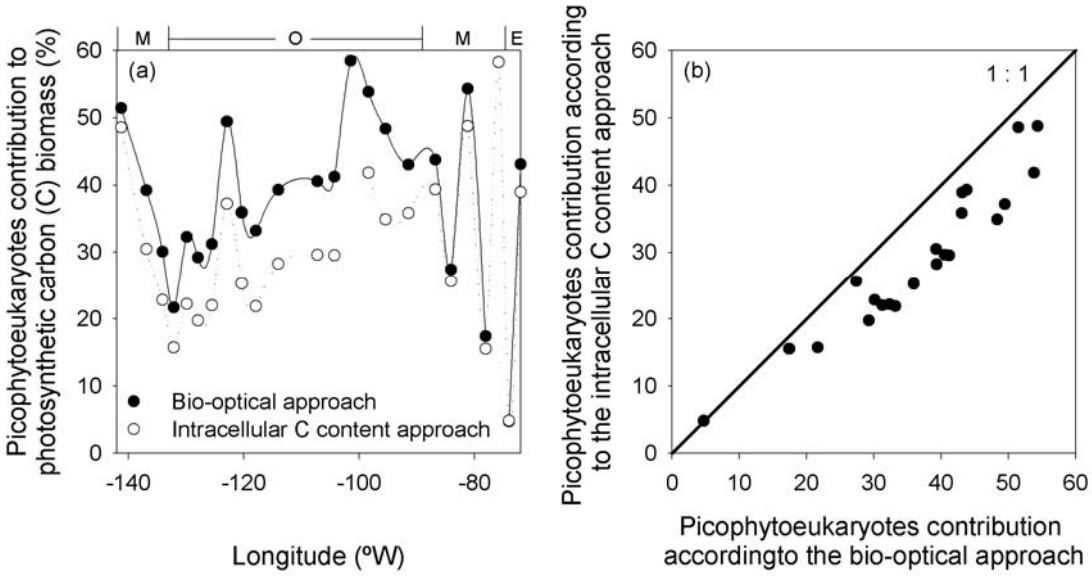

Fig. 9. Picophytoeukaryotes contribution to the photosynthetic carbon biomass as derived from c_{euk}'s contribution to c_{veg} by applying Eq. 5 (bio-optical method) and as obtained using intracellular carbon contents in Fig. 3b to estimate picophytoplankton carbon biomass (a). When comparing the results obtained using both approaches, it can clearly be seen that the contributions estimated using the intracellular carbon (C) content approach are lower than those estimated using the bio-optical approach, with almost all data points being below the 1-to-1 line relating both estimates (b).

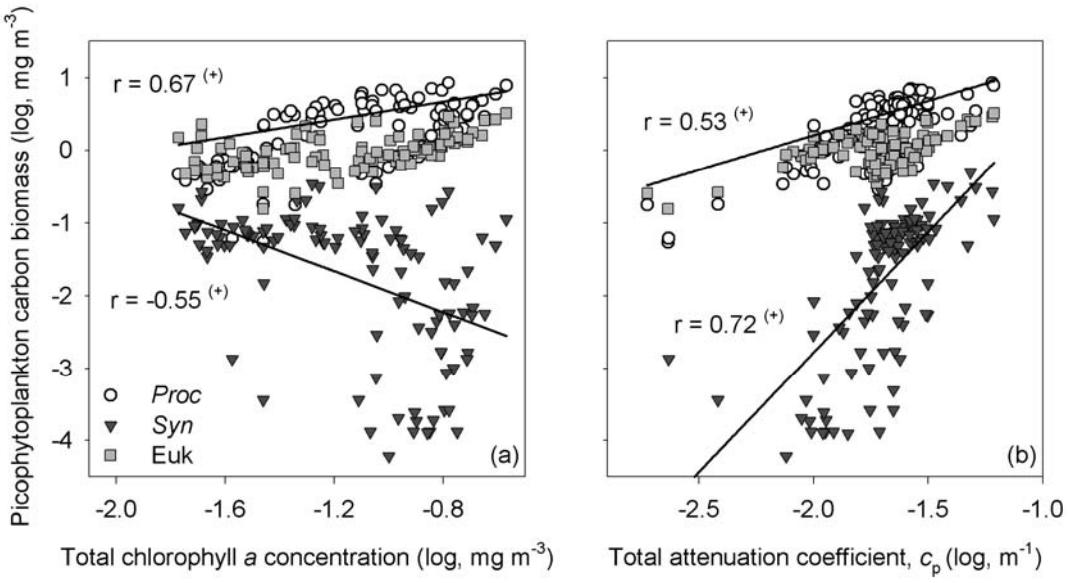

Fig. 10. Log-log relationships for *Prochlorococcus* (*Proc*), *Synechococcus* (*Syn*) and picophytoeukarytos (Euk) carbon biomass (mg m^{-3}) with total chlorophyll *a* concentration in mg m^{-3} (a) and total particulate attenuation coefficient in m^{-1} (b). Only data from Stations 3 to 15 and GYR and between the surface and 1.5 Ze are included (see Section 2.2). Correlation coefficients (r) were calculated for the sum of *Proc* and Euk (upper values) and for *Syn* carbon biomass (lower values) with Tchl*a* (a) and c_p (b). $^{(+)}$ indicates $p < 0.001$.

CHAPTER 5

DISCUSSION AND CONCLUSIONS

5. DISCUSSION AND CONCLUSIONS

It has been known since the early eighties that picophytoplankton constitutes an important fraction of the total photosynthetic biomass and primary production in the open ocean. For the eastern tropical Pacific, Li et al. (1983) reported contributions to biomass and PP in the range of 25 to 90% and 20 to 80%, respectively. In 1988, Li & Wood reported that in the central North Atlantic the picophytoplankton was numerically dominated by very small-fluorescing bodies detected through flow cytometry. That same year these cells were identified as prochlorophytes (Chisholm et al., 1988). The unexpectedly large prochlorophyte abundance lead to the paradigm that open-ocean carbon biomass and production in the < 2-μm size fraction is dominated by this group.

Studies on group-specific carbon biomasses and primary production have revealed, however, that the contribution by picophytoeukaryotes can in some cases be very important. Already in the early nineties, Li et al. (1992 & 1993) showed that in terms of carbon biomass, eukaryotic phytoplankton (usually < 3.4 μm) dominated the ultraplankton (< 5 μm) photosynthetic biomass in the northern Sargasso Sea (Li et al., 1992) and in the eastern Mediterranean Sea (Li et al., 1993). Zubkov et al. (1998 & 2000) found that, across the North and South Atlantic Subtropical Gyres, picophytoeukaryotes constituted a considerable fraction of the picophytoplanktonic carbon biomass.

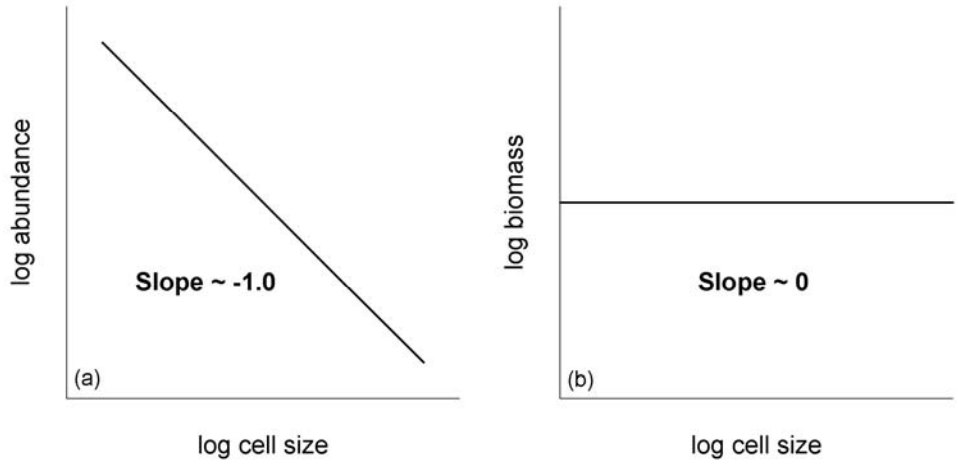

Fig. 17. Schematic representation of the log-log relationships between mean cell size and abundance (a) and between mean cell size and carbon biomass (b) expected from ecological theory.

All of the above agrees with ecological theory, which states that smaller cells (e.g., *Prochlorococcus*) are much more abundant than larger ones (e.g., picophytoeukaryotes), whereas in terms of carbon biomass the difference between size classes is expected to be small. In other words, whereas the slope of the log-log relationship between cell size and abundance usually approaches -1 (Fig. 17a; Chisholm, 1992), the slope of the relationship between size and carbon biomass is expected to be close to 0 (Fig. 17b; Sheldon et al., 1972).

Specific rates of pigment synthesis, a proxy for specific growth rates, have been estimated through carotenoid-^{14}C labeling experiments at the class and higher taxonomic levels (Goericke & Welschmeyer, 1993) for different size fractions (Goericke, 1998). For instance, using this approach Goericke (1998) estimated rates of carbon fixation for cyanobacteria (i.e., *Prochlorococcus* + *Synechococcus*) from the ^{14}C labelling of zeaxanthin, their characteristic pigment. At the group-specific level, on the other hand, *in situ* growth rates for synchronized *Prochlorococcus* populations have been estimated using cell cycle analyses (Vaulot et al., 1995). Unfortunately, this approach has been applied without success to determine *Synechococcus* growth rates (D. Marie, *pers. comm.*).

Using flow cytometry cell sorting combined with ^{14}C measurements, Li (1994) took one step forward and made the only simultaneous group-specific primary production rates measurements available in the literature for *Prochlorococcus*, *Synechococcus* and picophytoeukaryotes. Even though he could only apply this methodology at 3 different stations in the North Atlantic Ocean and at a single depth per station (see Chapter 6), Li (1994) results showed that picophytoeukaryotes contribution to picophytoplankton primary production increased as the *Prochlorococcus* to picophytoeukrayotes abundances ratio decreased. Through dilution experiments, Worden et al. (2004) also reported the highest picophytoplankton growth rates and contributions to the net community production and carbon biomass for the picophytoeukaryotes, this time in the Southern California Bight (coastal Pacific site) and on annual bases.

It was not until the year 2001, however, that molecular-based studies revealed an unexpected diversity within this group in the equatorial Pacific (Moon-van der Staay et al., 2001) and deep Antarctic (López-García et al., 2001) oceans. It was latter shown that in the English Channel the picophytoeukaryotic compartment is mainly dominated

by the division Chlorophyta (Not et al, 2002), with *Micromonas pusilla* being the most represented species (Not et al., 2004). *Micromonas*-like cells would also dominate this group in an oligotrophic Mediterranean site during certain periods of the year (J. Gasol, *pers. comm.*). The same kind of cells, as well as *Ostreococcus sp.* and *Bathycoccus sp.* have been identified in a coastal Pacific site located in the Southern California Bight (Worden et al., 2004; Worden, 2006). Nevertheless, very little is known about the real magnitude of picophytoeukaryotes genetic diversity since new clusters within this group are discovered every day under different trophic conditions (e.g., Not et al., 2007; R. Massana, *pers. comm.*).

Flow cytometry data on picoplankton abundance has been collected at a sufficiently large scale to make macroecological analyses applicable (e.g., Li, 2002; Li et al., 2004; Li, *in press*). However, large-scale studies based on group-specific carbon biomasses distribution in the open ocean are still lacking. In the present thesis work, picoplankton carbon biomasses across the eastern South Pacific were assessed using cytometrically-derived cell abundances and applying conversion factors from the literature (first part) or estimating group-specific contributions to c_p, a proxy for POC (second part). The overall work focused on the picophytoeukaryotes, the least known picophytoplanktonic group, because of their potential role in carbon production and cycling suggested by the limited information available for this group (see above).

5.1 Picoplankton abundances and distribution

The general tendency observed in picoplankton abundances across the eastern South Pacific was consistent during both cruises, increasing from oligo- (or hyper-oligo-) to mesotrophic conditions with a slight decrease towards eutrophic conditions, except for *Prochlorococcus* that was not detected in the latter (see Chapters 3 and 4). This general trend is in accord with what has been reported elsewhere (e.g., Partensky et al. 1996; Zubkov et al. 1998 & 2000; Shalapyonok et al. 2001; Worden et al. 2004). Whereas *Synechococcus* water-column integrated abundances were very similar during both cruises (Fig. 18b), those of picophytoeukaryotes were slightly higher during BIOSOPE in the eastern oligo- and mesotrophic regions (Fig. 18c). Under oligotrophic conditions, on the other hand, *Prochlorococcus* (Fig. 18a) and bacterioplankton (Fig. 18d) abundances were clearly more important during the BIOSOPE cruise.

In the case of *Prochlorococcus* and picophytoeukaryotes, the higher integrated abundances estimated during BIOSOPE can be attributed to the important subsurface maximum observed during this cruise in the oligotrophic region (see Fig. 4 in Chapter 4) and that was not detected during BEAGLE (see Fig. 3 in Chapter 3). In the same region, deep bacterioplankton abundances were much higher during BIOSOPE, probably due to the presence of the picophytoplankton subsurface maxima that could be fueling this group with DOC.

Prochlorococcus populations have been studied well enough to be able to explain their abundances distribution in terms of their physiology, ecology, diversity and phylogeny (e.g., Partensky et al., 1999b and references therein). For instance, the success of this group in colonizing oligotrophic regions has been attributed to the fact that they would grow on organic nitrogen compounds (Zubkov et al., 2003), such as amino acids (e.g., Zubkov et al., 2004 & 2005), rather than on nitrate (e.g., Moore et al., 2002). The presence of an important subsurface abundance maximum in such environments, such as the one observed during BIOSOPE, seems to be a common feature in the oligotrophic open ocean (e.g., Campbell & Vaulot, 1993; Vaulot & Marie, 1999). This feature has been attributed to the presence of a low light-adapted ecotype, different from the high-light-adapted one that dominates in surface populations (e.g., Partensky et al., 1999b and references therein). Finally, *Prochlorococcus* growth rates would be inhibited at temperatures below 10ºC and at high mixing levels (e.g., Partensky et al., 1999a and references therein) such as the ones observed at the coast, where this group was not detected. Thus, *Prochlorococcus* abundance distribution across the eastern South Pacific followed a general pattern that agrees well with what is already known about this group's ecology, physiology and genetic diversity.

The shallower depths reached by *Synechococcus*, on the other hand, have been associated with a limitation by low irradiances for this organism. Although the role of nutrients in determining this group's abundance distribution is less clear (e.g., Partensky et al, 1999a), *Synechococcus* does tend to increase towards higher nutrient concentrations (Fig. 18b). Furthermore, both light and nutrients have been suggested as important factors determining ecotype differentiation in this group (e.g., Ahlgren & Rocap, 2006). Far less is known on the factors controlling picophytoeukaryotes distribution. Based on the positive correlations found between this group's abundances and those of *Synechococcus*, which were also observed in the present work (see

Chapters 3 and 4), it has been hypothesized that these two groups would have similar nutrient requirements (e.g., Worden et al., 2004). However, direct studies on *in situ* picophytoeukaryotes nutrient's metabolism are lacking. Even though there has been a few laboratory works dealing with picophytoeukaryotic physiology for certain species (e.g., Timmersman et al., 2005; Rodríguez et al., 2005), these results cannot be readily extrapolated to the field, since the taxa present within this heterogeneous group are mostly unknown.

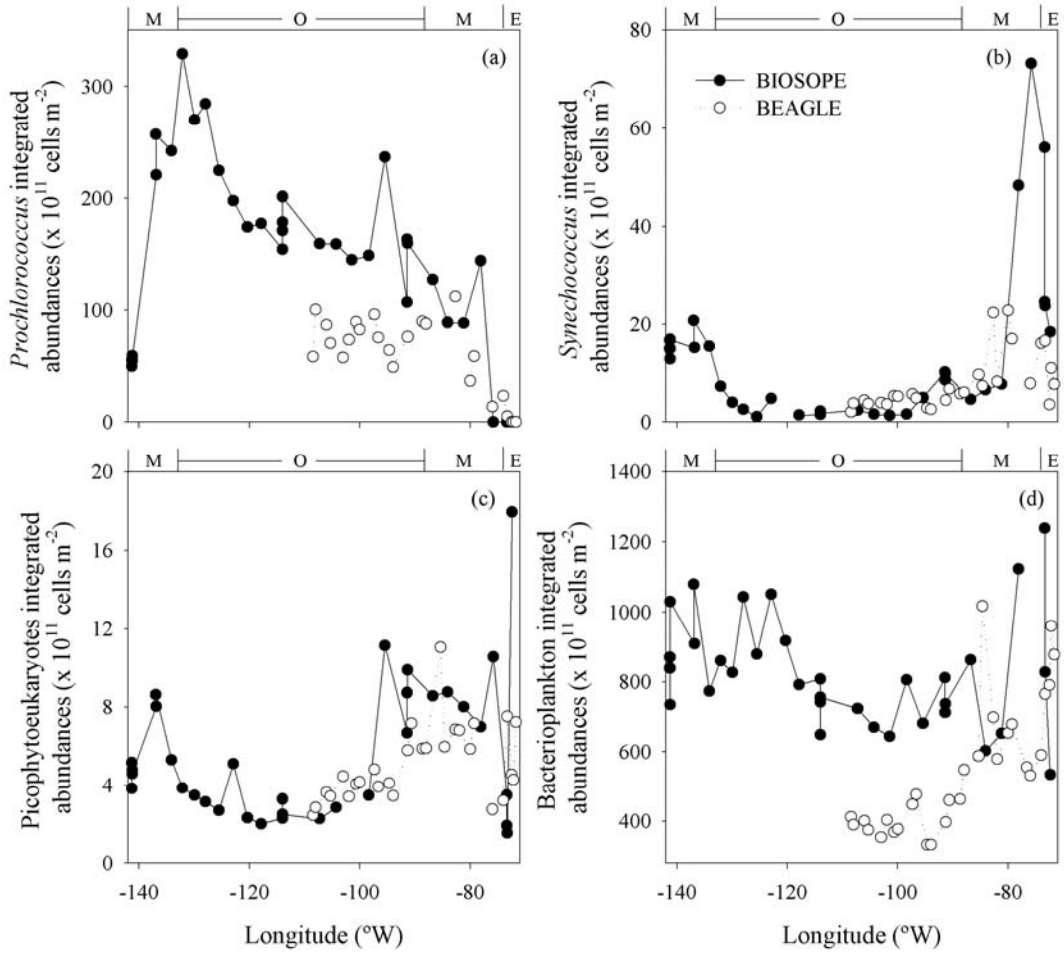

Fig. 18. Water-columned integrated *Prochlorococcus* (a), *Synechococcus* (b), picophytoeukaryotes (c) and bacterioplankton abundances (x 10^{11} cells m^{-2}) estimated during both cruises. Although during the BEAGLE cruise the data was integrated between the surface and 200 m, the abundances registered below 200 m were negligible enough for these results to be comparable to those integrated between the surface and 1.5 Ze during BIOSOPE.

The deep picophytoeukaryotes abundance maximum observed at the centre of the gyre during BIOSOPE has also been reported for other oligotrophic sites (e.g., Li et al., 1992 & 1993; Vaulot & Marie, 1999; Veldhuis et al., 2005). Pigment data indicates that picophytoeukaryotes within this subsurface maximum corresponded mainly to

Prymnesiophytes (Ras et al., *submitted*). However, it is not possible to say if such subsurface maximum is due to the presence of different taxa or only to different ecotypes. Again, although the occurrence of different ecotypes has been reported for *Ostreococcus tauri* populations isolated from different environments and depths (Rodríguez et al., 2005), there is little information on the distribution of this species in the open ocean. It is therefore not possible to establish the origin of the observed subsurface maximum (different taxa v/s different ecotypes) without previously identifying the groups that are present there.

A very interesting feature observed during the present work is that picophytoeukaryotes within the subsurface maximum, located around 160-170 m, increased in abundance during the 4 days of sampling at the GYR station (Fig. 19a), associated with an important increase in light availability (Fig. 20). This is remarkable, since at this depth nitrate concentrations are still at minimum levels ($\leq$ 1 μmol L^{-1}). It was mentioned above that *Prochlorococcus* would not grow on nitrate (e.g., Moore et al., 2002), so the fact that this group's abundance increased with increasing light availability is not surprising (Fig. 19b & Fig. 20), since at this depth they would be expected to be limited by light. The similar behavior observed in picophytoeukaryotes suggests that, like *Prochlorococcus* (e.g., Moore et al., 2002), this group could be growing on nutrients other than nitrate and their main limiting factor at this depth could also be light. The above has been shown for at least one picophytoeukaryotic group, i.e., *Aureococcus anophagefferens*, which was able to grow on high-molecular weight dissolved organic nitrogen (Berg et al., 2003). However, the ability of the picophytoeukaryotes to grow under such conditions could also be related to the capacity of eukaryotic cells to concentrate nutrients in internal vacuoles that are not present in prokaryotes. This group could therefore have stored nutrients in these vacuoles during periods where light availability was insufficient to grow and then used them when light increased. A decrease in the grazing pressure on *Prochlorococcus* and picophytoeukaryotes cannot be ruled out, although there is no information available regarding this matter. Nevertheless, the ecological and biogeochemical role of picophytoeukaryotes in the deep oligotrophic ocean could be as important as that of *Prochlorococcus*. Until now, this cyanobacterium is believed to be the most important picophytoplanktonic group in such environments.

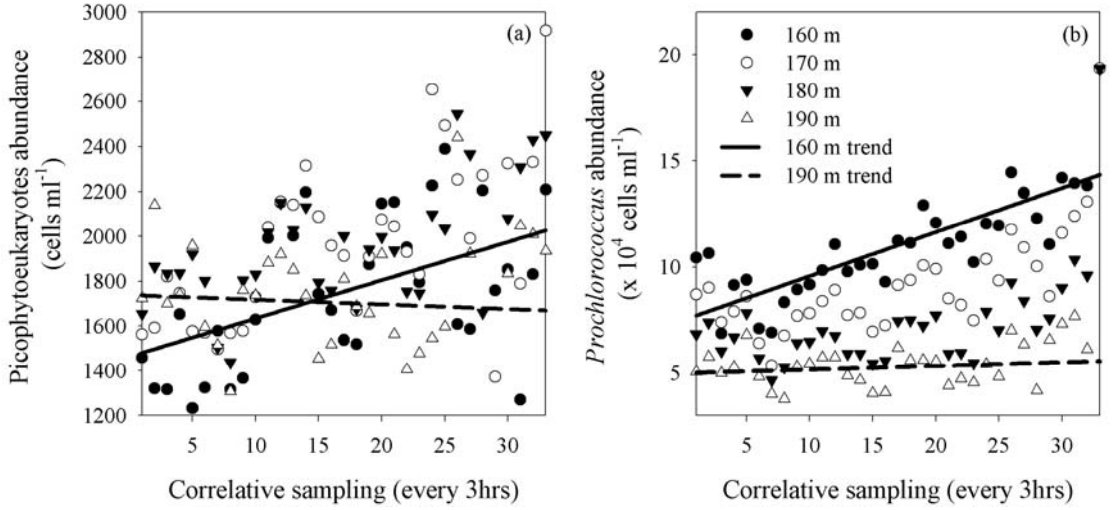

Fig. 19. Picophytoeukaryotes (a) and *Prochlorococcus* (b) general increasing trends observed at 160-170 m (solid lines) as a response to an increase in light availability during the 4 days of sampling at GYR station (see Claustre et al., *submitted*). The slightly negative (a) and almost negligible (b) trends observed at 190 m (dashed lines) are presented to highlight the increases observed at 160-170 m. Each dot corresponds to one data point.

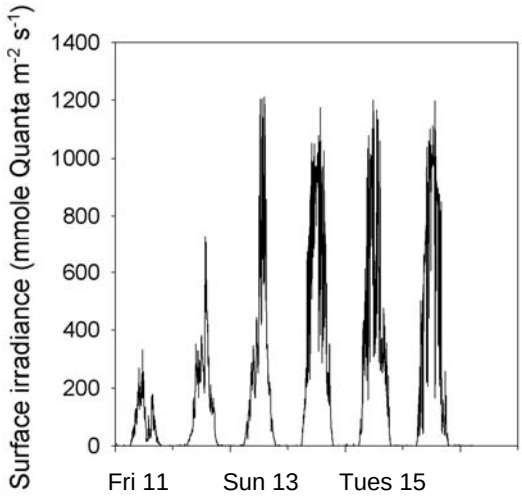

Fig. 20. Surface irradiance (mmole quanta m-2 s-1) the day before arriving to GYR station (Fri, Friday 11th) and during the 4 days of sampling at this station (Monday 12th to Wednesday 16th), November 2003. From Claustre, *pers. comm.*

5.2 Picoplankton carbon biomasses and contributions to total particulate organic carbon (POC)

In the first part of this thesis work picoplankton carbon biomasses were estimated using cell-specific conversion factors from the literature (Chapter 3). In the second part, however, these biomasses were estimated from group-specific particle beam attenuation coefficients (optically-based approach), assuming that all group's contributions to c_p were equivalent to their contributions to POC, an assumption proven to be valid for the picophytoeukaryotes (Chapter 4). In both cases the conclusion was the same:

picophytoeukaryotes represent a significant fraction of the picophytoplanktonic carbon biomass (> 50% in most of the study area), as well as a non-negligible fraction of the total picoplanktonic carbon biomass (~20 and 55%) across the eastern South Pacific.

The carbon conversion factors from the literature used for oceanic picophytoplankton during the BEAGLE cruise were, however, 2 times higher than the mean intracellular carbon contents estimated during BIOSOPE. The above implies that *Prochlorococcus*, *Synechococcus* and picophytoeukaryotes absolute carbon biomasses were overestimated by 100% during BEAGLE. Such overestimations would result in picophytoplankton contributions to the total POC concentrations observed during BIOSOPE in the order of 40 to 100% instead of 20 to 50% (see Fig. 7, Chapter 4) across the eastern South Pacific. A 100% picophytoplankton contribution to the entire POC pool leaves no room for the presence of bacterioplankton, heterotrophic flagellates and detritus in the water column, which is unrealistic. It is therefore necessary to highlight the importance of using *in situ* measurements instead of using conversion factors from the literature in order to reasonably estimate picophytoplankton carbon biomass.

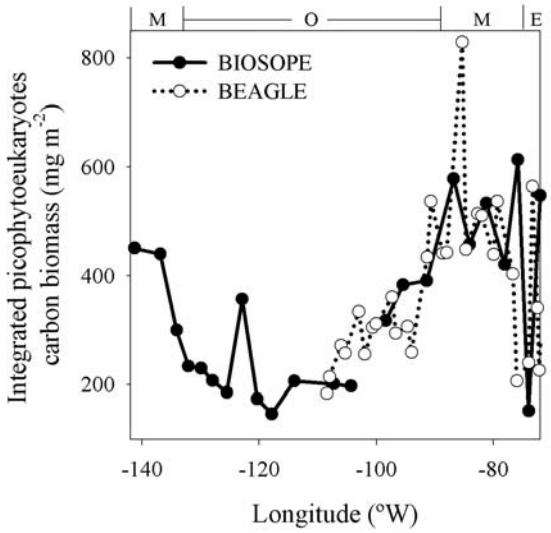

Fig. 21. Water-column integrated picophytoeukaryotes carbon biomasses estimated across the eastern South Pacific. In order to compare the data from both cruises, BEAGLE data were divided by 2, according to the mean picophytoeukaryotes intracellular carbon content estimated during BIOSOPE. The latter was 2 times lower than the conversion factors from the literature used during the BEAGLE cruise. O, M and E (top of the figure panel) stand for oligo-, meso- and eutrophic conditions.

Given the 2-fold difference observed between carbon biomasses estimated during BEAGLE and BIOSOPE, in order to compare the results obtained during both cruises for picophytoeukaryotes we divided the open-ocean results obtained during BEAGLE by 2. The resulting picophytoeukaryotes carbon biomasses were very similar to those estimated during BIOSOPE (Fig. 21), consistent with their abundances distribution in both cases (see above). Integrated biomasses varied between 200 and 600 mg m^{-2}, except for one BEAGLE station (~85ºW; Fig. 21), where cell abundance was

particularly high. The lowest biomasses were always detected under oligotrophic conditions (Fig. 21). It is worth noticing that even though the BEAGLE data were integrated between the surface and 200 m, the abundances registered below 200 m were negligible enough for biomasses to be comparable to those integrated between the surface and 1.5 Ze during BIOSOPE.

Picophytoplankton carbon biomasses were overestimated by a factor of 2 during the BEAGLE cruise. Assuming that this was also the case for bacterioplankton, then the contributions by picophytoeukaryotes to picoplankton and picophytoplankton carbon biomasses estimated during both cruises can be compared as well (Fig. 22). The first hypothesis of this thesis stated that the spatial variability of picophytoplanktonic carbon biomass in the euphotic zone of the eastern South Pacific is essentially determined by the picophytoeukaryotes. The overall results show that picophytoeukaryotes constitute an important fraction of the integrated picoplankton, picophytoplankton and total phytoplankton carbon biomasses (Fig. 22), in all cases more important than previously thought. This group constituted more than 50% of the total picophytoplankton carbon biomass in most of the transect, except for the hyper-oligotrophic centre of the gyre sampled during BIOSOPE (Fig. 22).

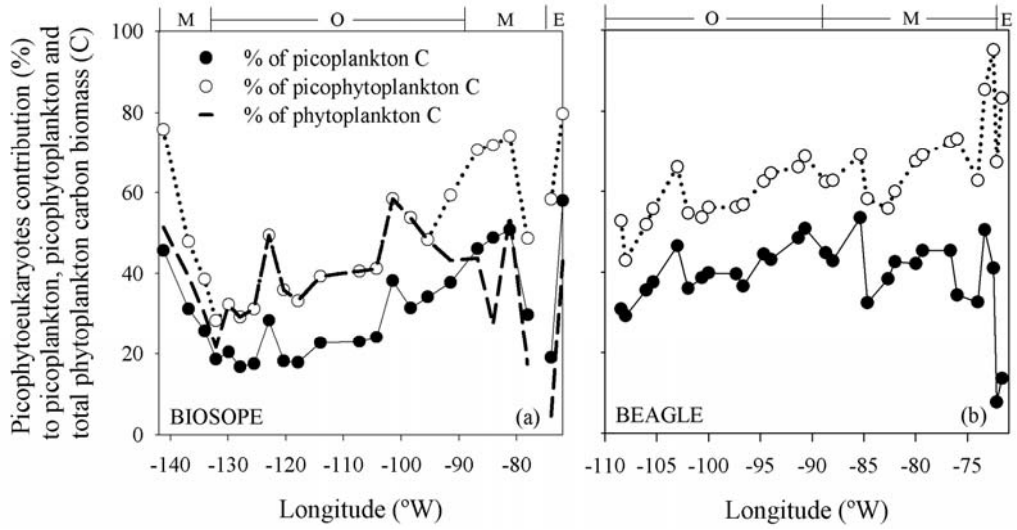

Fig. 22. Picophytoeukaryotes contribution to integrated picoplankton (filled circles and solid line) and picophytoplanktonic (empty circles and dotted line) carbon biomass (C) during the BIOSOPE (a) and BEAGLE (b) cruises. For the BIOSOPE cruise (a), picophytoeukaryotes contribution to total phytoplankton carbon biomass (dashed line) is also presented. Note that BEAGLE integrated data starts at 110ºW, whereas that of BIOSOPE begins at 142ºW.

On the light of these results, it can therefore be said that picophytoeukaryotes are indeed essential in determining the spatial variability on picophytoplankton biomass across the eastern South Pacific (Fig. 22), and the first hypothesis can hence be accepted. Picophytoeukaryotes contribution to picoplankton carbon biomass, on the other hand, varied between a minimum of ~20% at the hyper-oligotrophic centre of the gyre and ~55% at the coastal- most station sampled during the BIOSOPE cruise (Fig. 22a), whereas it was quite stable at around 40% during BEAGLE (Fig. 22b). The above implies that the spatial variability on the picoplanktonic carbon biomass can, in some cases, also be determined by the picophytoeukaryotes.

5.2.1 Spatial variability in group-specific contributions to total particulate organic carbon (POC)

Group-specific contributions to the total particulate organic carbon (POC) were estimated from their contributions to the total particle beam attenuation coefficient (c_p) during the second part of the present work only. Across the eastern South Pacific c_p, and therefore POC, was dominated in magnitude by the non-vegetal compartment (50 to 83%; see Chapter 4). Nevertheless, the spatial variability in the vegetal compartment was more important in shaping this inherent optical property in the water column (see Chapter 4). Picophytoeukaryotes being a non-negligible fraction of the open-ocean vegetal compartment (39 to 51%), the conclusion is that this group was important in determining the spatial variability in c_p across the eastern South Pacific (see Chapter 4).

The lack of spatial variability in the non-vegetal compartment relative to c_p can clearly be seen when comparing this coefficient's ratios to c_{veg} and c_{nveg} (Fig. 23). The non-vegetal compartment is constituted by bacterioplankton, heterotrophic protists and detritus. Within this compartment, c_{bact}'s variability across the open ocean trophic gradient studied was, as expected (e.g., Oubelkheir et al., 2005), lower than that of phytoplankton (see Chapter 4). Consequently, c_{het}'s variability was also low (see Eq. 4). c_{det} being obtained by difference (Eq. 5), its variability is expected to be determined by the contributors to c_p with larger variability. The almost negligible variability (relative to c_p) in c_{nveg} compared to c_{veg} is therefore not surprising.

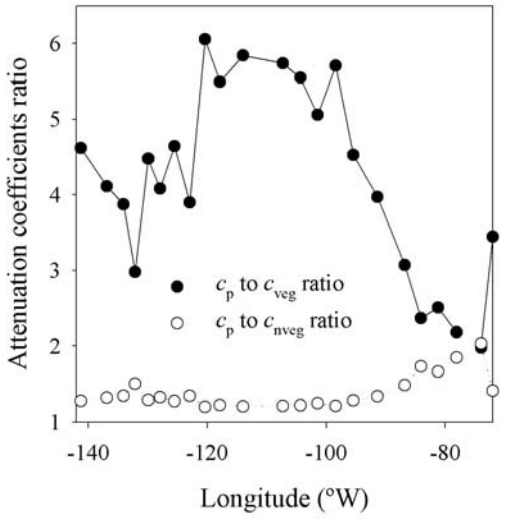

Fig. 23. Total particle beam attenuation coefficient (c_p) ratios to the vegetal compartment attenuation coefficient (c_{veg}) and to the non-vegetal compartment attenuation coefficient (c_{nveg}). Notice the much higher variability in the c_p to c_{veg} ratio. Data from the BIOSOPE cruise.

The results presented in Chapter 4 also showed that the spatial variability in open-ocean picophytoplankton carbon biomass can be equally well traced by changes in Tchl*a* (Tchl*a*, mono+divinyl chlorophyll *a*) and c_p (see Fig. 8 in Chapter 4). Such conclusion was drawn from the fact that both correlation coefficients were not significantly different from a statistical point of view ($p > 0.05$, t-test on the z-transform of the correlation coefficient; Zokal & Rohlf, 1994). Unlike c_p, chlorophyll *a* is unique to phytoplankton and has been universally used to estimate primary production. c_p has the advantage, however, of being insensitive to changes in intracellular chlorophyll content. Across the eastern South Pacific c_p seems to be a good proxy for the dominant photosynthetic carbon biomass. However, the applicability of this proxy to larger spatial scales is still controversial. For instance, when comparing the performance of diverse proxies for phytoplankton biomass, Huot et al. (*submitted*) came to the conclusion that Tchl*a* was more efficient than c_p. Beherenfeld & Boss (2003 & 2006), on the other hand, found that c_p was a good proxy for the autotrophic carbon biomass in surface oceanic waters.

Although our results indicate that both Tchl*a* and c_p are good proxies for the photosynthetic biomass, it is important to point out that in order to estimate such biomass from c_p it is necessary to have information or make some assumptions on the contributions by vegetal and non-vegetal particles to this coefficient. In this regard, Oubelkheir et al. (2005) found that the contribution to c_p by phytoplankton was equivalent under different trophic conditions. However, this was not the case across the eastern South Pacific, where phytoplankton contribution to integrated c_p varied between

~20 and 55%. In this case, an empirical relationship was established between c_p and the picophytoplankton biomass dominating the oceanic region of the eastern South Pacific. By using this relationship it would be possible to estimate the photosynthetic carbon biomass at the very high vertical resolution for which c_p measurements are available. The limitations and errors associated with this approach are determined by the variance in the relationship established. Tchl*a* measurements, on the contrary, are only available at discrete depths.

Establishing a direct relationship between c_p and the photosynthetic carbon biomass for the entire ocean would therefore not be straight forward. However, because of the advantages of determining c_p over Tchl*a* in terms of time and expenses, further research should be done to test the ability of c_p in tracing phytoplankton biomass in the ocean.

5.2.2 Temporal variability

Diel cycles

High frequency samplings to address diel variability were only performed during the BIOSOPE cruise. Of the 5 long stations sampled, however, marked diel cycles on picophytoplanktonic groups were only observed at MAR (Fig. 24). In the other long stations, the data did not follow a pattern clear enough to determine, for instance, when abundances stopped decreasing and when they started increasing, like it could clearly be seen for picophytoeukaryotes at MAR (Fig. 24a). For this reason, picophytoeukaryotes' contribution to the diel variability in total particulate organic carbon (POC) concentration could only be evaluated in this mesotrophic station.

In the present work it was assumed that diel changes in picophytoeukaryotes attenuation cross-section were mainly driven by changes in cell size and not in the refractive index, as observed in *Nannochloris sp.* (DuRand & Olson, 1998) and *Micromonas pusilla* (DuRand et al., 2002) from culture. At the surface (5 m), the estimated attenuation cross-sections (σ_c) varied from a minimum of 1.29 m^2 $cell^{-1}$ at 6 h and a maximum of 2.36 m^2 $cell^{-1}$ at 15 h (Fig. 24b), corresponding to a ~84% increase. However, since cell abundance followed the exact opposite pattern of σ_c, the resulting group-specific attenuation coefficients (i.e., $c_{euk} = \sigma_c$ x cell abundance; see Chapter 2.3.1) increased only 37.5%. It is worth noticing that picophytoeukaryotes σ_c followed the same pattern between the surface and 60 m, with similar differences between the morning minimum

and the afternoon maximum above 30 m and lower differences below this depth (Fig. 24b).

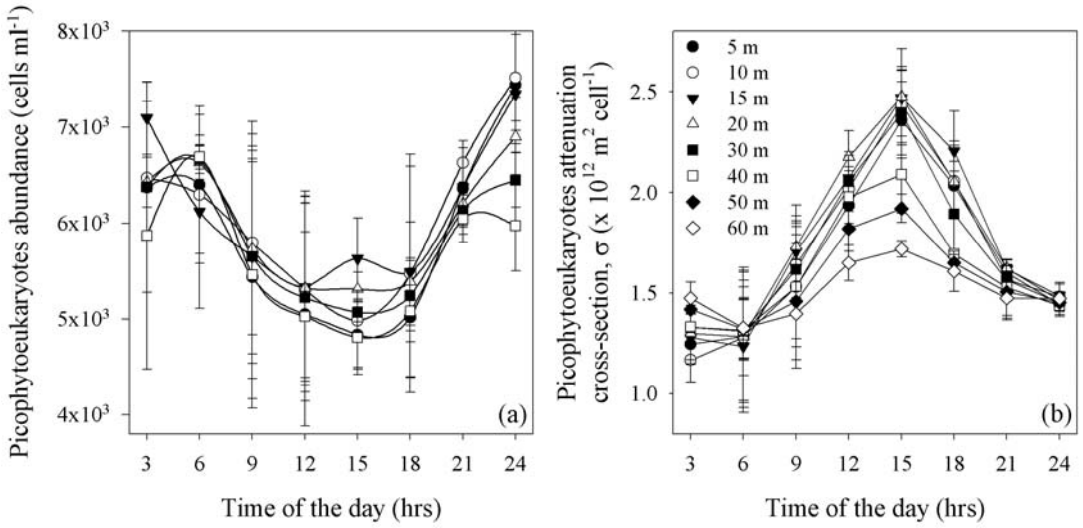

Fig. 24. Mean diel cycles of picophytoeukaryotes abundance in cells ml^{-1} (a) and attenuation cross-section (σ_c) in x 10^{12} m^2 $cell^{-1}$ (b) between the surface and 60 m, at MAR station. The average and standard deviation values for each sampling time (i.e., 3, 6, 9, 12, 15, 18, 21 and 24 h) were obtained using the data collected during the 2 sampling days. σ_c for each time of the day were obtained as indicated in Chapter 2.3.1.

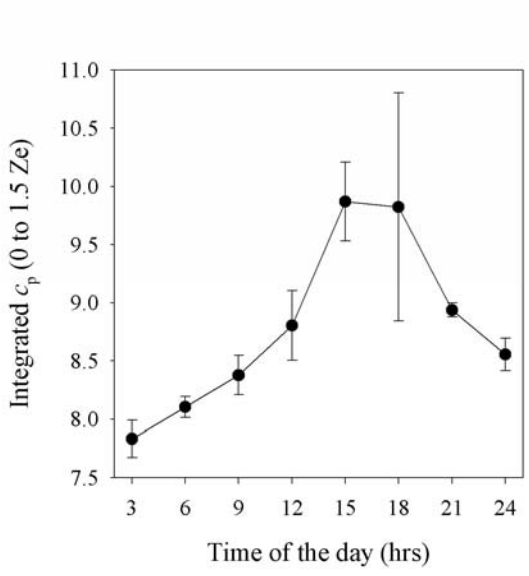

Fig. 25. Mean diel cycle of integrated (0 to 1.5 Ze) particle beam attenuation (cp) at MAR station.

The results presented above indicate that although diel variability at the individual cell's level (i.e., in σ_c) was important (Fig. 24b), opposing changes in cell abundance (Fig. 24a) resulted in a much lower variability in c_{euk}. The observed inverse trends in σ_c and cell abundance are typical of synchronized cells growth and division as part of their life cycle. Mean integrated c_p (0 to 1.5 Ze), on the other hand, increased from 7.8 to 9.9 m^{-1} between the early morning (3h) and early afternoon (15-18h), i.e., ~26% during the diel cycle (Fig. 25). Interestingly, c_{euk} represented a very stable ~10% of c_p, and therefore of POC (see Chapter 4), along the whole diel cycle and at all depths (Table 1). Therefore, the picophytoeukaryotes contribution to the diel variability in the total particulate organic carbon concentration

was not significant (~10%). The second hypothesis of this work can hence be rejected, at least for now since it could only be tested at the mesotrophic Marquesas Islands station.

Table 1. Percentage of the total attenuation coefficient (c_p) corresponding to picophytoeukaryotes (%) at MAR Station. Three different depths are presented as representative of the surface (15 m), intermediate (30 m) and deep (60 m) water column

	Time of the day (h)							
Depth (m)	**3**	**6**	**9**	**12**	**15**	**18**	**21**	**24**
15	9	10	10	10	8	10	10	9
30	10	9	11	10	8	9	10	10
60	9	10	11	10	9	9	9	11

Daily rates of change

In terms of daily rates of change (d^{-1}) estimated over the whole sampling periods (see Chapter 2.5), the MAR station did not follow the same pattern observed at HNL, GYR and EGY, and was therefore not included when establishing a significant correlation ($p < 0.001$) between biomass and c_p rates of change (Fig. 26a). The conclusion that can be drawn from these results is that this bio-optical property (i.e., c_p) was useful in tracing short-term variability in picophytoplanktonic carbon biomass.

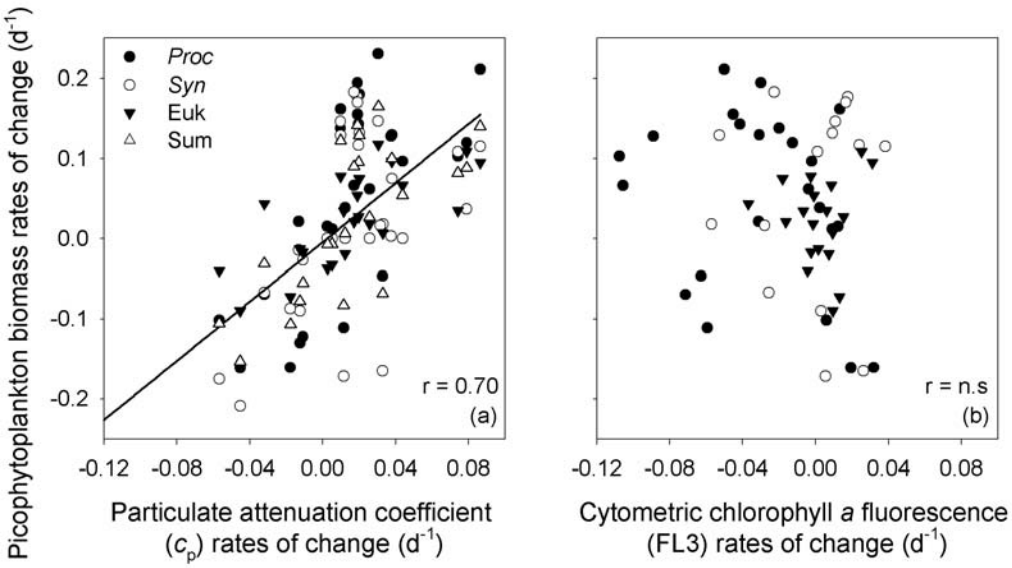

Fig. 26. Relationship between daily rates of change (d-1) in *Prochlorococcus* (Proc), *Synechococcus* (Syn) and picophytoeukaryotes (Euk) carbon biomass and daily rates of change of total particle attenuation (cp) (a) and cytometric chlorophyll fluorescence (FL3) (b). In (a), the correlation coefficient (r) was calculated for the mean rates of change (considering all *Proc, Syn* and Euk biomasses rates of change) and *cp.* In (b), n. s. stands for not significant.

Rates of change on the chlorophyll fluorescence cytometric signal (FL3), a useful proxy for Tchl*a* concentration (Li et al., 1993), were not correlated to rates of change in picophytoplankton carbon biomass (Fig. 26b). Although we do not have diel pigment data to calculate the actual Tchl*a* rates of change, the above suggests that changes in carbon biomass should be better traced by changes in c_p than in Tchl*a*. At GYR, for instance, even though the diel increase in deep picophytoplankton carbon biomass was associated with an important increase in light availability (Claustre et al., *submitted*), changes in FL3 were minimal. Daily rates of change in c_p (d^{-1}) could therefore be a good proxy, probably better than Tchl*a*, for short term (i.e., days) changes in the photosynthetic biomass.

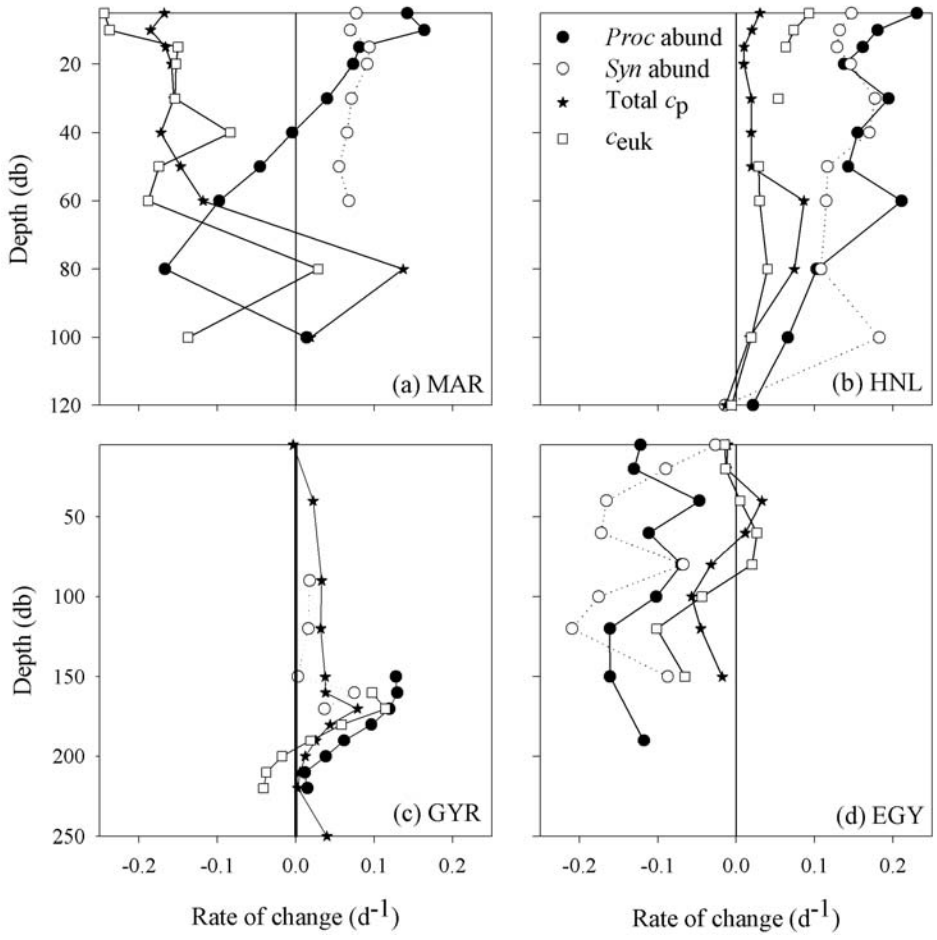

Fig. 27. Daily rates of change (d-1) of *Prochlorococcus* (Proc) and *Synechococcus* (Syn) abundances (abund), total particle beam attenuation coefficient (Total *cp)* and picophytoeukaryotes attenuation coefficient (ceuk) at MAR (a), HNL (b), GYR (c) and EGY (d). In the case of cyanobacteria, daily rates of change in abundance are representative of daily rates of change in their attenuation coefficients, because the latter were estimated using an average cell size (see Chapter 2.3.1).

When comparing these 4 long stations, c_{euk} daily rates of change seemed to follow changes in c_p more closely than cyanobacteria (Fig. 27). Remember that rates of change in cyanobacteria abundance are equivalent to their rates of change in attenuation coefficient, because we used a unique cell size to calculate the latter. These results seem to agree with the constant c_{euk}'s contribution to c_p observed for the average diel cycle (Table 1).

5.3 Significance of the thesis results in a global context

Across the eastern South Pacific, picophytoeukaryotes contributed significantly to picophytoplankton (cyanobacteria + picophytoeukaryotes) and picoplankton (bacterioplankton + picophytoplankton) carbon biomass, and to the c_p-derived total particulate organic carbon concentration (POC) (see Chapters 3 and 4). c_p, on the other hand, seemed to be a good proxy for tracing picophytoplankton biomass spatial variability (see Chapter 4) provided that information on the contributions by vegetal and non-vegetal particles is available. Regarding temporal variability, the influence of picophytoeukaryotes remains unclear because their contribution to the diel variability of c_p could only be tested at one station (i.e, MAR), where it was rather low (~10%). These results are valid for the area of the open-ocean eastern South Pacific covered during the BEAGLE and BIOSOPE cruises during austral spring time. But what general conclusions can we draw from these results? What if these results were also valid at larger spatial and temporal scales?

5.3.1 Implications for global marine primary production

In the present work it was shown that average picophytoeukaryotes contribution to the total open-ocean phytoplanktonic carbon biomass is in the range of ~40 to 60% (Fig. 22). If *Prochlorococcus* and picophytoeukaryotes PP rates normalized to their carbon biomass were to be equivalent, then the picophytoeukaryotes contribution to PP would be in the same order than that of *Prochlorococcus*. For instance, if we assume the contribution by *Synechococccus* to be almost negligible and take the 56% picophytoplanktonic contribution to total integrated PP reported by Marañón et al. (2001) for the North and South Atlantic Subtropical Gyres, then we can say that when representing ~40% of the photosynthetic carbon biomass the picophytoeukaryotes would be responsible for ~29% of the open-ocean PP. If we then consider that about 86% of total marine primary production takes place in the open ocean (Chen et al.,

2003), this group would be responsible for about 34%, i.e., more than one third of the global marine PP. The picophytoeukaryotes could hence be much more important to carbon production and cycling then previously though, not only in the open ocean but also at the global scale. Nevertheless, much work needs to be done in order to determine the contribution by the different picophytoplanktonic groups to the PP in this size fraction (see Chapter 6).

The data presented here was collected across the eastern South Pacific during austral spring time. Despite taking place during the same season of the year, the water column was more stratified during BIOSOPE than during BEAGLE. The former cruise was characterized by important subsurface maxima in Tchl*a* concentrations, *Prochlorococccus* and picophytoeukaryotes abundances, whereas during the latter the presence of such deep maxima were not detected. Nevertheless, the general results pointed out to the same conclusions, i.e., picophytoeukaryotes constitute an important fraction of picophytoplankton carbon biomass in the open ocean. Therefore, this statement could be considered to be valid regardless of the degree of stratification of the water column and hence probably regardless of the period of the year.

Surface chlorophyll *a* concentrations at the centre of the South Pacific Subtropical Gyre seem to be consistently low all year round (Claustre & Maritorena, 2003). Seasonal SeaWiFS data indicates that the area of lowest surface chlorophyll *a* concentrations (< 0.07 mg m^{-3}) in this region is at its maximum during austral summer and at its minimum during austral winter (McClain et al., 2004). The above suggests that the eastern South Pacific was predominantely oligotrophic during the period of sampling.

Picophytoeukaryotes contribution to the photosynthetic carbon biomass and PP (according to assumptions and estimations presented above) increases from oligo- to mesotrophic conditions. In the oceanic region of the eastern South Pacific their contribution to biomass and PP would therefore be highest during austral winter time, when the area covered by oligotrophic conditions is at its minimum. Yuras et al. (2005) have also reported maximum surface chlorophyll *a* concentration during austral winter for this region. If we now consider that the same pattern of seasonal expansion and contraction of the oligotrophic area of all Subtropical Gyres (McClain et al., 2004), then picophytoeukaryotes contribution to the global open-ocean carbon biomass and PP would be highest during austral winter. Therefore, the estimates derived from this thesis

work concerning picophytoeukaryotes contribution to the global open-ocean photosynthetic biomass and PP would be close to the annual lowest.

Near the coast, on the other hand, at ~36.5ºS picophytoeukaryotes abundance reaches its maximum during late autumn, the variability on chlorophyll *a* concentration being dominated by large phytoplankton (> 5µm) year round (G. Alarcón, *pers. comm.*). Picophytoeukaryotes contribution to the coastal photosynthetic biomass and PP would therefore be low most of the year. However, because of the large area covered by the open ocean, all of the above indicates that despite their low contribution in coastal regions, on annual bases picophytoeukaryotes would still be very important in terms of carbon biomass and PP at a global scale.

5.3.2 Implications for open-ocean carbon export

Richardson et al. (2006) stated that offshore in the Arabian Sea carbon originating from the picophytoplankton made the highest contributions to export through three different pathways: POC export (detritus flux), DOC advection and consumption of mesozooplankton by higher trophic levels. Through inverse and network analyses, Richardson & Jackson (2007) showed that the relative contributions of various phytoplankton size classes to carbon export are proportional to their contributions to total net primary production. Until now, export by picophytoplankton was thought to be almost negligible and their biomass assumed to be remineralized within the microbial food web through direct excretion of dissolved organic matter (DOC) and DOC released after grazing by unicellular zooplankton (Fig. 28). Richardson & Jackson (2007) proposed three additional export pathways: formation of organic aggregates that are directly grazed by large zooplankton (pathway 3 in Fig. 28), grazing by tunicates and pteropods that contribute to particulate organic detritus by defecation (pathway 4 in Fig. 28) and direct sinking to particulate organic detritus (pathway 5 in Fig. 28). The organic matter being exported through these additional pathways is believed to be underestimated through traditional export measurements such as sediment traps.

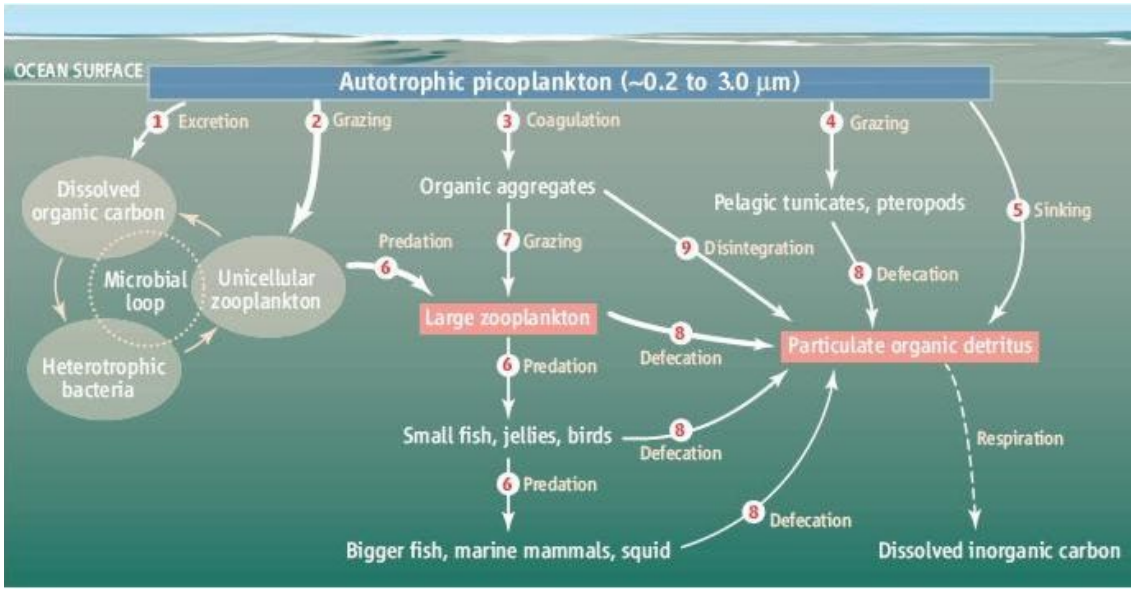

Fig. 28. The picoplankton food web: This oceanic food web based on picoplankton shows the paths of organic carbon flux determined by Richardson & Jackson (2007). On the left is the classical "microbial loop" (grey). The two red boxes (large zooplankton and particulate organic detritus) are two carbon pools that, according to Richardson and Jackson, receive substantial export of picoplankton carbon. This new information suggests that the role of picoplankton in carbon export and fish production needs further investigation in both observations and models. Modified from Barber, 2007.

Again, if picophytoeukaryotes were to be as significant contributors to carbon production as they were to carbon biomass, then this group's role in open-ocean carbon export could be much more important than previously thought. Their role could be particularly relevant at the subsurface maximum, where this population was able to respond (Fig. 19a) to an increase in light availability (Fig. 20), just like *Prochlorococcus* did (Fig. 19b). The probability of the carbon produced at 160-170 m to be exported to the ocean's interior and escape instant remineralization is higher than for the one produced near the surface. Considering the premise that larger predators eat larger preys, on the other hand, this group could also be important in channelling carbon flow towards higher trophic levels more efficiently than the smaller-sized *Prochlorococcus*. Further studies are however needed in order to determine the actual role of picophytoeukaryotes in carbon flow and export.

5.3.3 Picophytoeukaryotes role under changing environmental conditions

Let us picture the following two probable future scenarios (1) increasing stratification due to global warming (Falkowski et al., 1998) and (2) increasing El Niño frequency with a decrease in PP and export production in upwelling regions such, as in the north of Chile (Iriarte & González, 2004).

Increasing stratification will lead to an increase area of oligotrophic low-latitude gyres (Falkowski et al., 1998), i.e., an increase area of the picophytoplankton-dominated photosynthetic biomass, leading to a reduction of primary production and carbon export at the global scale. If picophytoeukaryotes and *Prochlorococcus* were to be equally contributing to the open-ocean PP (see Chapter 5.3.1), then these two groups would play an equivalently important role in the future's ocean global primary production. The above would be particularly true if picophytoeukaryotes were to have the ability to grow on nutrients other than nitrate, as suggested by the increase in abundance observed at the GYR station (Fig. 19a), since in this future stratified ocean inorganic nitrogen is expected to be scarce.

Regarding more productive regions, the background bloom hypothesis states that picophytoplankton constitutes the background photosynthetic biomass (e.g. Denman, 2003). It has been shown for the north of Chile that during El Niño events primary and export production are reduced because of an increased dominance of pico- and nanophytoplankton (Iriarte & González, 2004). A higher frequency of El Niño events would increase the occurrence of these open-ocean-like conditions in coastal waters. Under such conditions, picophytoplankton could be equally important than nano- and microphytoplankton in terms of PP (see Fig. 2 in Iriarte & González, 2004). Given that picophytoeukaryotes usually dominate the coastal picophytoplanktonic carbon biomass this group could be responsible for up to one third (see Fig. 2 in Iriarte & González, 2004) of the coastal PP and therefore play an important role under such scenario.

Considering the high genetic diversity found within this group (e.g., López-García et al., 2001; Moon-van der Staay et al., 2001; Not et al., 2007), there is room for one more speculation about the importance of picophytoeukaryotes under changing environmental conditions. Not et al. (2007) suggested that this unexpected high diversity could probably act as reservoirs of genetic capacity that would be activated under particular circumstances. If we consider this possibility, then under changing conditions such as the ones mentioned above this group could eventually pull the trigger on this genetic reservoir and adapt to lower inorganic nutrient conditions and turn to different metabolic pathways in order to keep up with their present high contribution to carbon biomass and probably production at the global scale.

It is impossible for now to predict the response of the Earth system to the ongoing environmental changes. Picophytoplanktonic groups form a very important part of the marine ecosystem and it is therefore fundamental to know more about their ecology in order to better understand how changes at the primary producer's level could modify the system's functioning. Compared to cyanobacteria, too little is known on the physiology, ecology and diversity of picophytoeukaryotes and much more work needs therefore to be done.

CHAPTER 6

PERSPECTIVES

6. PERSPECTIVES

In this work I highlighted the importance of picophytoeukaryotes in terms of their contribution to the photosynthetic carbon biomass and to total particulate organic carbon in the euphotic layer of the open-ocean. Here, picophytoeukaryotes attenuation coefficients were estimated from actual cell size instead of assuming one like did Claustre et al. (1999). Picophytoplankton populations were isolated *in situ* using flow cytometry cell sorting and measured with a particle counter to establish a direct relationship between mean cell size and the cytometric forward scatter signal (FSC). To my knowledge, this is the first time that such direct measurements have been done. The deconvolution of c_p into its different contributors seems clearly to be a promising tool for estimating group-specific contributions to the total carbon biomass if actual cell sizes are known (optically-based approach).

Based on the success of the optically-based approach to determine picophytoeukaryotes biomass (see Chapter 2.3.1), the first perspective rising from the present work is testing the applicability of the same kind of methodology for other phytoplankton groups. Unfortunately, this could not be tested here for cyanobacteria, because flow cytometric forward scatter signals (FSC) were only partially available for *Synechococcus* (see Chapter 2.1.3) and *Prochlorococcus* was not included in the relationship established between FSC and intracellular carbon content. For future studies (1) flow cytometry data should be acquired using different settings in order to include not only all picophytoplankton groups, but also larger phytoplankton cells (i.e., nano- and microphytoplankton) if possible, and (2) the size range used to establish the FSC-size and FSC-intracellular carbon content relationships should be expanded.

The total particle beam attenuation coefficient (c_p) was found to be a useful proxy for picophytoplankton biomass. If carbon biomasses for all phytoplankton groups (i.e., pico-, nano- and microphytoplankton) were to be efficiently determined through the optically-based approach (as was done here for the picophytoeukaryotes), then the usefulness of c_p as a proxy for spatial and temporal variability in the photosynthetic carbon biomass (see Chapter 4, 5.1 and 5.2) could be explored at larger spatial and temporal scales. c_p being more easily obtained than Tchl*a* concentrations on the field, this could be an important step forward in determining the photosynthetic carbon biomass and primary production in the ocean.

Fast cell sorting proved to be very useful to isolate non-preserved *in situ* picophytoplankton population to determine further group-specific characteristics such as their actual mean cell size. Unfortunately, due to their low intracellular carbon content and abundance, collecting enough cells to estimate carbon concentrations on per-cell bases would be extremely long. However, given the improvement that this technique has experimented in the last decades, it would not be surprising if we were able to do so in the near future. Cell sorting has another great advantage, which is that combined with ^{14}C measurements it allows the determination of group-specific primary production rates for picophytoplankton (Li, 1994). Nevertheless, because of the low sorting rates available until recently, gathering enough cells to measure the radioactive signal was extremely time consuming (Li, *pers. comm.*) and could be performed only at 3 different stations and at a unique depth per station (Li, 1994). The new generation of fast cell sorters opens the possibility of reproducing this kind of measurements that, to my knowledge, have only been performed once (Li, 1994). Furthermore, this technique could be applied to study bio-optical properties at the individual cell level from natural populations, since until now this kind of study has only been performed on cells from culture under controlled conditions (e.g., Stramski et al., 1995; DuRand & Olson, 1998; DuRand et al., 2002; Claustre et al., 2002).

Isolating enough cells of an individual picoplanktonic population has also proven to be useful to identify different groups based on their genetic sequences. By combining fast cell sorting and molecular biology it has been possible to discover an unexpectedly high diversity within this size fraction (e.g., Not et al., 2007). This combination of techniques could, for instance, be a very powerful tool to explore the speculation made on the potential role of such diversity and their ability to activate particular genes as a response to a particular external forcing or to changing environmental conditions (see Chapter 5.3.3). Furthermore, it opens the door for group-specific studies on nutrient metabolism, which would help, for instance, to answer the questions about nitrate utilization by picophytoeukaryotes (see Chapter 5.1).

Finally, although the present work constitutes one step forward on picophytoplankton research, it only considered carbon stocks and not fluxes. In order to better understand the role of the different picophytoplanktonic groups in the global carbon cycle, the next step is to consider energy and matter flows from this primary producers' compartment towards higher trophic levels within the oceanic food web. Given the little that is known

about picophytoeukaryotes metabolism, it would be very interesting to determine the importance of mixotrophy within this group and how this metabolic process could alter carbon and energy flow in the open and coastal oceans.

LITERATURE CITED

Ahlgren, N. A. and Rocap, G.: Culture isolation and culture-independent clone libraries reveal new marine *Synechococcus* ecotypes with distinctive light and N physiologies. Appl Environ Microb, 72, 7193-7204, 2006.

Antoine, D., André, J. M. , and Morel, A.: Oceanic primary production II. Estimation at global scale from satellite (Coastal Zone Color Scanner) chlorophyll. Global Biogeochem Cycles, 10, 57-69, 1996.

Barber, R. T.: Picoplankton Do Some Heavy Lifting. Science, 315, 777-778, 2007.

Behrenfeld, M. J. and Boss, E.: The beam attenuation to chlorophyll ratio: an optical index of phytoplankton physiology in the surface ocean? Deep Sea Res Part I, 50, 1537–1549, 2003.

Behrenfeld, M. J. and Boss, E.: Beam attenuation and chlorophyll concentration as alternative optical indices of phytoplankton biomass. J Mar Res, 64, 431–451, 2006.

Berg, G. M., Repeta, D. J. , and LaRoche, J.: The role of the picoeukaryote *Aureococcus anophagefferens* in cycling of marine high–molecular weight dissolved organic nitrogen. Limnol Oceanogr, 48, 1825–1830, 2003.

Binder, B. J. and DuRand, M. D.: Diel cycles in surface waters of the equatorial Pacific. Deep Sea Res II, 49, 2601–2617, 2002.

Blanchot, J. and Rodier, M.: Picophytoplankton abundance and biomass in the western Tropical Pacific Ocean during the 1992 El Nino year: Results from flow cytometry. Deep-Sea Res, 43, 877-896, 1996.

Blanchot, J., André, J.-M., Navarette, C., Neveux, J. , and Radenac, M.-H.: Picophytoplankton in the equatorial Pacific: vertical distributions in the warm pool and in the high nutrient low chlorophyll conditions. Deep-Sea Res Part I, 48, 297-314, 2001.

Bricaud, A., Morel, A. , and Prieur, L.: Absorption by dissolved organic matter of the sea (yellow substance) in the UV and visible domains. Limnol Oceanogr, 26, 43-53, 1981.

Campbell, L. and Vaulot, D.: Photosynthetic picoplankton community structure in the subtropical North Pacific Ocean near Hawaii (station ALOHA). Deep Sea Res Part I, 40, 2043-2060, 1993.

Carr, M.-E., Friedrichs, M. A. M., Schmeltz, M., Aita, M. N., Antoine, D., Arrigo, K. R., Asanuma, I., Aumont, O., Barber, R., Behrenfeld, M., Bidigare, R., Buitenhuis, E. T., Campbell, J., Ciotti, A., Dierssen, H., Dowell, M., Dunne, J., Esaias, W., Gentili, B., Gregg, W., Groom, S., Hoepffner, N., Ishizaka, J., Kameda, T., Quéré, C. L., Lohrenz, S., Marra, J., Mélin, F., Moore, K., Morel, A., Reddy, T. E., Ryan, J., Scardi, M., Smyth, T., Turpie, K., Tilstone, G., Waters, K. , and Yamanaka, Y.: A comparison of global estimates of marine primary production from ocean color. Deep Sea Research II, 53, 741–770, 2006.

Chen, C.-T. A., Liu, K.-K. , and MacDonald, R. W.: Continental margin exchanges. Ocean Biogeochemistry, in: The Role of the Ocean Carbon Cycle in Global Change, edited by Fasham, M. J. R., IGBP Book Series, Springer, 53-97, 2003.

Chisholm, S. W., Olson, R. J., Zettler, E. R., Goericke, R., Waterbury, J. B. , and Welschmeyer, N. A.: A novel free-living prochlorophyte occurs at high cell concentrations in the oceanic euphotic zone. Nature, 334, 340-343, 1988.

Chisholm, S. W., 1992: Phytoplankton size. Primary Productivity and Biogeochemical Cycles in the Sea, edited by. Falkowski, P. G. and Woodhead, A. D., Plenum Press, 213-237.

Chung, S. P., Gardner, W. D., Richardson, M. J., Walsh, I. D. , and Landry, M. R.: Beam attenuation and microorganisms: spatial and temporal variations in small particles along 14O”W during the 1992 JGOFS EqPac transects. Deep Sea Research II, 43, 1205-1226, 1996.

Chung, S. P., Gardner, W. D., Landry, M. R., Richardson, M. J. , and Walsh, I. D.: Beam attenuation by microorganisms and detrital particles in the Equatorial Pacific. J Geophys Res, 103 (C6), 12,669-12,681, 1998.

Claustre, H., Morel, A., Babin, M., Cailliau, C., Marie, D., Marty, J. C., Tailliez, D. , and Vaulot, D.: Variability in particle attenuation and chlorophyll fluorescence in the Tropical Pacific: Scales, patterns, and biogeochemical implications. J Geophys Res, 104 (C2), 3401-3422, 1999.

Claustre, H., Bricaud, A., Babin, M., Bruyant, F., Guillou, L., Gall, F. L., Marie, D. , and Partensky, F.: Diel variations in *Prochlorococcus* optical properties. Limnol Oceanogr, 47, 1637–1647, 2002.

Claustre, H. and Maritorena, S.: The Many Shades of Ocean Blue. Science, 302, 1514-1515, 2003.

Denman, K. L.: Modelling planktonic ecosystems: parameterizing complexity. Prog Oceanogr, 57, 429–452, 2003.

DuRand, M. D. and Olson, R. J.: Contributions of phytoplankton light scattering and cell concentration changes to diel variations in beam attenuation in the equatorial Pacific from flow cytometric measurements of pico-, ultra- and nanoplankton. Deep Sea Res Part II, 43, 891-906, 1996.

DuRand, M. D. and Olson, R. J.: Diel patterns in optical properties of the chlorophyte *Nannochloris sp.*: Relating individual-cell to bulk measurements. Limnol Oceanogr, 43, 1107-1118, 1998.

DuRand, M. D., Green, R. E., Sosik, H. M. , and Olson, R. J.: Diel variations in optical properties of *Micromonas pusilla* (Prasinophyceae). J Phycol, 38, 1132-1142, 2002.

Falkowski, P. G., Barber, R. T. , and Smetacek, V.: Biogeochemical Controls and Feedbacks on Ocean Primary Production. Science, 200-206, 1998.

Fuhrman, J. A., Sleeter, T. D., Carlson, C. A. , and Proctor, L. M.: Dominance of bacterial biomass in the Sargasso Sea and its ecological implications. Mar Ecol Prog Ser, 57, 207-217, 1989.

Fuhrman, J. A.: Bacterioplankton roles in cycling on organic matter: The microbial food web, in: Primary productivity and biogeochemical cycles in the sea, edited by Falkowski, P. and Woodhead, A.D., Plenum, 361-383, 1992.

Field, C. B., Behrenfeld, M. J., Randerson, J. T. , and Falkowski, P.: Primary Production of the Biosphere: Integrating Terrestrial and Oceanic Components. Science, 281, 237-240, 1998.

Gasol, J. M. and Duarte, C. M.: Comparative analyses in aquatic microbial ecology: how far do they go? FEMS Microbiol Ecol, 31, 99-106, 2000.

Goericke, R. and Welschmeyer, N. A.: The carotenoid-labeling method: measuring specific rates of carotenoid synthesis in natural phytoplankton communities. Mar Ecol Prog Ser, 98, 157-171, 1993.

Goericke, R.: Response of phytoplankton community structure and taxon-specific growth rates to seasonally varying physical forcing in the Sargasso Sea off Bermuda. Limnol Oceanogr, 43, 921-935, 1998.

Huot, Y., Babin, M., Bruyant, F., Grob, C., Twardowski, M. S. , and Claustre, H.: Does chlorophyll a provide the best index of phytoplankton biomass for primary productivity studies?, *submitted*.

Iriarte, J. L. and González, H. E.: Phytoplankton size structure during and after the 1997/98 El Niño in a coastal upwelling area of the northern Humboldt Current System. Mar Ecol Prog Ser, 269, 83–90, 2004.

Legendre, L. and Fèvre, J. L.: Microbial food web and the export of biogenic carbon in oceans. Aquat Microb Ecol, 9, 69-77, 1995.

Li, W. K. W., Rao, D. V. S., Harrison, W. G., Smith, J. C., Cullen, J. J., Irwin, B. , and Platt, T.: Autotrophic Picoplankton in the Tropical Ocean. Science, 219, 292 - 295, 1983.

Li, W. K. W. and Wood, M.: Vertical distribution of North Atlantic ultraphytoplankton: analysis by flow cytometry and epifluorescence microscopy. Deep Sea Res, 35, 1615-1638, 1988.

Li, W. K. W., Dickie, P. M., Irwin, B. D. , and Wood, A. M.: Biomass of bacteria, cyanobacteria, prochlorophytes and photosynthetic eukaryotes in the Sargasso Sea. Deep-Sea Res, 39, 501-519, 1992.

Li, W. K. W., Zohary, T., Yacobi, Y. Z. , and Wood, A. M.: Ultraphytoplankton in the eastern Mediterranean Sea: Towards deriving phytoplankton biomass from flow cytometric measurements of abundance fluorescence and light scatter. Mar Ecol Prog Ser, 102, 79-87, 1993.

Li, W. K. W.: Primary production of prochlorophytes, cyanobacteria, and eucaryotic ultraphytoplankton: Measurements from flow cytometric sorting. Limnol Oceanogr, 39, 169-175, 1994.

Li, W. K. W.: Composition of ultraphytoplankton in the Central North Atlantic. Mar Ecol Prog Ser, 122, 1-8, 1995.

Li, W. K. W.: Macroecological patterns of phytoplankton in the northwestern North Atlantic Ocean. Nature, 419, 154-157, 2002.

Li, W. K. W., Head, E. J. H. , and Harrison, W. G.: Macroecological limits of heterotrophic bacterial abundance in the ocean. Deep-Sea Res Part I, 51, 1529-1540, 2004.

Li, W. K. W.: Plankton Populations and Communities, in: Marine Macroecology, edited by Witman, J. and Kaustuv, R., University of Chicago Press, *in press*.

Loisel, H. and Morel, A.: Light scattering and chlorophyll concentration in case 1 waters: A reexamination. Limnol Oceanogr, 43, 847-858, 1998.

Longhurst, A., Sathyendranath, S., Platt, T. , and Caverhill, C.: An estimate of global primary production in the ocean from satellite radiometer data. J Plankton Res, 17, 1245-1271, 1995.

López-García, P., Rodríguez-Valera, F., Pedrós-Alió, C. , and Moreira, D.: Unexpected diversity of small eukaryotes in deep-sea Antarctic plankton. Nature, 409, 603-607, 2001.

Marañón, E., Holligan, P. M., Barciela, R., González, N., Mouriño, B., Pazó, M. J. , and Varela, M.: Patterns of phytoplankton size structure and productivity in contrasting open-ocean environments. Mar Ecol Prog Ser, 216, 43-56, 2001.

Marie, D., Partensky, F., Simon, N., Guillou, L. , and Vaulot, D.: Flow cytometry analysis of marine picoplankton. In: Diamond R.A., DeMaggio S. (ed.). In Living Colors: Protocols in Flow Cytometry and Cell sorting. Vol., 421-454 pp., 2000.

Marie, D., Simon, N. & Vaulot, D., Phytoplankton cell counting by flow cytometry, p. 253-267. In Andersen, R. A. [ed.], Algal Culturing Techniques. Academic Press, 2005.

Moon van der Staay, S. Y., Wachter, R. D. , and Vaulot, D.: Oceanic 18S rDNA sequences from picoplankton reveal unsuspected eukaryotic diversity. Nature, 409, 607-610, 2001.

Moore, L. R., Post, A. F., Rocap, G. , and Chisholm, S. W.: Utilization of different nitrogen sources by the marine cyanobacteria *Prochlorococcus* and *Synechococcus*. Limnol Oceanogr, 47, 989-996, 2002.

Morel, A. and Ahn, Y.-H.: Optics of heterotrophic nanoflagellates and ciliates: A tentative assessment of their scattering role in oceanic waters compared to those of bacterial and algal cells. J Mar Res, 49, 177-202, 1991.

Morel, A., Gentili, B., Claustre, H., Babin, M., Bricaud, A., Ras, J. , and Tièche, F.: Optical properties of the "clearest" natural waters. Limnol Oceanogr, 52, 217-229, 2007.

Not, F., Simon, N., Biegala, I. C. , and Vaulot, D.: Application of fluorescent in situ hybridization coupled with tyramide signal amplification (FISH-TSA) to assess eukaryotic picoplankton composition. Aquat Microb Ecol, 28, 157-166, 2002.

Not, F., Latasa, M., Marie, D., Cariou, T., Vaulot, D. , and Simon, N.: A Single Species, *Micromonas pusilla* (Prasinophyceae), Dominates the Eukaryotic Picoplankton in the Western English Channel. Appl Environ Microb, 70, 4064–4072, 2004.

Not, F., Valentin, K., Romari, K., Lovejoy, C., Massana, R., Töbe, K., Vaulot, D. , and Medlin, L. K.: Picobiliphytes: A Marine Picoplanktonic Algal Group with Unknown Affinities to Other Eukaryotes. Science, 315, 253-255, 2007.

Olson, R. J., Zettler, E. R., DuRand, M.D., Phytoplankton analysis using flow cytometry. In: Kemp PF, Sherr BF,Sherr EB, Cole JJ (eds) Handbook of methods in aquatic microbial ecology. Lewis Publ, p 175-186, 1993.

Oubelkheir, K., Claustre, H. , and Babin, A. S.: Bio-optical and biogeochemical properties of different trophic regimes in oceanic waters. Limnol Oceanogr, 50, 1795–1809, 2005.

Partensky, F., Blanchot, J., Lantoine, F., Neveux, J. , and Marie, D.: Vertical Structure of picophytoplankton at different trophic sites of tropical northeastern Atlantic Ocean. Deep-Sea Res Part I, 43, 1191-1213, 1996.

Partensky, F., Blanchot, J. , and Vaulot, D.: Differential distribution and ecology of *Prochlorococcus* and *Synechococcus* in oceanic waters: a review. Bulletin de l'Institut océanographique, Monaco, nº special 19, 457-475, 1999a.

Partensky, F., Hess, W. R. , and Vaulot, D.: *Prochlorococcus*, a marine photosynthetic prokaryote of global significance. Microbiol Mol Biol R, 63, 106-127, 1999b.

Preisendorfer, R. W.: Application of radiative transfer theory to light measurements in the sea. Monogr., 10, 11-30, Int Union Geod Geophys, Paris, 1961.

Raven, J. A., Physiological consequences of extremely small size for autotrophic organisms in the sea. In: Platt T, WKW Li (eds) Photosynthetic picoplankton. Canadian Bulletin of Fisheries and Aquatic Sciences, 214: 1-60, 1986.

Raven, J. A., Finkel, Z. V. , and Irwin, A. J.: Picophytoplankton: bottom-up and top-down controls on ecology and evolution. Vie Milieu, 55, 209-215, 2005.

Richardson, T. L., Jackson, G. A., Ducklow, H. W. , and Roman, M. R.: Spatial and seasonal patterns of carbon cycling through planktonic food webs of the Arabian Sea determined by inverse analysis. Deep Sea Res Part II, 53, 555–575, 2006.

Richardson, T. L. and Jackson, G. A.: Small Phytoplankton and Carbon Export from the Surface Ocean. Science, 315, 838-840, 2007.

Rodríguez, F., Derelle, E., Guillou, L., Gall, F. L., Vaulot, D. , and Moreau, H.: Ecotype diversity in the marine picoeukaryote *Ostreococcus* (Chlorophyta, Prasinophyceae). Environ Microbiol, 7, 853-859, 2005.

Shalapyonok, A., Olson, R. J. , and Shalapyonok, L. S.: Arabian Sea phytoplankton during Southwest and Northeast Monsoons 1995: composition, size structure and biomass from individual cell properties measured by flow cytometry. Deep-Sea Res Part II, 48, 1231-1261, 2001.

Sheldon, R. W., Prakash, A. , and Sutcliffe, W. H.: The size distribution of particles in the ocean. Limnol Oceanogr, 17, 327-340, 1972.

Sherr, E. B., Sherr, B. F. , and Wheeler, P. A.: Distribution of coccoid cyanobacteria and small eukaryotic phytoplankton in the upwelling ecosystem off the Oregon coast during 2001 and 2002. Deep Sea Research II, 52, 317–330, 2005.

Sieburth, J. M., Smetacek, V. , and Lenz, J.: Pelagic Ecosystem Structure: Heterotrophic Compartments of the Plankton and Their Relationship to Plankton Size Fractions. Limnol Oceanogr, 23, 1256-1263, 1978.

Sokal, R. R., and F. J. Rohlf. Biometry the principles and practice of statistics in biological research, W.H. Freeman and Company, New York, 1994.

Stramski, D., Shalapyonok, A. , and Reynolds, R.: Optical characterization of the oceanic unicellular cyanobacterium *Synechococcus* grown under a day-night cycle in natural irradiance. J Geophys Res, 100, 13295-13307, 1995.

Timmermans, K. R., Wagt, B. v. d., Veldhuis, M. J. W., Maatman, A. , and Baar, H. J. W. d.: Physiological responses of three species of marine pico-phytoplankton to ammonium, phosphate, iron and light limitation. J Sea Res, 53, 109– 120, 2005.

Van de Hulst, H. C.: Light scattering by small particles, Wiley, New York, 1957.

Vaulot, D.: CYTOPC: Processing software for flow cytometric data. Signal and Noise, 2:8. 1989.

Vaulot, D., Marie, D., Olson, R. J. , and Chisholm, S. W.: Growth of Prochlorococcus, a Photosynthetic Prokaryote, in the Equatorial Pacific Ocean. Science, 268, 1480 - 1482, 1995.

Vaulot, D. and Marie, D.: Diel variability of photosynthetic picoplankton in the equatorial Pacific. J Geophys Res, 104 (C2), 3297-3310, 1999.

Veldhuis, M. J. W., Timmermans, K. R., Croot, P. , and Wagt, B. v. d.: Picophytoplankton; a comparative study of their biochemical composition and photosynthetic properties. J Sea Res, 53, 7 – 24, 2005.

Waterbury, J. B., Watson, S. W., Guillard, R. R. L. , and Brand, L. E.: Widespread occurrence of a unicellular, marine planktonic, cyanobacterium. Nature, 277, 293-294, 1979.

Worden, A. Z., Nolan, J. K. , and Palenik, B.: Assessing the dynamics and ecology of marine picophytoplankton: The importance of the eukaryotic component. Limnol Oceanogr, 49, 168–179, 2004.

Worden, A. Z.: Picoeukaryote diversity in coastal waters of the Pacific Ocean. Aquat Microb Ecol, 43, 165–175, 2006.

Zubkov, M. V., Sleigh, M. A., Tarran, G. A., Burkill, P. H. , and Leakey, R. J. G.: Picoplanktonic community structure on an Atlantic transect from 50ºN to 50ºS. Deep-Sea Res Part I, 45, 1339-1355, 1998.

Zubkov, M. V., Sleigh, M. A., Burkill, P. H. , and Leakey, R. J. G.: Picoplankton community structure on the Atlantic Meridional Transect: a comparison between seasons. Prog Oceanogr, 45, 369–386, 2000.

Zubkov, M. V., Fuchs, B. M., Tarran, G. A., Burkill, P. H. , and Amann, R.: High Rate of Uptake of Organic Nitrogen Compounds by Prochlorococcus Cyanobacteria as a Key to Their Dominance in Oligotrophic Oceanic Waters. Appl Environ Microb, 69, 1299–1304, 2003.

Zubkov, M. V., Tarran, G. A. , and Fuchs, B. M.: Depth related amino acid uptake by *Prochlorococcus* cyanobacteria in the Southern Atlantic tropical gyre. FEMS Microbiol Ecol, 50, 153–161, 2004.

Zubkov, M. V. and Tarran, G. A.: Amino acid uptake of *Prochlorococcus spp.* in surface waters across the South Atlantic Subtropical Front. Aquat Microb Ecol, 40, 241–249, 2005.

CURRICULUM VITAE

María Carolina Grob Varas
Born in Jun 14th 1978, Concepción, Chile

1997-2002: Marine Biologist with Mention in Oceanography and Environmental Quality, University of Concepción, Chile.

2003-2007: Ph. D. in Oceanography, University of Concepción, Chile and University of Paris VI, France.

Publications:

Grob C., R. Quiñones & D. Figueroa (2003), "Cuantificación de flujos costa-océano en el sector centro-sur de Chile (35.4-37.2ºS) ", Gayana 67 (1): 55-67.

Grob C., O. Ulloa, W.K.W. Li, G. Alarcón, M. Fukasawa, S. Watanabe, "Picoplankton abundance and biomass across the eastern South Pacific Ocean along 32.5ºS". Mar Ecol Prog Ser, 332, 53–62, 2007.

Grob C., O. Ulloa, H. Claustre, Y. Huot, G. Alarcón & D. Marie, "Contribution of picoplankton to the particle beam attenuation coefficient (c_p) and organic carbon concentration (POC) in the eastern South Pacific", *submitted to Biogeosciences.*

Bonnet S., C. Guieu, F. Bruyant, O. Prasil, P. Raimbault, M. Gorbunov, J.P. Zehr, **C. Grob**, S.M. Masquelier, S. Blain, T. Moutin, F. Van Wambeke & H. Claustre, "What controls primary productivity in the hyper-oligotrophic South Pacific gyre?", *submitted to Biogeosciences.*

Huot Y., M. Babin, F. Bruyant, **C. Grob**, M. S. Twardowski & H. Claustre, "Does chlorophyll *a* provide the best index of phytoplankton biomass for primary productivity studies?", *submitted to Biogeosciences.*

Research areas:

Main: Biological oceanography
Secondary: Bio-optics